



HHS Public Access

Author manuscript

J Med Chem. Author manuscript; available in PMC 2019 July 05.

Published in final edited form as:

J Med Chem. 2018 February 22; 61(4): 1450–1473. doi:10.1021/acs.jmedchem.7b00738.

Design and Synthesis of Orally Bioavailable Piperazine Substituted 4(1*H*)-Quinolones with Potent Antimalarial Activity: Structure–Activity and Structure–Property Relationship Studies

Raghupathi Neelarapu[§], Jordany R. Maignan[§], Cynthia L. Lichorowic[†], Andrii Monastyrskiy[§], Tina S. Mutka[¶], Alexis N. LaCrue[¶], Lynn D. Blake[¶], Debora Casandra[¶], Sherwin Mashkouri[¶], Jeremy N. Burrows[€], Paul A. Willis[€], Dennis E. Kyle[¶], and Roman Manetsch^{*,†,⊥}

[§] Department of Chemistry, University of South Florida, CHE 205, 4202 East Fowler Avenue, Tampa, Florida 33620, United States [†] Department of Chemistry and Chemical Biology, Northeastern University, 102 Hurtig Hall, 360 Huntington Avenue, Boston, Massachusetts 02115, United States [¶] Department of Global Health, College of Public Health, University of South Florida, 3720 Spectrum Boulevard, Suite 304, Tampa, Florida 33612, United States [€] Medicines for Malaria Venture, 20, Route de Pre-Bois, P.O. Box 1826, 1215 Geneva, Switzerland [⊥] Department of Pharmaceutical Sciences, Northeastern University, 102 Hurtig Hall, 360 Huntington Avenue, Boston, Massachusetts 02115, United States

Abstract

Malaria deaths have been decreasing over the last 10–15 years, with global mortality rates having fallen by 47% since 2000. While the World Health Organization (WHO) recommends the use of artemisinin-based combination therapies (ACTs) to combat malaria, the emergence of artemisinin resistant strains underscores the need to develop new antimalarial drugs. Recent in vivo efficacy improvements of the historical antimalarial ICI 56,780 have been reported, however, with the poor solubility and rapid development of resistance, this compound requires further optimization. A series of piperazine-containing 4(1*H*)-quinolones with greatly enhanced solubility were developed utilizing structure–activity relationship (SAR) and structure–property relationship (SPR) studies. Furthermore, promising compounds were chosen for an in vivo scouting assay to narrow selection for testing in an in vivo Thompson test. Finally, two piperazine-containing 4(1*H*)-quinolones were

*Corresponding Author Phone: (617) 373-6316. r.manetsch@neu.edu.

Author Contributions

R.N. and J.R.M. contributed equally. The manuscript was written through contributions of all authors. All authors have given approval to the final version of the manuscript.

■ ASSOCIATED CONTENT

Supporting Information

The Supporting Information is available free of charge on the ACS Publications website at DOI: [10.1021/acs.jmed-chem.7b00738](https://doi.org/10.1021/acs.jmed-chem.7b00738).

Additional solubility and log *D* data for selected compounds (PDF)

Molecular formula strings (CSV)

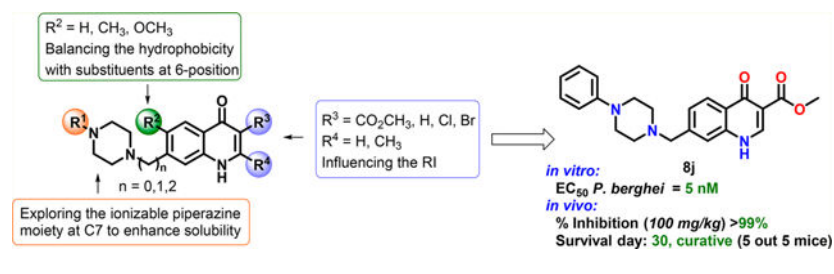
PDB coordinates of **8ae** bound to Q₀ and Q_i sites of bc₁ (PDB)

PDB coordinates of **8ac** bound to Q₀ and Q_i sites of bc₁ (PDB)

The authors declare no competing financial interest.

curative in the conventional Thompson test and also displayed *in vivo* activity against the liver stages of the parasite.

Graphical Abstract



INTRODUCTION

Malaria is one of the deadliest public health problems in the world, accounting for nearly half a million casualties annually.¹ A protozoan parasitic species, *Plasmodium* is responsible for transmitting the disease to humans through a mosquito vector. The various developmental stages of the parasite within the host make the design and development of curative antimalarial agents challenging. In addition, the widespread parasite resistance to almost all antimalarial drugs in use emphasizes the pressing need for new drugs with novel chemotypes that are safe and effective against multiple stages of highly resistant parasites.^{2,3} In the past few years, several research groups reported their optimization efforts in developing antimalarial 4(1*H*)-pyridone- and 4(1*H*)-quinolone-based agents, which are structurally related.^{4–13}

One of the major challenges in advancing these 4(1*H*)-quinolones into antimalarial drugs is the poor aqueous solubility of these scaffolds, which limits the oral bioavailability.¹⁴ Quinolone ester ICI 56,780^{15,16} (**1**, Figure 1) is one of these antimalarial 4(1*H*)-quinolones displaying very potent activity against blood, liver, and transmission stages of the parasite.^{7,16,17} Quinolone ester **1** even produced radical cures (eradicated dormant exoerythrocytic stages of the parasite) in *Plasmodium cynomolgi* infected rhesus monkeys.¹⁵ However, the development of **1** was halted as resistance emerged after only one passage in *Plasmodium berghei* (*Pb*) infected mice.¹⁶ Nevertheless, recent improvements in preclinical efficacy models and compound property assessment motivated the laboratories of Guy,^{4,5} Ward and O'Neill,¹⁸ and Manetsch and Kyle^{7,17} to reexamine studies on the antimalarial 4(1*H*)-quinolone ester from slightly different angles. Previous work completed by our laboratory resulted in a set of 46 compounds with *in vitro* activities against clinically relevant, multidrug resistant malarial strains W2 and TM90-C2B. Because cytochrome *bc*₁ is known to be the biological target of antimalarial 4(1*H*)-quinolones, cross resistance with atovaquone is a concern for any new antimalarial chemotype series. Therefore, all compounds were routinely tested against W2, a chloroquine and pyrimethamine resistant strain, and TM90-C2B, a chloroquine-, mefloquine-, pyrimethamine-, and atovaquone-resistant strain, to determine the resistance index (RI) as the calculated ratio of the effective concentrations of W2 and the atovaquone resistant TM90-C2B ($\text{RI} = \text{EC}_{50}(\text{TM90-C2B}) / \text{EC}_{50}(\text{W2})$).

Lead compound 3-bromo-6-butyl-2-methyl-7-(2-phenoxyethoxy)quinolin-4(1*H*)-one (**2**, Figure 1) addressed atovaquone cross resistance concerns over **1** by lowering the resistance index (RI) to 4.7 and exemplified a potent liver stage activity of 2.12 nM.¹⁷ It further exemplified the need to not only improve potency but also optimize aqueous solubility. Therefore, the main objective for the next optimization phase focused on the design and synthesis of a series of 6- and 7- substituted 4(1*H*)-quinolones with enhanced aqueous solubility without compromising blood and liver stage activity. Herein, we report detailed structure–activity relationship and structure–property relationship studies, leading to a set of analogues with improved aqueous solubility and oral bioavailability for which a subset has been further assessed for in vivo efficacy in targeting the blood and liver stages of the parasite.

■ RESULTS AND DISCUSSION

Design and Synthesis.

The rationale for the design of the next generation 4(1*H*)-quinolones was based on insights gained from structure–activity relationship (SAR) studies on 4(1*H*)-quinolone esters reported by us and others.^{7,15,18} The 4(1*H*)-quinolone core, the ester group in the 3-position, and the phenoxyethoxy substituent in the 7-position were identified to be key structural elements rendering this chemotype's potent antimalarial activity. Substituents in 2- and 6-positions were considered to be of secondary importance, with a negligible influence on the RI and/or the overall hydrophobicity of the 4(1*H*)-quinolone ester analogues. As a starting point for the next compound design, we decided to proceed with a 4(1*H*)-quinolone pharmacophore containing a 3-carboxylic acid ester and a 7-piperazinyl group (Figure 2). The piperazinyl moiety was selected for the following reasons: (1) an ionizable piperazine will enhance the aqueous solubility of 4(1*H*)-quinolones, (2) a straightforward, base-mediated or reductive *N*-alkylation of a piperazine provides an easy route to access highly functionalized 4(1*H*)-quinolone ester analogues, and (3) the commercial availability of various *N*-substituted piperazines allows the straightforward synthesis of a diversified set of piperazinyl-substituted 4(1*H*)-quinolones. In addition to the design of piperazine-substituted 4(1*H*)-quinolones, a general synthetic route was chosen by introducing the 4(1*H*)-quinolone core at the end of the synthesis sequence, reducing the number of cumbersome synthetic and purification steps which are complicated due to solubility limitations typical for 4(1*H*)-quinolone moieties.

Initially, a set of 7-piperazinyl-4(1*H*)-quinolone esters with differing alkyl chain lengths between the 4(1*H*)-quinolone core and the piperazinyl moiety were synthesized. The connectivity ranged from a direct attachment of the piperazine to the 4(1*H*)-quinolone's 7-position to a methylene or ethylene chain with each linker requiring a different synthetic path. The nucleophilic aromatic substitution was initially attempted for analogues with the piperazinyl moiety directly attached to the 4(1*H*)-quinolone core, using substituted nitrobenzenes **3** along with the required substituted piperazine. The substitution reaction was followed by a reduction of the nitro group and a thermal cyclization to yield 4(1*H*)-quinolones **8a**–**8b**. This synthetic approach, however, was only successful when the 4(1*H*)-quinolone core was sufficiently electron deficient (Scheme 1).¹⁹

For analogues in which the 4(1*H*)-quinolone core was not sufficiently electron deficient, a two-step sequence was required to obtain the necessary nitro intermediates **4**. First, the corresponding para-substituted aniline or benzylamine **9** was reacted with 2 equiv of 2-chloroethanol to give diols **10**. Diols **10** were chlorinated, and their products were reacted with substituted nitroanilines to yield piperazines **4**.²⁰ Subsequent reduction with tin(II) chloride gave piperazine-substituted anilines **5**, which were further reacted using standard Gould—Jacob sequence of reactions to afford final products **8c—8i** (Scheme 2).^{7,21}

Compounds with a methylene unit between the 4(1*H*)-quinolone core and the piperazine were synthesized starting with 3-amino-benzyl alcohol **11**, which was reacted with dimethyl 2-(methoxymethylene)malonate (**6**) to yield the corresponding enamines **12**. The alcohol was oxidized using Dess—Martin periodinane²² to the corresponding benzaldehyde **13**, which was subjected to direct reductive amination conditions to yield substituted piperazines **7j—7ab**.²³ These piperazinyl-substituted enamines were then cyclized using a microwave reactor to yield 4(1*H*)-quinolones **8j—8ab** (Scheme 3).

Compounds with an ethylene between the piperazine and 4(1*H*)-quinolone core were synthesized through a four-step reaction sequence that was initiated by an alkylation of 3-nitrophenethyl bromide with corresponding piperazines **14** to yield intermediates **4**.²⁴ The nitrophenyl intermediates **4** were reduced to anilines **5** using tin(II) chloride, which were subjected to the standard Gould—Jacob reaction sequence to give 4(1*H*)-quinolone esters **8ac—8ae** (Scheme 4).

A similar approach described for **8j—8ab** was used for the synthesis of 6-piperizino-4(1*H*)-quinolone esters, however, 4-amino-benzyl alcohol **11d** was used instead. The same four-step reaction sequence involving the enamine formation, a Dess—Martin oxidation, a direct reductive amination, followed by the cyclization was performed to yield 6-piperizino-4(1*H*)-quinolone esters **8af—8ai** (Scheme 5).

Finally, 7-piperazinyl-3-halo-4(1*H*)-quinolones **8aj—8at** were synthesized by alkylation of substituted piperazines **14**²⁴ with nitrophenethyl bromides to give nitro intermediates **4**, followed by a reduction using tin(II) chloride. The resulting piperazine aniline **5aj** was reacted with Meldrum's acid,²⁵ resulting in enamine **15aj**, which was further reacted in a thermal cyclization to give 7-((4-(4-fluorophenyl)piperazin-1-yl)-methyl)quinolin-4(1*H*)-one **8aj**. This was followed by the use of an appropriate *N*-halo succinimide to obtain the required 3-halo-7-piperazinyl-4(1*H*)-quinolones **8ak** and **8al**. The same approach was used for the preparation of 3-halo-2-methyl-4(1*H*)-quinolones, with the exception being that a Conrad—Limpach cyclization using ethyl acetoacetate was used following the formation of anilines **5aj—5as** instead of the abovementioned cyclization with Meldrum's acid to give compounds **8am**, **8ap**, and **8as**. These 4(1*H*)-quinolones were reacted with the appropriate *N*-halo succinimide to procure compounds **8an**, **8ao**, **8aq**, **8ar**, and **8at** (Scheme 6).

Antimalarial Activity and Cytotoxicity.

All compounds were tested against clinically relevant multidrug resistant malarial strains W2 (pyrimethamine- and chloroquine-resist-ant) and TM90-C2B (mefloquine-, chloroquine-, atovaquone-, and pyrimethamine-resistant) as previously reported.^{6,9,26}

Because of the emergence and rapid acquisition of cross-resistance,²⁷ each compound was also evaluated based on its RI (EC₅₀) for TM90-C2B and W2 strains (RI = EC₅₀ TM90-C2B/ EC₅₀ W2). Ideally, the RI of a compound should lie between 0.3 and 3.0 in order to avoid rapidly inducing resistance in the parasite. This range is based upon the natural resistance patterns observed for drugs like chloroquine and mefloquine.^{28,29} Selected compounds were also tested for in vitro liver stage activity using *Pb* sporozoites expressing luciferase, harvested from mosquito salivary glands and allowed to infect HEPG2 hepatoma cells in order to assess if the compounds possessed causal prophylactic activity.²⁶ Additionally, each compound was tested for cytotoxicity using mammalian J774 cell lines in a 96-well plate format.^{6,8,9,26}

Structure—Activity Relationships.

The poor aqueous solubility of our 4(1*H*)-quinolone esters⁷ motivated us to design and prepare a set of ionizable piperazinyl-substituted analogues with the primary aim being to significantly enhance the aqueous solubility without compromising antimalarial activity. The initial, small set of 6-hydrogen-7-piperazinyl-4(1*H*)-quinolones containing various linkages between the piperazinyl moiety and the 4(1*H*)-quinolone's benzenoid ring was prepared to identify the optimal spacer length (Table 1). In general, compounds with an ethylene between the 4(1*H*)-quinolone core and the piperazine showed the poorest blood stage activity of the group, with *N*-phenylpiperazinyl-4(1*H*)-quinolone **8ac** displaying EC₅₀ values of 26 nM for W2 and 1500 nM for TM90-C2B, while benzyl-substituted analogue **8ad** was less active, with EC₅₀ values of 120 nM for W2 and >2.0 μM for TM90-C2B. In contrast, *p*-methoxybenzylpiperazinyl-4(1*H*)-quinolone **8ae** was the most active for W2, with EC₅₀ values of 12 nM, but the least active for TM90-C2B, showing activities greater than 2.0 μM. Compounds with piperazines directly attached to the 4(1*H*)-quinolone core were more active than compounds containing an ethylene linker. *N*-Phenylpiperazinyl-4(1*H*)-quinolone **8a** was the most active member, with EC₅₀ values of 4.5 and 250 nM for W2 and TM90-C2B. In comparison, *N*-benzylpiperazinyl-4(1*H*)-quinolone **8b** was 4-fold less potent, with an EC₅₀ of 16 nM for W2, along with 860 nM for TM90-C2B, respectively.

Compounds with a methylene spacer between the piperazine and 4(1*H*)-quinolone were the most active analogues of this first set of 4(1*H*)-quinolones. Compounds **8j**, **8k**, and **8l** were similarly potent, with low single-digit nM inhibitory concentrations for W2. However, the same compounds displayed reduced activity against TM90-C2B, producing RI values ranging from 100 to 390 for analogues **8j**, **8k**, and **8l**.

A selection of this first set of piperazinyl-4(1*H*)-quinolones (Table 1) was tested for in vitro liver stage activity using *P. berghei* sporozoites expressing luciferase as previously described.¹⁹ The best results were obtained with analogues whose piperazinyl moiety was attached to the quinolone's benzenoid ring via a methylene unit. *N*-Phenylpiperazinyl-4(1*H*)-quinolone **8j** was the most potent compound, with an EC₅₀ of 4.7 nM for *Pb*, while its benzyl analogue **8k** or its 4-methoxybenzyl analogue **8l** were approximately 10-fold less potent, with EC₅₀ values of 44–83 nM. All the other analogues **8a**, **8b**, and **8ad**, with the piperazinyl group substituted to the 4(1*H*)-quinolone's core directly or via an ethylene, were even less potent.

Follow-up SAR studies focused solely on piperazines directly attached to the 4(1*H*)-quinolone core or via one methylene unit, as the antimalarial activity of the *N*-phenyl or *N*-benzylpiperazinyl-4(1*H*)-quinolones appeared to be more potent than ethylene-connected analogues. This, in conjunction with previous observations that substituents in the 6-position alter antimalarial activity predominantly against TM90-C2B, led to the design of a small series of 6-methyl- or 6-methoxy-4(1*H*)-quinolone esters retaining in 7-position an *N*-phenyl-, *N*-benzyl-, or 4-methoxybenzyl-substituted piperazine. Piperazinyl-4(1*H*)-quinolones **8q**, **8r**, **8w**, and **8x** with a methylene spacer were approximately 10-fold more potent against W2 than their structurally related analogues **8c**, **8g**, **8d**, and **8h**, whose 4(1*H*)-quinolone core is directly substituted with the piperazine moiety (Table 2). In contrast, the 7-piperazinyl-4(1*H*)-quinolones **8c**, **8g**, **8d**, and **8h** possessed approximately 10-fold more favorable RI values in comparison to the analogues **8q**, **8r**, **8w**, and **8x** with a methylene spacer. Furthermore, for both the *N*-phenylpiperazinyl- or *N*-benzylpiperazinyl-substituted 4(1*H*)-quinolones, the 6-methyl substituent appeared to improve antimalarial activity, whereas the opposite effect was true for the 6-methoxy-substituted analogues. 6-Methyl-7-phenylpiperazinyl-4(1*H*)-quinolone **8q** was the most potent of the group against W2, with an EC₅₀ value of 0.44 nM and 0.15 μM against TM90-C2B. When the *N*-phenylpiperazinyl moiety of **8q** was exchanged by an *N*-benzylpiperazine, activity for analogue **8r** fell slightly for W2, with an EC₅₀ value of 1.5 nM, and more noticeable for TM90-C2B, with an EC₅₀ value of 0.89 μM. Additional potency losses were observed with compound **8s** when the *N*-phenyl-piperazinyl moiety of **8q** was exchanged by a 4-methoxybenzylpiperazine. Exchange of the 6-methyl group of 4(1*H*)-quinolone **8q** by a 6-methoxy substituent in compound **8w** dropped the potency approximately 3-fold for both W2 and TM90-C2B.

The compounds displaying the best W2 activity were also tested for in vitro liver stage activity. Analogues **8q**, **8r**, and **8x** were the most potent ones, with EC₅₀ values of 6.9, 9.5, and 9.3 nM, respectively.

Next, a subseries was designed to determine how steric and/ or electronic effects of the *N*-phenylpiperazinyl moiety influences the antimalarial activity (Table 3). The para position of the *N*-phenylpiperazinyl group was substituted with a fluorine, a trifluoromethyl, or a methoxy group, while simultaneously the quinolone's 6-position was probed with a hydrogen, a methyl, or a methoxy group. The previously observed trend was confirmed as analogues **8n** and **8z** with the methylene spacer between the piperazine and the 4(1*H*)-quinolone's core were more potent against W2 than compounds **8e** and **8f** with a directly attached piperazine. Furthermore, independently of the 4-substituent of the *N*-phenylpiperazine moiety, activity data against W2 indicated that the 6-methyl-substituted compounds are slightly more potent than the 6-methoxy analogues, which in comparison to the 6-hydrogen, analogues are equipotent or less potent. Finally, substituting the 4-position of the *N*-phenylpiperazinyl moiety with the electron donating methoxy group generally produced compounds that were slightly less potent than analogues with an electron withdrawing group.

The fluorinated methylene-spaced compounds **8o**, **8u**, and **8aa** showed significant antimalarial activity against all strains. Analogues **8o** and **8aa** were equipotent against W2, with EC₅₀ values of 1.8 nM, whereas compound **8u** displayed subnanomolar potency. The

trifluoromethylphenylpiperazinyl-4(1*H*)-quinolones **8p**, **8v**, and **8ab** were more potent than the fluorophenyl-substituted analogues **8o**, **8u**, and **8aa**, suggesting a strong electron-withdrawing effect on the phenyl group to be beneficial. Compound **8v** was the most potent analogue of the entire series, with an EC₅₀ value of 66 pM against W2 and an EC₅₀ value of 100 nM against TM90-C2B.

Compounds in this series also displayed very potent liver stage activity. Of the compounds chosen for testing, *p*-methoxyphenyl-substituted analogue **8n** was the most potent one, with an EC₅₀ value of 120 pM. Fluorophenyl- or methoxyphenyl-substituted 4(1*H*)-quinolones **8o**, **8u**, and **8t** displayed single-digit nanomolar activity.

We next considered whether a positional change of the piperazine moiety from the 7-position to the 6-position would retain or improve the antimalarial activity and possibly improve the RI value. A set of analogues **8af–8ai** was prepared by switching the piperazine moiety from the 7-position to 6-position of the 4(1*H*)-quinolone's benzenoid ring and evaluated for their activity (Table 4). These piperazinyl analogues **8af–8ai** lost significantly in activity in comparison to their 7-substituted counterparts, with EC₅₀ values ranging from 45 to 160 nM against W2. Against TM90-C2B, these compounds were considered to be nearly inactive. Surprisingly, compounds **8af** and **8ai** showed moderate activity against *Pb*, with EC₅₀ values of 85–90 nM. However, the lack of potency against W2, TM90-C2B, and *Pb* further substantiated our initial hypothesis that for antimalarial activity the piperazine moiety must be attached at the 4(1*H*)-quinolone's 7-position.

Previously, 3-halo-substitutions were shown to significantly improve the RI values of phenoxyethoxy-4(1*H*)-quinolones and several piperazinyl-substituted analogues were prepared for this purpose (Table 5). With the exception of compounds **8ar** and **8at**, all other 3-halo-4(1*H*)-quinolones **8ak–8aq** possessed acceptable RI values smaller than 3. Like the 7-phenoxyethoxy-4(1*H*)-quinolone analogues, the addition of a 2-methyl substituent gave rise to more potent compounds, with the 3-chloro-substituted 4(1*H*)-quinolone **8ao** having EC₅₀ values of 39 and 52 nM for W2 and TM90-C2B, respectively, producing an RI of 1.4. The 3-bromo **8an** was even more potent, with EC₅₀s of 25 nM for both W2 and TM90-C2B with an RI of 1.0. However, there was a 30-fold difference in *Pb* activities between the 2-unsubstituted and 2-methyl substituted with **8ak** displaying subnanomolar activity while **8an** had an EC₅₀ of 26 nM. Finally, trifluoromethylphenyl-substituted piperazine variants were synthesized to give 3-chloro **8ar** and 3-bromo **8aq**. Both compounds showed a significant decrease in activity compared to their fluoro-substituted piperazine counterparts **8ao** and **8an**.

Proposed Structural Basis of Antimalarial Activity and Molecular Docking.

Plasmodium cytochrome *bc*₁ complex is an effective and validated target in the treatment and prophylaxis of malaria. Many different classes of compounds, including 4(1*H*)-pyridone^{30,31} and related 4(1*H*)-quinolone^{6–9,26,32} derivatives developed by our and other groups, have been identified as potent inhibitors of *bc*₁ mitochondrial electron transport chain component. Nevertheless, only one *bc*₁ inhibitor, atovaquone, has been approved for clinical use as a key component of the fixed-dose antimalarial combination therapy, marketed as Malarone, since

2000. Unfortunately, several point mutations at Q_o atovaquone binding site of the bc₁ complex lead to clinically relevant atovaquone-resistant strains of *P. falciparum* (one of these atovaquone-resistant strains is TM90-C2B that we routinely used for our SAR campaign in this study). Up until 2015, majority of the investigated bc₁ inhibitors were believed to target Q_o site of the protein. Disclosing the structure of bovine heart cytochrome bc₁ complex with 4(1*H*)-pyridones GW844520 and GSK932121 revealed clear evidence of these compounds unexpectedly binding to the reductive Q_i site.³³ These findings explain the ability of 4(1*H*)-pyridones (and related 4(1*H*)-quinolones) to overcome parasite Q_o-based atovaquone resistance. Additionally, TM90-C2B cross resistance and RI data itself could be used as an indicator of preferential Q_o/Q_i site binding. The discovery of preferred binding of the 4(1*H*)-pyridones class of inhibitors to Q_i site as well as RI data provided critical structural and biological information that we applied to structure-guided drug design efforts of herein disclosed piperazine substituted 4(1*H*)-quinolone inhibitors.

To understand the structural basis of observed antimalarial activity, we performed molecular docking studies using coordinates of the bc₁GW844520 (Q_i site, PDB 4D6T³³) and bc₁ atovaquone (Q_o site, PDB 4PD4³⁴). Receptor grids were generated and validated by docking GW844520 and atovaquone into Q_i and Q_o sites accordingly (Figure 3E,F). The docked models for both inhibitors were in good agreement with the reported crystal structures coordinates. We then selected two representative piperazine substituted 4(1*H*)-quinolone inhibitors with high RI (**8ae**, RI > 495, Table 1) suggesting preferential Q_o site inhibition and low (**8ao**, RI = 1.35, pan Q_i/ Q_o or selective Q_i inhibition, Table 5) RI values. The binding poses of both **8ao** and **8ae** (Figure 3A–D) as well as historic atovaquone, GW844520 (Figure 3E,F) and quinolones ELQ-300²⁶ and **1** (data not shown) in the Q_o and Q_i sites of bc₁ were subsequently analyzed.

On the basis of the phenotypic readout (EC₅₀ W₂ = 12 nM, TM90-C2B > 5740 nM) and RI data (RI > 495), we hypothesize that **8ae** is a preferential Q_o site binder. Indeed, **8ae** docked well into Q_o binding pocket similarly to atovaquone (docking scores: atovaquone, -9.86; **8ae**, -8.77) with 4(1*H*)-quinolone core occupying space in between Val146 and Leu275 (Figure 3A) and C7 piperazine tale extending outside of the pocket. On the other hand, the orientation of compound **8ae** docked into the Q_i site of the protein (Figure 3B) was opposed to the orientation of GW844520 (Figure 3F) in the original crystal structure, suggesting diminished mode of action and confirming the loss of activity against TM90-C2B. The 4(1*H*)-pyridone core of GW844520 sits deep in the Q_i site, making favorable π - π interactions with Phe220 and hydrogen bond interactions with Ser35 of loop A (Figure 3F, also see the original report³³ for more details). Instead, docking of **8ae** into Q_i site revealed positioning of the quinolone core in the hydrophobic pocket away from the heme (Figure 3B). Switching the 3-ester group of **8ae** to halogen led to compound **8ao**. Interestingly, compound **8ao** (EC₅₀ W₂ = 39 nM, TM90-C2B = 52 nM) docked well in the Q_i site of bc₁ with quinolone core sitting deep in the binding pocket making similar to GW844520 interactions and piperazine tale extending out of the channel (Figure 3D,F). This mode of action can explain the ability of **8ao** bind to Q_i site, hence the activity against Q_o-based atovaquone resistance TM90-C2B strain. Compounds **8ao** and GW844520 also docked well in Q_o site (WT) of the bc₁ (Figure 3C,E).

Molecular docking studies performed in combination with biological data suggest that 3-halo-substituted 4(*1H*)-quinolones (Table 5) are Q_i site inhibitors showing significantly improved RI values and activity against TM90-C2B strain. At the same time, it is very likely that vast majority of piperazine-containing 4(*1H*)-quinolone esters (Tables 1–4) are selective inhibitors of Q_o site of cytochrome *bc*₁ complex.

Cytotoxicity.

All compounds were tested in vitro for cytotoxicity to J774 mammalian cells using a protocol, which was used in all of our previous published studies with various 4(*1H*)-quinolone derivatives as a guide and to produce selectivity index data to assist with the SAR optimization of the compounds (Tables 1–5).^{6–9} Of all the compounds tested, only a few compounds displayed signs of cytotoxicity at concentrations lower than 20 μ M. Onset of cytotoxicity was recorded for compounds **8j**, **8l**, **8n**, and **8o** with EC₅₀ values of 3.94, 5.13, 4.73, and 2.00 μ M, respectively. Nevertheless, these analogues and the majority of the piperazinyl-4(*1H*)-quinolones can be considered selective chemotypes as they display single-digit nanomolar or subnanomolar activity against W2.

Structure–Property Relationships.

Calculated properties such as molecular weight, polar surface area, and number of H-bond donors and acceptors were within the recommended ranges typically needed for good oral bioavailability, suggesting that the piperazinyl-4(*1H*)-quinolone design provided excellent spatial leeway for structural modifications to occupy physicochemical space unique for orally bioavailable compounds. Furthermore, to profile the properties of the piperazinyl-4(*1H*)-quinolones, and to identify potential limitations, aqueous solubility and lipophilicity log D were experimentally determined via LC/MS-based assays as described by the Manetsch laboratory previously^{6,8,35,36} (see Supporting Information, Tables S1–S5). Encouragingly, the piperazinyl-4(*1H*)-quinolones were much more soluble (average solubility 50 μ M) than the previously described phenoxyethoxy-4(*1H*)-quinolones (average solubility 5 μ M) or 3-phenyl-substituted analogues (average solubility 5 μ M).¹⁷ As expected, the solubility of all compounds was affected by pH, with better solubility under more acidic conditions.

The piperazine analogues such as **8ac**, **8ad**, **8ae**, **8j**, or **8k** with an ethylene or a methylene spacer between the piperazine and the quinolone moiety displayed good aqueous solubility of 80 μ M or more at both pH 2.0 and pH 6.5. Only compounds such as **8a** with an *N*-phenylpiperazinyl group directly attached to the 4(*1H*)-quinolone core had reduced solubility below 20 μ M at pH 2.0 and pH 6.5. Replacement of the *N*-phenylpiperazinyl group in 4(*1H*)-quinolone **8a** by an *N*-benzylpiperazinyl group in compound **8b** reestablished the solubility in the ranges of 60–80 μ M. The aqueous solubility was also in good correlation with calculated p*K*_a values of the piperazine nitrogens. Specifically, compounds with an ethylene spacer (**8ac**, **8ad**, **8ae**) showed a p*K*_a of approximately 6–7, compounds with a methylene spacer (**8j** and similar) between the piperazine and the quinolone showed a p*K*_a of approximately 5.0, while compounds with the piperazinyl group directly attached to the 4(*1H*)-quinolone core (**8c** and similar) displayed a p*K*_a of 3.8 or less.

Additional solubility dependencies were observed with the various 4(*H*)-quinolone compound series. Analogues in which the piperazinyl moiety was moved from the 4(*H*)-quinolone's 7-position to the 6-position were slightly less soluble at pH 6.5 (see Supporting Information, Tables S1–S5). Furthermore, 3-halo-4(*H*)-quinolones had marked solubility differences between pH 2.0 and 6.5, displaying significantly higher solubility at low pH. The addition of a 2-methyl group to the 4(*H*)-quinolone further lowered solubility, with 3-bromo-2-methyl-4(*H*)-quinolone **8an** being more than 20 times less soluble at pH 6.5 compared to its 2-hydrogen counterpart **8ak** (see Supporting Information, Tables S1–S5). This observation is in agreement with calculated pK_a values of 4(*H*)-quinolone's nitrogens of 4.2 for **8ak** and 2.8 for **8an**, respectively.

In Vivo Efficacy Evaluation of Selected Compounds in an Efficacy Scouting Assay Against Blood Stages of the Parasite.

Of all prepared and tested 4(*H*)-quinolones, 29 with potent in vitro activity against both *P. falciparum* strains were chosen to undergo a scouting assay in *Pb*-infected mice. The screening involved a single oral 50 mg/kg dose 1 day post infection (PI) and an assessment of parasitemia on days 3 PI and 6 PI (Table 6). The threshold for active compounds was inhibition greater than 50% on days 3 and 6 PI. Compounds **8h**, **8m**, **8t**, and **8ad** all showed no inhibition on day 6 PI, whereas 4(*H*)-quinolones **8b** and **8l** were just under the 50% threshold of activity with both showing inhibition in the low 40% ranges. Compounds **8a**, **8c**, **8d**, **8k**, **8n**, **8q**, **8r**, **8s**, **8x**, **8y**, and **8ag** displayed little to moderate protection on day 6 PI, delaying the parasite's growth. Lastly, compounds **8o**, **8p**, **8u**, **8v**, **8w**, **8z**, **8aa**, **8ab**, **8ak**, **8al**, **8an**, and **8ao** all showed excellent activities in these scout assays with trifluoromethylpiperazinyl-4(*H*)-quinolone esters **8p**, **8v**, and **8ab** and 3-bromo-4(*H*)-quinolone **8an** having completely inhibited parasite growth even on day 6 PI. These results clearly underscore the significant advantages the piperazinyl-substituted 4(*H*)-quinolones have over the previously reported 4(*H*)-quinolone esters.¹⁷

In Vivo Efficacy Evaluation of Frontrunner Compounds Against Blood Stages of the Parasite.

Using a modified Thompson test model, frontrunner compounds **8o**, **8p**, **8u**, **8v**, **8ab**, **8ak**, **8an**, and **8ao** were evaluated in vivo. These frontrunner compounds were selected for further in vivo efficacy testing as they displayed full inhibition on day 3 PI and over 85% inhibition on day 6 PI in the scouting assay. Mice were infected with 1×10^6 *P. berghei*-*GFP* parasites, and compounds were dosed orally on days 3, 4, and 5 PI with a dose of 10 mg/kg of compound suspended or dissolved in HEC/Tween or PEG 400. Parasitemia was observed by flow cytometry on days 3, 6, 9, 13, 21, and 30 PI. Compounds with animal survival up to day 30 PI, and parasitemia levels of less than 1% on day 30 PI were considered to be cures. Lastly, animals with more than 40% parasitemia levels were euthanized. For all experiments, atovaquone was used as the positive control.^{9,26}

4(*H*)-Quinolone esters **8ak** and **8ao** and 3-bromo-4(*H*)-quinolone **8an** all had the same day of death as the untreated control animals. While 4(*H*)-quinolone esters **8ak** and **8ao** displayed a low inhibition on day 6 PI, analogue **8an** was much more potent with a 90.9% inhibition on day 6 PI. These results suggest that compound **8an** is possibly rapidly cleared

after day 6 PI. Compounds **8o**, **8p**, and **8u** had greater 100% inhibition on day 6 PI, nevertheless, all animals succumbed to the parasite by day 21 PI, possibly indicating a longer half-life than 3-bromo-4(1*H*)-quinolone **8an**. The remaining compounds, **8v** and **8ab**, both produced cures in more than half of the animals, curing 3 of the 5 animals (Table 7).

In Vivo Efficacy Evaluation of Frontrunner Compounds Against Liver Stages of the Parasite.

The potent in vitro activity of piperazinyl-substituted 4(1*H*)-quinolones against liver stages of the parasite prompted a study to determine in vivo these compounds in *P. berghei* sporozoite infected mice. Five animals per group were dosed as previously reported only 1 h after infection with piperazinyl-substituted 4(1*H*)-quinolones **8j** and **8l**. At 44 h PI, day 6 PI, day 9 PI, and day 13 PI, compound efficacy was determined by bioluminescence imaging via injection of D-luciferin. Both compounds were administered orally or subcutaneously at increasing doses of 25, 50, and 100 mg/kg in PEG 400. of the two piperazinyl-substituted 4(1*H*)-quinolones, **8j** performed significantly better than **8l** (Figure 4). With the exception of an infection on days 6, 9, 13 PI of a single mouse, which was orally dosed with 50 mg/kg, no luminescence was observed for **8j** at any other doses and time points. In comparison, compound **8l** displayed full protection at all time points only at an oral dose of 100 mg/kg. Progression of parasitemia was monitored up to 30 days after infection (Table 8). Differences between the two test 4(1*H*)-quinolones were more obvious following survival cures (Figure 5) as **8j** cured two or more out of five animals. In contrast, one of five animals was cured only at a high dose of 100 mg/kg of **8l**. These results with **8j** and **8l** underscore that piperazinyl-substituted 4(1*H*)-quinolones have potential as single-dose prophylactic and curative agents.

CONCLUSIONS

In 1970, Ryley and Peters demonstrated that 4(1*H*)-quinolone ester **1** possesses causal prophylactic activity (kill growing exoerythrocytic stage parasites) and erythrocytic stage inhibition in avian malaria models but not against malaria parasites in mammals.¹⁶ Twenty years after Ryley and Peters' work was published, Puri and Dutta showed that **1** produced radical cures (eradicate dormant EE parasites) in *Plasmodium cynomolgi* infected rhesus monkeys.¹⁵ Despite the promise of this 4(1*H*)-quinolone ester, the development of this compound was challenged due to major physicochemical property limitations requiring parenteral dosing. Furthermore, the propensity for rapid acquisition of resistance following exposure to **1** hampered its further development.¹⁶

Recent optimization studies led to the synthesis and identification of 4(1*H*)-quinolones that displayed potent in vitro antimalarial activity against the liver and the blood stages of the parasite. In particular, 4(1*H*)-quinolones, whose ester group in 3-position was replaced by a halogen, appeared to significantly reduce cross resistance with atovaquone and the best compound of this subseries displayed significantly better in vivo efficacy than compound **1**. Nevertheless, as a follow-up, 46 additional piperazinyl-substituted 4(1*H*)-quinolone esters or 3-halo-4(1*H*)-quinolones were synthesized with the objective to increase the aqueous solubility while maintaining or improving the antimalarial activity against the blood and

liver stages of the parasite. As a secondary objective, compound optimization also focused on equipotency against W2, a chloroquine- and pyrimethamine-resistant strain, and against TM90-C2B, a chloroquine-, mefloquine-, pyrimethamine-, and atovaquone-resistant strain.

Structure—activity relationship studies concentrated primarily on analogues in which (a) a piperazine containing moiety was installed either in 6- or 7-position, (b) the 2-position was probed with a methyl or a hydrogen, and (c) the 3-position was varied with a methyl ester or a halogen. The best antimalarial activity was observed when the piperazine-containing moiety was installed in 7-position, while the 3-position was equipped with a methyl ester group. Of the 7-substituted 4(1*H*)-quinolones, analogues with an ethylene spacer between the piperazine and the 4(1*H*)-quinolone core were approximately 10-fold less potent than counterparts in which the piperazine was directly attached to the 4(1*H*)-quinolone moiety or via a methylene spacer. Furthermore, *N*-phenylpiperazinyl-4(1*H*)-quinolones were slightly better than *N*-benzylpiperazinyl-substituted counterparts. Antimalarial activity was lost if the piperazine-containing substituent was moved from the 7-position to the 6-position or when the methyl ester in the 3-position was replaced by a halide. Nevertheless, 3-halo-substituted 4(1*H*)-quinolones possessed significantly improved resistance indices as they displayed equipotent activity against W2 and TM90-C2B. Specifically, analogues **8p**, **8q**, **8t**, **8u**, **8v**, and **8w** were among the most potent 4(1*H*)-quinolone esters, displaying low single-digit nanomolar or subnanomolar EC₅₀ values against W2, double- or triple-digit nanomolar activity against TM90-C2B, and single- or double-digit nanomolar activity against the *Pb* liver stages. In contrast, despite 3-bromo-4(1*H*)-quinolone **8an** and other 3-halo-4(1*H*)-quinolones being slightly less potent against W2, they maintained the potency against TM90-C2B and consequently produced excellent resistance indices smaller than 3. Follow-up docking studies with cytochrome bc₁ the molecular target of antimalarial 4(1*H*)-quinolones or 4(1*H*)-pyridones, revealed that 3-ester-substituted 4(1*H*)-quinolones presumably prefer binding to the Q_o site of the cytochrome, while 3-halosubstituted 4(1*H*)-quinolones bind to the Q_i site. This data is in full agreement with the phenotypic data as Y268S mutations in Q_o site is directly associated with resistance to atovaquone.

The preferred candidates for in vivo efficacy studies were selected based on log *D* and aqueous solubility data at two different pHs. The majority of the piperazinyl-substituted 4(1*H*)-quinolones displayed good aqueous solubility of 40 μM or higher. The 29 best compounds were tested for in vivo efficacy, first in a scouting assay, and the eight most promising 4(1*H*)-quinolones were subsequently assessed for in vivo efficacy in the conventional Thompson test at a lower oral dose. *N*-Trifluoromethylpiperazinyl-substituted analogues **8v** and **8ab** were the most efficacious 4(1*H*)-quinolone esters, reducing parasitemia on day 6 PI completely and curing three out of five animals, whereas **8o**, **8p**, and **8u** were slightly less potent with a survival period of mice to 21 days PI. 3-Bromo-4(1*H*)-quinolone **8an** displayed a 91% inhibition of parasitemia on day 6 PI, nevertheless, mice were sacrificed on day 13 PI due to increased level of parasitemia. Finally, compounds **8j** and **8l** displaying good activity in vitro against liver stages were also tested for in vivo efficacy against liver stages. The more in vitro potent 4(1*H*)-quinolone **8j** was highly efficacious in vivo, generating cures at oral doses of 25 mg/kg or higher. This in conjunction with the promising in vivo activity against the blood stages renders the piperazinyl-

substituted 4(1*H*)-quinolone compound series potential for further optimization as an orally bioavailable antimalarial compound series.

■ EXPERIMENTAL SECTION

General.

All reagents and solvents were obtained from Aldrich Chemical Co. and used without further purification. NMR spectra were recorded at ambient temperature on a 400 or 500 MHz Varian NMR spectrometer in the solvent indicated. All ¹H NMR experiments are reported in δ units, parts per million (ppm) downfield of TMS, and were measured relative to the signals of chloroform (7.26 ppm) and dimethyl sulfoxide (39.5 ppm) with ¹H decoupled observation. Data for ¹H NMR are reported as follows: chemical shift (δ ppm), multiplicity (s = singlet, d = doublet, t = triplet, q = quartet, p = pentet, m = multiplet), integration and coupling constant (Hz), whereas ¹³C NMR analyses were reported in terms of chemical shift. NMR data was analyzed by using MestReNova Software version 6.0.2–5475. The purity of the final compounds was determined to be 95% by highperformance liquid chromatography (HPLC) using an Agilent 1100 LC/MSD-VL with electrospray ionization. Low-resolution mass spectra were performed on an Agilent 1100 LC/MSD-VL with electrospray ionization. High-resolution mass spectra (HRMS) were acquired on an Agilent LC/MSD TOF system G3250AA. Analytical thin layer chromatography (TLC) was performed on silica gel 60 F254 precoated plates (0.25 mm) from EMD Chemical Inc., and components were visualized by ultraviolet light (254 nm). EMD silica gel 230–400 (particle size 40–63 μ m) mesh was used for all flash column chromatography. Microwave heating was performed in a single-mode Anton Paar Monowave 300, and all microwave-irradiated reactions were conducted in heavy-walled glass vials sealed with Teflon septa.

In Vitro Antimalarial Activity against Blood Stages of *P. falciparum* (W2 and TM90-C2B).

In vitro antimalarial activity against blood stage parasites W2 and TM90-C2B was determined as previously reported.^{6–9,17,37} *P. falciparum* clone W2 (Indochina) and TM90C2B (Thailand) were grown in continuous culture using RPMI 1640 media containing 10% heat-inactivated type A+ human plasma, sodium bicarbonate (2.4 g/L), HEPES (5.94g/L), and 4% washed human type A+ erythrocytes. Cultures were gassed with a 90% N₂, 5% O₂, and 5% CO₂ mixture followed by incubation at 37 °C. Test compounds in DMSO at 10.0 mM concentration were diluted at least 1:400 and then serially diluted in duplicate over 11 concentrations. *P. falciparum* cultures with >70% ring stage parasites were diluted to 0.5–0.7% parasitemia and 1.5% hematocrit in RPMI 1640 media. In 96-well plates, a volume of 90 μ L/well of parasitized erythrocytes was added on top of 10 μ L/well of the test compound. A separate plate containing chloroquine, dihydroartemisinin, and atovaquone was added to each set of assay plates as control drugs. A Beckman Coulter Biomek 3000 was used to dispense test compounds, control drugs, and parasitized erythrocytes into the microtiter plates. Positive and negative controls were included in each plate. Positive controls consisted of drug-free parasitized erythrocytes, and negative controls consisted of parasitized erythrocytes dosed with a high concentration of chloroquine or dihydroartemisinin that ensured 100% parasite death. Assay plates were placed into a plastic gassing chamber and equilibrated with 90% N₂, 5% O₂, and 5% CO₂ mixture then incubated

at 37 °C for 48 h, then ³H-hypoxanthine was added and plates incubated another 24 h. After 72 h of incubation, the assay plates were frozen at –80 °C until later processing for parasite growth determinations. Assay plates were removed from –80 °C and allowed to thaw at room temperature. Using a plate harvester, the contents of the plate were collected on filtermats and then CPMs counted in a Topcount liquid scintillation counter. Data analysis was performed using a custom database manager (Dataspects, Inc.). Nonlinear regression analysis was used to calculate EC₅₀.

In Vitro J774 Cytotoxicity Assay.

In vitro J774 cytotoxicity was determined as previously reported.^{6–9,17,37} Mouse macrophage cell line J774 was cultured in RPMI-1640 media with phenol-red containing L-glutamine then supplemented with 10% fetal bovine serum, penicillin (50 Units/mL), and streptomycin (50 µg/mL). For seeding into 96-well plates, the J774 cells were diluted to 5 × 10⁵ cells/mL. Cells were dispensed into 96-well plates at a volume of 100 µL/well, giving a final concentration of 5 × 10⁴ cells/well. Plates were incubated for 24 h at 37 °C and 5% CO₂ to allow the attachment of J774 to the bottom of the plate wells. Test compounds were prepared by diluting to 10 µg/mL or 20 µM, followed by 1:2 serial dilutions over 11 concentrations. After 24 h, the media was removed from the wells and serially diluted test compounds were added to each well. Positive and negative control wells were included on each assay plate. Plates containing cells and test compounds were then incubated for 72 h at 37 °C and 5% CO₂. After the incubation period, cell proliferation was assessed using CellTiter 96 Aqueous One Solution Cell Proliferation Assay reagent (Promega). To each well 20 µL of reagent were added followed by incubation for 4 h at 37 °C and 5% CO₂. A Spectramax M2e (Molecular Devices) plate reader was used to read absorbance at 490 nm. IC₅₀ values were determined using a custom database manager (Dataspects, Inc.). Nonlinear regression analysis was used to calculate IC₅₀s.

In Vitro Antimalarial Activity against *P. berghei* Liver Stages.

In vitro antimalarial activity against liver stage parasites was determined as previously reported.^{2,37} HepG2 cells (75000 per well) were seeded into collagen-coated, black 96-well plates with optically clear bottoms (Beckton Dickson, Franklin Lakes, NJ) for viewing on the IVIS spectrum system (Caliper Life Sciences, Hanover, MD) and white 96-well plates for analysis with the TopCount microplate luminometer (Packard, Meriden, CT). Cells were maintained at 37 °C in 5% CO₂ in Dulbecco's Modified Eagle Medium (DMEM) supplemented with 10% fetal bovine serum, 1.0% penicillin-streptomycin (Sigma), and 1.0% L-glutamine. Mosquito salivary glands were dissected as described above, and 5000 sporozoites were added per well. Plates were incubated at 37 °C for 3 h and then washed three times with PBS. Serial dilutions of test compounds were prepared as previously described, added to parasite-infected HepG2 cells in triplicate, and incubated at 37 °C for 44 h. Following the incubation, cells were washed once with PBS and then lysed with 10 µL of cell culture lysis reagent (Promega Luciferase Assay system kit; Promega, Madison, WI). Immediately after cell lysis, 100 µL of luciferase assay substrate was added and then the parasite lysates were analyzed.

In Vivo Blood Stage Antimalarial Activity (Thompson Test, *P. berghei*).

In vivo antimalarial activity against blood stage parasites was determined as previously reported.^{9,17,37} We used a “modified Thompson model”, in which infections were established by an intraperitoneal inoculation of 2×10^6 *P. berghei* (GFP)-infected red blood cells. By day 3, the first day of drug treatment, parasitemia typically reached 1% (i.e., 1% of the RBC will be parasitized). Test compounds were administered per os once-daily (qd) for 3 days. Atovaquone was included as a standard drug for comparison. Infected mice, compound treated on days 3–5 post parasite inoculum, were followed for 30 days total. Parasitemia was determined from blood collected from the tail vein on days 3, 6, 9, 12, 15, 18, 21, 24, 27, and 30; parasitemia was quantified by microscopic examination of Giemsa-stained blood smears. We also monitored whether (and when) recrudescence occurred. End points for the efficacy analysis were the ED₅₀ and ED₉₀ (dose of drug that suppressed 50% and 90% of parasitemia on day 6, respectively), the no recrudescence dose (ie., no parasitemia following initial clearance of parasitemia), and percent cure at 30 days. This study was conducted in compliance with the Guide for the Care and Use of Laboratory Animals of the National Research Council for the National Academies. The protocol was approved by the University of South Florida Institutional Animal Care and Use Committee.

In Vivo Antimalarial Activity against Liver Stages (*P. berghei*).

In vivo antimalarial activity against liver stage parasites was determined as previously reported.^{2,37} There were five mice per treatment group. Experimental groups were treated with 50 or 25 mg/kg sc or administered at 100 or 50 mg/kg po. Mice were treated once at 2 h after infection. Untreated, noninfected, and infected mice (infection controls) as well as compound-treated and atovaquone-treated mice (drug controls) were also included. In vivo imaging was performed 44 h post infection to assess liver stage development and on days 6, 9, and 13 PE to monitor blood stage development using methods described previously.³⁸ Briefly, the luciferase activities of whole animals were assessed using IVIS Spectrum (Caliper Life Sciences, Hanover, MD). Prior to analysis, the abdomens of all mice were shaved. Animals ($n = 5$) were injected ip with D-luciferin (100 mg/kg), anesthetized with isoflurane, and imaged 5 min postinjection. While animals were continuously exposed to isoflurane, images were acquired with a 23 cm field of view (FOV), medium binning factor, and an exposure time of 20 to 120 s. Images were analyzed using the Living Image 3.0 software (Caliper Life Sciences, Hanover, MD). This study was conducted in compliance with the Guide for the Care and Use of Laboratory Animals of the National Research Council for the National Academies. The protocol was approved by the University of South Florida Institutional Animal Care and Use Committee.

Molecular Modeling.

The original co-crystal structures of bc₁ atovaquone (Q_o site, PDB 4PD4³⁴) and bc₁GW844520 (Q_i site, PDB 4D6T³³) were refined using the Protein Preparation Wizard³⁹ implemented in the Maestro 11.2 (Schrodinger Release 2017–2) interface, and invalid atom types were corrected using this same wizard. The protein structure was imported into workspace and preprocessed to assign bond orders, add hydrogen atoms, create disulfide bonds, and to delete water molecules beyond 5 Å from hetero groups. Additionally, the

protein structure was refined via automated H-bond assignment and restrained minimization with OPLS 2005 force field by converging heavy atoms to 0.5 Å RMSD. Ligand structures were sketched in ChemDraw and prepared with LigPrep in the Maestro interface. A receptor grid was generated from the refined structures using default values while centered on the position of the ligand (atovaquone or GW844520) that occupied either Q_o and Q_i sites of bc₁. Selected inhibitors were docked into the grid using Glide 7.4⁴⁰⁻⁴² in standard precision (SP) mode, without any constraints, by sampling of the conformational and positional degrees of freedom of the ligand. The binding poses of inhibitors in the Q_o and Q_i sites of bc₁ were further refined using minimization of the binding pocket around the docked ligands and subsequently analyzed.

General Procedure A.—A mixture of piperazine (1 equiv), 3-nitrobenzyl bromide/3-nitrophenethyl bromide (1.1 equiv), and Et₃N (1.5 equiv) in anhydrous THF was stirred for overnight at RT. The reaction mixture was diluted with water (20 mL) and extracted with EtOAc (3 × 20 mL). The combined organic extracts were dried over Na₂SO₄, filtered, and concentrated under reduced pressure. The crude was purified by flash chromatography (90:20 → 70:30, hexanes/ EtOAc) to afford the title compounds.

General Procedure B.—A mixture of nitro compound (1 equiv) and SnCl₂ (3 equiv) in absolute ethanol was refluxed for 3 h. The reaction was neutralized with 4N KOH solution and extracted with EtOAc. The combined organic extracts were dried over Na₂SO₄, filtered, and concentrated under reduced pressure. The crude was purified by flash chromatography using 100% EtOAc.

General Procedure C.—A neat mixture of aniline/aminobenzyl alcohol (1 equiv) and dimethyl 2-(methoxymethylene)malonate (1.05 equiv) was heated at 110 °C for 30 min. The reaction mixture was allowed to cool to RT while precipitation arose. Diethyl ether was added to the mixture to improve the precipitation. The solid was filtered off and washed with diethyl ether, dried under vacuum, and used directly for the further transformations.

General Procedure D.—To a solution of alcohol (1 equiv) in anhydrous CH₂Cl₂ was added the Dess–Martin periodinane (1.5 equiv) at RT. The resulting mixture was stirred for 3 h at RT. The mixture was treated with aqueous NaHCO₃ solution and filtered through a sintered funnel while washing with CH₂Cl₂. The organic phase was separated, dried over Na₂SO₄, filtered, and concentrated to give the aldehyde in an almost pure form which was used directly for further transformations.

General Procedure E.—To a mixture of aldehyde (1 equiv) and piperazine/piperazine hydrochloride (1.2 equiv) in anhydrous THF were added anhydrous MgSO₄ (2 equiv) followed by *N,N*-diisopropylethylamine (2.5 equiv) at RT, and the resulting solution was stirred vigorously for 30 min. To this was then added sodium triacetoxyborohydride (2 equiv). The reaction was stirred for an additional 4 h at RT, quenched with saturated NaHCO₃ solution, and extracted with EtOAc. The combined organic fractions were washed with brine, dried over Na₂SO₄, and concentrated under reduced pressure. The crude was purified by flash chromatography gradient elution (80:20 → 30:70, hexanes/EtOAc) to afford the title compounds.

General Procedure F.—The enamine in toluene was subjected to microwave heating at 280 °C for 4 min. The reaction mixture was allowed to cool to RT while precipitation rose. Diethyl ether was added to the mixture to improve the precipitation. The solid was filtered off and washed with diethyl ether. The solid containing the unreacted enamine and quinolone regio-isomers was then refluxed in methanol (in most of the cases unless it is mentioned otherwise) for 1 h and filtered hot to give the title quinolones in purest form.

General Procedure G.—To a solution of quinolone (1 equiv) in anhydrous CH₂Cl₂ was added freshly recrystallized NBS/NCS (1.2 equiv) at RT, and the resulting mixture was stirred overnight. The reaction was concentrated, and the crude was purified by either recrystallization or HPLC.

General Procedure H.—To a stirred solution of diol 10 (12.5 mmol) in anhydrous CH₂Cl₂ (50 mL) was added thionyl chloride (2.5 mL, 34.7 mmol) dropwise. The mixture was heated at reflux for 1 h. The reaction was concentrated, and the residue was diluted with MeCN (200 mL). To this was then added KI (100 mg, 0.62 mmol) followed by nitroaniline (13 mmol), and the resulting mixture was refluxed for 7 days. The reaction was concentrated, and the crude product was used for the next reaction without further purification.

1-(3-nitrophenyl)-4-phenylpiperazine 4a.—To a solution of 1-fluoro-3-nitrobenzene (2 g, 14.2 mmol) in DMSO (28.5 mL) was added 1-phenylpiperazine (6.5 mL, 42.5 mmol) and DIPEA (9.9 mL, 56.8 mmol). The reaction was refluxed for 2 days. DI water was added, then extracted with EtOAc 3 times. The organic layer was dried over sodium sulfate, filtered, and concentrated under reduced pressure followed by separation by flash column chromatography to give 4a as a yellow solid in 50% yield. ¹H NMR (399 MHz, (CD₃XCO) δ 7.77 (t, *J* = 2.3 Hz, 1H), 7.63 (ddd, *J* = 7.9, 2.1, 1.0 Hz, 1H³), 7.50 (t, *J* = 8.1 Hz, 1H), 7.44 (ddd, *J* = 8.3, 2.5, 0.9 Hz, 1H), 7.29–7.23 (m, 2H), 7.05–7.00 (m, 2H), 6.84 (tt, *J* = 7.4, 1.0 Hz, 1H), 3.49 (dd, *J* = 6.3, 3.9 Hz, 4H), 3.37 (dd, *J* = 6.3, 3.9 Hz, 4H). ¹³C NMR (100 MHz, (CD₃)₂CO) δ 153.1, 152.4, 150.5, 131.0, 130.1, 122.4, 120.7, 117.2, 114.2, 110.1, 49.9, 49.2.

1-Benzyl-4-(3-nitrophenyl)piperazine 4b.—To a solution of 1-fluoro-3-nitrobenzene (2 g, 14.2 mmol) in DMSO (28.5 mL) were added 1-benzylpiperazine (7.4 mL, 42.5 mmol) and DIPEA (9.9 mL, mmol). The reaction was refluxed for 2 days. DI water was added, then extracted with EtOAc 3 times. The organic layer was dried over sodium sulfate, filtered, and concentrated under reduced pressure followed by separation by flash column chromatography to give 4b as a yellow solid in 65% yield. ¹H NMR (399 MHz, (CD₃)₂CO) δ 7.69 (t, *J* = 2.3 Hz, 1H), 7.59 (ddd, *J* = 8.0, 2.1, 0.8 Hz, 1H³), 7.45 (t, *J* = 8.2 Hz, 1H), 7.40–7.31 (m, 5H), 7.29–7.23 (m, 1H), 3.57 (s, 2H), 3.35–3.31 (m, 4H), 2.62–2.58 (m, 4H). ¹³C NMR (100 MHz, (CD₃)₂CO) δ 152.4, 149.6, 138.7, 130.1, 129.1, 128.4, 127.2, 121.2, 112.9, 109.0, 62.7, 52.9, 48.3.

1-(3-Nitrophenethyl)-4-phenylpiperazine 4ac.—4ac was obtained as a pale-yellow semisolid (600 mg, 62% yield) by alkylation of 1-phenylpiperazine (500 mg, 3.08 mmol) with 3-nitrophenethyl bromide (780 mg, 3.4 mmol) following general procedure A. ¹H

NMR (400 MHz, CDCl₃): δ 8.16–8.04 (m, 2H), 7.57 (d, J = 7.6 Hz, 1H), 7.46 (t, J = 7.9 Hz, 1H), 7.33–7.23 (m, 2h), 7.00–6.82 (m, 3H), 3.31–3.17 (m, 4H), 2.96 (t, J = 7.8 Hz, 2H), 2.73–2.69 (m, 6h). ¹³C NMR (101 MHz, CDCl₃): δ 151.2, 148.3, 142.3, 135.0, 129.2, 129.1 (2C), 123.6, 121.3, 119.8, 116.1 (2C), 59.5, 53.2 (2C), 49.1 (2C), 33.1. HRMS (ESI-TOF) calcd for C₁₈H₂₂N₃O₂ [M + H]⁺ 312.1712, found 312.1719.

1-Benzyl-4-(3-nitrophenethyl)piperazine 4ad.—4ad was obtained as an orange-yellow oil (800 mg, 63% yield) by alkylation of 1-benzylpiperazine (690 mg, 4.0 mmol) with 3-nitrophenethyl bromide (1.0 g, 4.3 mmol) following general procedure A. ¹H NMR (400 MHz, CDCl₃): δ 8.06 (t, J = 2.0 Hz, 1h), 8.03 (ddd, J = 8.1, 2.4, 1.1 Hz, 1H), 7.54–7.50 (m, 1H), 7.41 (t, J = 7.9 Hz, 1H), 7.32–7.20 (m, 5H), 3.51 (s, 2H), 2.91–2.85 (m, 2H), 2.65–2.59 (m, 2H), 2.59–2.45 (m, 8H). ¹³C NMR (101 MHz, CDCl₃): δ 148.3, 142.5, 138.0, 135.0, 129.2, (2C), 129.1, 128.2 (2C), 127.0, 123.6, 121.2, 63.0, 59.6, 53.1 (2C), 53.0 (2C), 33.1. HRMS (ESI-TOF) calcd for C₁₉H₂₄N₃O₂ [M + H]⁺ 326.1869, found 326.1869.

1-(4-Methoxybenzyl)-4-(3-nitrophenethyl)piperazine 4ae.—4ae was obtained as an orange-yellow oil (1.3 g, 59% yield) by alkylation of 1-(4-methoxybenzyl)piperazine (1.3 g, 6.3 mmol) with 3-nitrophenethyl bromide (1.5 g, 6.9 mmol) following general procedure A. ¹H NMR (400 MHz, CDCl₃): δ 8.07–7.95 (m, 2H), 7.48 (t, J = 8.3, 1H), 7.37 (dd, J = 16.5, 8.6, 1H), 7.23–7.15 (m, 2H), 6.86–6.78 (m, 2h), 3.74 (s, 3H), 3.42 (s, 2H), 2.87–2.80 (m, 2H), 2.59 (dd, J = 9.0, 6.7, 2H), 2.54–2.40 (m, 8H). ¹³C NMR (101 MHz, CDCl₃): δ 158.7, 148.2, 142.5, 135.0, 130.3 (2C), 130.0, 129.1, 123.5, 121.1, 113.5 (2C), 62.4, 59.5, 55.2, 53.1 (2C), 52.9 (2c), 33.1. HRMS (ESI-TOF) calcd for C₂₀H₂₅N₃O₃ [M + H]⁺ 356.1974, found 356.1981.

1-(4-Fluorophenyl)-4-(3-nitrobenzyl)piperazine 4aj.—4aj was obtained as a white solid (8.5 g, 97% yield) by alkylation of 1-(4-(trifluoromethyl)phenyl)piperazine (5.0 g, 27.7 mmol) with 3-nitro-benzyl bromide (6.6 g, 30.5 mmol) following general procedure A. ¹H NMR (400 MHz, CDCl₃): δ 8.21 (t, J = 2.0 Hz, 1H), 8.09 (ddd, J = 8.2, 2.4, 1.1 Hz, 1H), 7.68 (dt, J = 7.7, 1.3 Hz, 1H), 7.47 (t, J = 7.9 Hz, 1H), 6.95–6.89 (m, 2H), 6.87–6.81 (m, 2H), 3.63 (s, 2H), 3.16–3.05 (m, 4H), 2.65–2.56 (m, 4H). ¹³C NMR (101 MHz, CDCl₃): δ 158.2, 155.8, 148.3, 147.8, 140.5, 134.9, 129.1, 123.6, 122.1, 117.7, 115.5, 115.3, 61.8, 53.0 (2C), 50.0 (2C). HRMS (ESI-TOF) calcd for C₁₇H₁₉FN₃O₂ [M + H]⁺ 316.1461, found 316.1466.

1-(3-Nitrobenzyl)-4-(4-(trifluoromethyl)phenyl)piperazine (4ao).—4ao was obtained as a pale-yellow solid (3.7 g, 90% yield) by alkylation of 1-(4-(trifluoromethyl)phenyl)piperazine (3 g, 13.0 mmol) with 3-nitrobenzyl bromide (2.2 g, 14.3 mmol) following general procedure A. ¹H NMR (399 MHz, CDCl₃) δ 8.25 (s, 1H), 8.12, (d, J = 8.2 Hz, 1H), 7.72 (d, J = 7.6 Hz, 1H), 7.51 (d, J = 7.9 Hz, 1H), 7.47 (d, J = 8.7 Hz, 2H), 6.91 (d, J = 8.7 Hz, 2H), 3.65 (s, 2H), 3.34–3.26 (m, 4H), 2.69–2.55 (m, 4H). ¹³C NMR (100 MHz, CDCl₃) δ 153.3, 148.5, 140.5, 135.1, 129.3, 126.4 (dd, J = 7.4, 3.7 Hz), 124.9 (d, J = 270.5 Hz), 123.7, 122.4, 120.4 (d, J = 32.7 Hz), 114.6, 62.0, 52.8, 48.0.

1-(2-Methoxy-5-nitrobenzyl)-4-(4-(trifluoromethyl)phenyl)-piperazine (4as).—4as was obtained as a white solid (1.4 g, 90% yield) by alkylation of 1-(4-

(trifluoromethyl)phenyl)piperazine (850 mg, 3.7 mmol) with 2-(bromomethyl)-1-methoxy-4-nitrobenzene (1 g, 4.1 mmol) following general procedure A. ^1H NMR (500 MHz, CDCl_3) δ 8.37 (d, J = 2.8 Hz, 1H), 8.19 (dd, J = 9.0, 2.8 Hz, 1H), 7.49 (d, J = 8.8 Hz, 2H), 6.95 (t, J = 8.1 Hz, 3H), 3.97 (s, 3H), 3.65 (s, 2H), 3.38–3.29 (m, 4H), 2.73–2.65 (m, 4h). ^{13}C NMR (126 MHz, CDCl_3) δ 162.7, 153.4, 141.5, 127.7, 126.4 (q, J = 3.9 Hz), 125.6, 124.9 (d, J = 270.9 Hz), 124.6, 120.4 (d, J = 32.7 Hz), 114.6, 110.1, 56.23, 55.5, 53.0, 48.1.

3-(4-Phenylpiperazin-1-yl)aniline 5a.—A nitro reduction reaction of **4a** (178 mg, 0.63 mmol) following general procedure B resulted in **5a**, isolated as a crude orange solid which was used in the next step without further purification.

3-(4-Benzylpiperazin-1-yl)aniline 5b.—A nitro reduction reaction of **4b** (658 mg, 2.21 mmol) following general procedure B resulted in **5b**, isolated as a crude orange solid which was used in the next step without further purification.

3-(2-(4-Phenylpiperazin-1-yl)ethyl)aniline 5ac.—A nitro reduction reaction of **4ac** (500 mg, 1.6 mmol) following general procedure B resulted in **5ac** as an orange-yellow semisolid (450 mg, 99% yield). ^1H NMR (400 MHz, CDCl_3): δ 7.30–7.24 (m, 2H), 7.08 (t, J = 7.7 Hz, 1H), 6.97–6.92 (m, 2H), 6.88–6.84 (m, 1H), 6.63 (dt, J = 7.6, 1.2 Hz, 1H), 6.56–6.52 (m, 2H), 3.60 (bs, 2H), 3.26–3.22 (m, 4h), 2.79–2.74 (m, 2H), 2.71–2.62 (m, 6H). ^{13}C NMR (101 MHz, CDCl_3): δ 151.3, 146.4, 141.4, 129.3, 129.1 (2C), 119.7, 119.0, 116.0, 115.4 (2C), 112.9, 60.4, 53.2 (2C), 49.1 (2C), 33.6. HRMS (ESI-TOF) calcd for $\text{C}_{18}\text{H}_{24}\text{N}_{32}$ $[\text{M} + \text{H}]^+$ 282.1970, found 282.1965.

3-(2-(4-Benzylpiperazin-1-yl)ethyl)aniline 5ad.—A nitro reduction reaction of **4ad** (700 mg, 2.1 mmol) following general procedure B resulted in **5ad** as a yellow oil (550 mg, 86% yield). ^1H NMR (400 MHz, CDCl_3): δ 7.32–7.29 (m, 4H), 7.28–7.20 (m, 1H), 7.04 (td, J = 7.3, 1.4 Hz, 1H), 6.58 (dt, J = 7.3, 1.3 Hz, 1H), 6.50 (dd, J = 7.1, 1.1 Hz, 2H), 3.91 (bs, 2H), 3.52 (s, 2H), 2.76–2.66 (m, 2H), 2.57 (ddd, J = 23.4, 12.1, 4.9 Hz, 10H). ^{13}C NMR (101 MHz, CDCl_3): δ 146.4, 141.3, 137.8, 129.2, 129.2 (2C), 128.1 (2C), 127.0, 118.9, 115.4, 112.9, 62.9, 60.2, 52.9 (2C), 52.7 (2C), 33.3.

3-(2-(4-(4-Methoxybenzyl)piperazin-1-yl)ethyl)aniline 5ae.—A nitro reduction reaction of **4ae** (1.0 g, 3.0 mmol) following general procedure B resulted in **5ae** as an orange-yellow semisolid (820 mg, 90% yield). ^1H NMR (400 MHz, CDCl_3): δ 7.20 (t, J = 8.4 Hz, 2H), 7.03 (t, J = 7.7 Hz, 1H), 6.83 (dd, J = 8.4, 5.8 Hz, 2H), 6.57 (d, J = 7.6 Hz, 1H), 6.49 (d, J = 7.0 Hz, 2H), 3.77 (s, 3H), 3.43 (s, 2H), 2.69 (dd, J = 10.6, 5.7 Hz, 2H), 2.64–2.39 (m, 10H). ^{13}C NMR (101 MHz, CDCl_3): δ 158.6, 146.4, 141.4, 130.3 (2C), 129.9, 129.2, 118.8, 115.3, 113.5 (2C), 112.8, 62.3, 60.3, 55.1, 53.0 (2C), 52.8 (2C), 33.5. HRMS (ESI-TOF) calcd for $\text{C}_{20}\text{H}_{28}\text{N}_3\text{O}$ $[\text{M} + \text{H}]^+$ 326.2232, found 326.2225.

3-((4-(4-Fluorophenyl)piperazin-1-yl)methyl)aniline 5aj.—A nitro reduction reaction of **4aj** (8.4 g, 26.6 mmol) following general procedure B resulted in **5aj** as a pale-yellow solid (7.3 g, 96% yield). ^1H NMR (400 MHz, methanol- d_4): δ 7.04 (t, J = 7.7 Hz, 1H), 6.92–6.82 (m, 4H), 6.68 (t, J = 2.0 Hz, 1H), 6.65 (dt, J = 7.5, 1.3 Hz, 1H), 6.60 (ddd, J = 8.0, 2.3, 1.0 Hz, 1H), 3.40 (s, 2h), 3.06–3.01 (m, 4h), 2.58–2.52 (m, 4H). ^{13}C NMR (101 MHz,

methanol-*d*₄) δ 159.5, 157.1, 148.9, 148.2, 138.7, 129.9, 120.4, 118.9, 117.4, 116.2, 116.0, 115.4, 63.9, 53.8 (2C), 50.7 (2C). HRMS (eSI-TOF) calcd for C₁₇H₂₁FN₃ [M + H]⁺ 286.1720, found 286.1730.

3-((4-(4-(Trifluoromethyl)phenyl)piperazin-1-yl)methyl)aniline 5ap.—A nitro reduction reaction of **4ap** (2.8 g, 7.55 mmol) following method B resulted in **5ap** as a pale-orange solid (2.4 g, 94% yield). ¹H NMR (399 MHz, CDCl₃) δ 7.48 (d, *J* = 8.7 Hz, 2H), 7.13 (t, *J* = 7.7 Hz, 1H), 6.92 (d, *J* = 8.7 Hz, 2H), 6.79–6.70 (m, 2h), 6.66–6.57 (m, 1H), 3.66 (bs, 2H), 3.49 (s, 2H), 3.35–3.22 (m, 4h), 2.70–2.56 (m, 4h). ¹³C NMR (100 MHz, CDCl₃) δ 153.4, 146.6, 139.1, 129.3, 126.4 (q, *J* = 3.6 Hz), 124.9 (d, *J* = 270.6 Hz), 120.3 (d, *J* = 32.5 Hz), 119.6, 115.8, 114.5, 114.2, 63.1, 52.9, 48.0.

4-Methoxy-3-((4-(4-(trifluoromethyl)phenyl)piperazin-1-yl)-methyl)aniline 5as.—A nitro reduction reaction of **4as** (1.5 g, 3.79 mmol) following method B resulted in **5as**, isolated as a crude orange solid which was used in the next step without further purification.

Dimethyl 2-(((3-((4-Phenylpiperazin-1-yl)methyl)phenyl)amino)-methylene)malonate 7j.—A direct reductive amination (DRA) reaction between aldehyde **13a** (1.0 g, 3.8 mmol) and 1-phenyl-piperazine (740 mg, 4.6 mmol) following general procedure E afforded **7j** as a brown yellow semisolid (1.1 g, 72% yield). ¹H NMR (400 MHz, CDCl₃): δ 11.02 (d, *J* = 13.6 Hz, 1H), 8.52 (dd, *J* = 13.7, 2.1 Hz, 1H), 7.31–(5.96 (m, 6H), 6.90–6.75 (m, 3H), 3.79 (d, *J* = 2.5 Hz, 3h), 3.73 (d, *J* = 2.2 Hz, 3H), 3.51 (d, *J* = 2.8 Hz, 2H), 3.16 (t, *J* = 4.9 Hz, 4H), 2.57 (t, *J* = 5.0 Hz, 4H). ¹³C NMR (101 MHz, CDCl₃): δ 169.0, 165.6, 151.9, 150.9, 139.8, 138.9, 129.4, 128.8 (2C), 125.5, 119.4, 117.6, 115.7 (2C), 115.6, 92.6, 62.3, 52.8 (2C), 51.3, 51.2, 48.7 (2C). HRMS (ESI-TOF) calcd for C₂₃H₂₇N₃O₄ [M + H]⁺ 410.2080, found 410.2105.

Dimethyl 2-(((3-((4-Benzylpiperazin-1-yl)methyl)phenyl)amino)-methylene)malonate 7k.—A direct reductive amination (DRA) reaction between aldehyde **13a** (500 mg, 1.9 mmol) and 1-benzylpiperazine (400 mg, 2.3 mmol) following general procedure E afforded **7k** as a yellow oil (600 mg, 75% yield). ¹H NMR (400 MHz, CDCl₃): δ 11.00 (d, *J* = 13.8 Hz, 1H), 8.52 (dd, *J* = 13.8, 1.2 Hz, 1H), 7.30–7.24 (m, 5H), 7.20 (ddt, *J* = 5.9, 4.8, 2.4 Hz, 1H), 7.11 (t, *J* = 1.8 Hz, 1H), 7.06 (dt, *J* = 7.6, 1.2 Hz, 1H), 7.02–6.98 (m, 1H), 3.83 (d, *J* = 1.4 Hz, 3H), 3.76 (d, *J* = 1.3 Hz, 3H), 3.49 (d, *J* = 1.2 Hz, 2H), 3.46 (s, 2H), 2.55–2.36 (m, 8H). ¹³C NMR (101 MHz, CDCl₃): δ 169.2, 165.9, 152.2, 140.5, 139.0, 137.9, 129.5, 129.1 (2C), 128.1 (2C), 126.9, 125.7, 117.8, 115.6, 92.6, 62.9, 62.5, 53.0 (2C), 52.9 (2C), 51.5, 51.4. HRMS (ESI-TOF) calcd for C₂₄H₃₀N₃O₄ [M + H]⁺ 424.2236, found 424.2250.

Dimethyl 2-(((3-((4-(4-Methoxybenzyl)piperazin-1-yl)methyl)-phenyl)amino)methylene)malonate 7l.—A DRA reaction between aldehyde **13k** (1.0 g, 3.8 mmol) and 1-(4-methoxybenzyl) piperazine (940 mg, 4.6 mmol) following general procedure E afforded **7l** as a yellow oil (1.2 g, 70% yield). ¹H NMR (400 MHz, CDCl₃): δ 10.99 (d, *J* = 13.8 Hz, 1H), 8.51 (d, *J* = 13.8 Hz, 1H), 7.27–7.23 (m, 1H), 7.19–7.15 (m, 2H), 7.10 (t, *J* = 1.9 Hz, 1H), 7.05 (dt, *J* = 7.6, 1.2 Hz, 1H), 6.99 (ddd, *J* = 8.1, 2.5, 1.0 Hz, 1H),

6.82–6.78 (m, 2H), 3.81 (s, 3H), 3.74 (s, 3H), 3.74 (s, 3H), 3.45 (s, 2H), 3.41 (s, 2H), 2.43 (s, 8h). ^{13}C NMR (101 MHz, CDCl_3): δ 169.2, 165.9, 158.6, 152.1, 140.5, 139.0, 130.3 (2C), 129.8, 129.5, 125.7, 117.7, 115.6, 113.4 (2C), 92.6, 62.5, 62.3, 55.1, 53.0 (2C), 52.7 (2C), 51.5, 51.3. HRMS (ESI-TOF) calcd for $\text{C}_{25}\text{H}_{32}\text{N}_3\text{O}_5$ $[\text{M} + \text{H}]^+$ 454.2342, found 454.2356.

Dimethyl 2-(((3-((4-(Benzo[d][1,3]dioxol-5-ylmethyl)piperazin-1-yl)methyl)phenyl)amino)methylene)malonate 7m.—

A DRA reaction between aldehyde **13a** (500 mg, 1.9 mmol) and 1-piperonylpiperazine (500 mg, 2.3 mmol) following general procedure E afforded **7m** as a yellow oil (600 mg, 67% yield). ^1H NMR (400 MHz, CDCl_3): δ 11.01 (d, $J = 13.7$ Hz, 1H), 8.53 (d, $J = 13.9$ Hz, 1H), 7.32–7.23 (m, 1H), 7.12 (t, $J = 1.9$ Hz, 1H), 7.07 (dt, $J = 7.7, 1.1$ Hz, 1H), 7.01 (ddd, $J = 8.0, 2.5, 0.9$ Hz, 1H), 6.82 (d, $J = 1.1$ Hz, 1H), 6.75–6.68 (m, 2H), 5.90 (d, $J = 0.6$ Hz, 2H), 3.83 (d, $J = 0.6$ Hz, 4H), 3.76 (d, $J = 0.5$ Hz, 3H), 3.48 (s, 2H), 3.41 (s, 2H), 2.46 (s, 8H). ^{13}C NMR (101 MHz, CDCl_3): δ 169.3, 166.0, 152.2, 147.5, 146.5, 140.5, 139.1, 131.7, 129.6, 125.8, 122.2, 117.8, 115.7, 109.5, 107.8, 100.8, 92.7, 62.6, 62.6, 53.0 (2C), 52.8 (2C), 51.5, 51.4. HRMS (ESI-TOF) calcd for $\text{C}_{25}\text{H}_{30}\text{N}_3\text{O}_6$ $[\text{M} + \text{H}]^+$ 468.2135, found 468.2142.

Dimethyl 2-(((3-((4-(4-Methoxyphenyl)piperazin-1-yl)methyl)phenyl)amino)methylene)malonate 7n.—

A DRA reaction between aldehyde **13a** (500 mg, 1.9 mmol) and 1-(4-methoxyphenyl)-piperazine hydrochloride (604 mg, 2.3 mmol) following general procedure E afforded **7n** as a pale-yellow semisolid (565 mg, 68% yield). ^1H NMR (400 MHz, CDCl_3): δ 11.03 (d, $J = 13.8$ Hz, 1H), 8.54 (d, $J = 13.8$ Hz, 1H), 7.30 (t, $J = 7.8$ Hz, 1H), 7.16 (t, $J = 1.9$ Hz, 1H), 7.11 (dt, $J = 7.6, 1.2$ Hz, 1H), 7.05–7.01 (m, 1H), 6.89–6.84 (m, 2H), 6.82–6.78 (m, 2H), 3.83 (s, 3H), 3.76 (s, 3H), 3.73 (s, 3H), 3.53 (s, 2H), 3.10–3.05 (m, 4H), 2.59 (dd, $J = 6.0, 3.8$ Hz, 4H). ^{13}C NMR (101 MHz, CDCl_3): δ 169.3, 166.0, 153.7, 152.2, 145.6, 140.4, 139.1, 129.6, 125.8, 118.2 (2C), 117.9, 115.8, 114.3 (2C), 92.7, 62.6, 55.5, 53.2 (2C), 51.5, 51.4, 50.5 (2C). HRMS (ESI-TOF) calcd for $\text{C}_{24}\text{H}_{30}\text{N}_3\text{O}_5$ $[\text{M} + \text{H}]^+$ 440.2185, found 440.2196.

Dimethyl 2-(((3-((4-(4-Fluorophenyl)piperazin-1-yl)methyl)phenyl)amino)methylene)malonate 7o.—

A direct reductive amination (DRA) reaction between aldehyde **13a** (500 mg, 1.9 mmol) and 1-(4-fluorophenyl)piperazine (410 mg, 2.3 mmol) following general procedure E afforded **7o** as a pale-yellow semisolid (580 mg, 72%). ^1H NMR (400 MHz, CDCl_3): δ 11.04 (d, $J = 13.6$ Hz, 1H), 8.54 (dd, $J = 13.9, 3.6$ Hz, 1H), 7.30 (td, $J = 7.8, 3.5$ Hz, 1H), 7.16 (s, 1H), 7.12 (d, $J = 7.5$ Hz, 1H), 7.06–7.01 (m, 1H), 6.92 (td, $J = 8.6, 3.5$ Hz, 2H), 6.84 (dt, $J = 9.0, 4.3$ Hz, 2H), 3.83 (d, $J = 3.2$ Hz, 3H), 3.76 (d, $J = 3.2$ Hz, 3H), 3.53 (bs, 2H), 3.11–3.08 (m, Hz, 4H), 2.60–2.58 (m, 4H). ^{13}C NMR (101 MHz, CDCl_3) δ 169.2, 165.9, 158.2, 155.8, 152.1, 147.8, 140.3, 139.1, 129.6, 125.6, 117.7, 117.6, 115.7, 115.4, 115.2, 92.7, 62.4, 53.0 (2C), 51.4, 51.3, 50.0 (2C). HRMS (ESI-TOF) calcd for $\text{C}_{24}\text{H}_{30}\text{N}_3\text{O}_5$ $[\text{M} + \text{H}]^+$ 428.1986, found 428.1990.

Dimethyl 2-(((3-((4-(4-(Trifluoromethyl)phenyl)piperazin-1-yl)methyl)phenyl)amino)methylene)malonate 7p.—

A direct reductive amination (DRA) reaction between aldehyde **13a** (500 mg, 1.9 mmol) and 1-(4-

trifluoromethylphenyl)piperazine (840 mg, 2.3 mmol) following general procedure E afforded **7p** as a pale-yellow semisolid (980 mg, 68% yield). ¹H NMR (400 MHz, CDCl₃): δ 11.03 (d, *J*=13.8 Hz, 1H), 8.53 (dd, *J*= 13.8, 1.0 Hz, 1H), 7.41 (d, *J*=8.7 Hz, 2H), 7.28 (t, *J*= 7.8 Hz, 1H), 7.14 (t, *J*=1.8 Hz, 1H), 7.09 (dd, *J*= 7.7, 1.3 Hz, 1H), 7.04–7.00 (m, 1H), 6.85 (d, *J* = 8.6 Hz, 2h), 3.81 (s, 3H), 3.74 (s, 3H), 3.50 (s, 2H), 3.23 (t, *J*= 5.1 Hz, 4H), 2.54 (dd, *J* = 6.1, 3.9 Hz, 4H). ¹³C NMR (101 MHz, CDCl₃) δ 169.1, 165.8, 153.1, 152.0, 140.1, 139.1, 129.6, 126.2, 126.2, 126.1, 126.1, 125.6, 117.6, 115.7, 114.3 (2C), 92.7, 62.4, 52.6 (2C), 51.4, 51.3, 47.7 (2C). HRMS (ESI-TOF) calcd for C₂₄H₂₇F₃N₃O₄ [M + H]⁺ 478.1954, found 478.1970.

Dimethyl 2-(((4-Methyl-3-((4-phenylpiperazin-1-yl)methyl)-phenyl)amino)methylene)malonate 7q.—A DRA reaction between aldehyde **13b** (600 mg, 2.2 mmol) and 1-phenylpiperazine (430 mg, 2.6 mmol) following general procedure E

afforded **7q** as a white semisolid (700 mg, 77%). ¹H NMR (400 MHz, CDCl₃): δ 11.02 (1H), 8.52 (d, *J*= 13.9 Hz, 1H), 7.23–7.20 (m, 2H), 7.15–7.12 (m, 2H), 6.95 (d, *J*= 8.2 Hz, 2H), 6.91–6.88 (dd, *J*= 8.8, 1.1 Hz, 2H), 6.84–6.80 (m, 1H), 3.83 (s, 3H), 3.75 (s, 3H), 3.47 (s, 2H), 3.19–3.13 (m, 4H), 2.62–2.55 (m, 4h), 2.32 (s, 3H). ¹³C NMR (101 MHz, CDCl₃) δ 169.2, 165.9, 152.2, 151.1, 138.0, 136.7, 134.1, 131.3, 128.9 (2C), 119.4, 118.5, 115.8 (2C), 115.3, 92.0, 60.2, 53.0 (2C), 51.3, 51.2, 49.0 (2C), 18.6. HRMS (ESI-TOF) calcd for C₂₄H₃₀N₃O₄ [M + H]⁺ 424.2236, found 424.2257.

Dimethyl 2-(((3-((4-Benzylpiperazin-1-yl)methyl)-4-methylphenyl)amino)methylene)malonate 7r.—A DRA reaction between aldehyde

13b (650 mg, 2.3 mmol) and 1-benzylpiperazine (500 mg, 2.8 mmol) following general procedure E afforded **7r** as a pale-yellow semisolid (630 mg, 63%). ¹H NMR (400 MHz, CDCl₃): δ 10.98 (d, *J*= 13.8 Hz, 1H), 8.50 (dd, *J*= 13.9, 0.9 Hz, 1H), 7.32–7.20 (m, 5H), 7.13–7.07 (m, 2H), 6.92 (dd, *J*= 8.1, 2.5 Hz, 1H), 3.83 (s, 3H), 3.76 (s, 3H), 3.50 (s, 2H), 3.41 (s, 2H), 2.47 (m, 8H), 2.28 (s, 3h). ¹³C NMR (101 MHz, CDCl₃): δ 169.3, 166.0, 152.3, 138.4, 137.9, 136.7, 134.1, 131.3, 129.1 (2C), 128.1 (2C), 126.9, 118.5, 115.2, 92.0, 62.9, 60.1, 53.1 (2C), 53.0 (2C), 51.4, 51.3, 18.5. HRMS (ESI-TOF) calcd for C₂₅H₃₂N₃O₄ [M + H]⁺ 438.2393, found 438.2394.

Dimethyl 2-(((3-((4-(4-Methoxybenzyl)piperazin-1-yl)methyl)-4-methylphenyl)amino)methylene)malonate 7s.—A DRA reaction between aldehyde

13b (200 mg, 1.4 mmol) and 1-(4-methoxybenzyl)-piperazine (350 mg, 1.7 mmol) following general procedure E afforded **7s** as a pale-yellow semisolid (430 mg, 70%). ¹H NMR (400 MHz, CDCl₃): δ 10.95 (d, *J*= 13.9 Hz, 1h), 8.46 (d, *J*= 13.9 Hz, 1H), 7.19–7.12 (m, 2H), 7.07–7.01 (m, 2H), 6.87 (dd, *J*= 8.1, 2.5 Hz, 1H), 6.79–6.75 (m, 2H), 3.78 (s, 3H), 3.71 (s, 3H), 3.70 (s, 3H), 3.38 (s, 2H), 3.36 (s, 2H), 2.40 (s, 8H), 2.23 (s, 3H). ¹³C NMR (101 MHz, CDCl₃): δ 169.1, 165.8, 158.4, 152.1, 138.3, 136.6, 133.9, 131.1, 130.0 (2C), 129.8, 118.3, 115.0, 113.3 (2C), 91.9, 62.1, 59.9, 54.9, 53.0 (2C), 52.7 (2C), 51.2, 51.1, 18.4.

Dimethyl 2-(((3-((4-(4-Methoxyphenyl)piperazin-1-yl)methyl)-4-methylphenyl)amino)methylene)malonate 7t.—A DRA reaction between aldehyde

13b (600 mg, 2.16 mmol) and 1-(4-methoxyphenyl)piperazine hydrochloride (690 mg, 2.6

mmol) following general procedure E afforded **7t** as a pale-yellow semisolid (685 mg, 70%). ¹H NMR (400 MHz, CDCl₃): δ 11.00 (d, *J* = 13.9 Hz, 1H), 8.52 (d, *J* = 13.9 Hz, 1H), 7.15–7.11 (m, 2H), 6.95 (dd, *J* = 8.2, 2.5 Hz, 1H), 6.90–6.85 (m, 2H), 6.83–6.78 (m, 2H), 3.83 (s, 3H), 3.75 (s, 3H), 3.73 (s, 3H), 3.48 (s, 2H), 3.09–3.05 (m, 4H), 2.60 (dd, *J* = 6.1, 3.7 Hz, 4h), 2.32 (s, 3H). ¹³C NMR (101 MHz, CDCl₃): δ 169.4, 166.1, 153.7, 152.4, 145.7, 138.3, 136.8, 134.3, 131.5, 118.7, (2C), 115.4, 114.4 (2C), 92.2, 60.3, 55.5, 53.3 (2C), 51.5, 51.4, 50.7 (2C), 18.7. HRMS (ESI-TOF) calcd for C₂₅H₃₂N₃O₅ [M + H]⁺ 454.2342, found 454.2351.

Dimethyl 2-(((3-((4-(4-Fluorophenyl)piperazin-1-yl)methyl)-4-methylphenyl)amino)methylene)malonate **7u.**—A DRA reaction between aldehyde

13b (600 mg, 2.16 mmol) and 1-(4-fluorophenyl)-piperazine (470 mg, 2.6 mmol) following general procedure E afforded **7u** as a yellow semisolid (800 mg, 84% yield). ¹H NMR (400 MHz, CDCl₃): δ 11.00 (d, *J* = 13.9 Hz, 1H), 8.49–8.42 (m, 1H), 7.46–7.39 (m, 2H), 7.22 (d, *J* = 2.9 Hz, 1H), 7.00 (dd, *J* = 8.8, 2.9 Hz, 1H), 6.89–6.82 (m, 3H), 3.81 (s, 3H), 3.79 (s, 3H), 3.73 (s, 3H), 3.57 (s, 2H), 3.27 (t, *J* = 5.0 Hz, 4H), 2.61 (t, *J* = 5.0 Hz, 4H). ¹³C NMR (101 MHz, CDCl₃) δ 169.4, 166.1, 158.3, 155.9, 152.4, 148.0, 138.1, 136.9, 134.3, 131.5, 118.7, 117.8, 117.7, 115.6, 115.5, 115.3, 92.2, 60.3, 53.2 (2C), 51.5, 51.4, 50.2 (2C), 18.7. HRMS (ESI-TOF) calcd for C₂₄H₂₉FN₃O₄ [M + H]⁺ 442.2142, found 442.2157.

Dimethyl 2-(((4-Methyl-3-((4-(4-(trifluoromethyl)phenyl)-piperazin-1-yl)methyl)phenyl)amino)methylene)malonate **7v.**—A DRA reaction between

aldehyde **13b** (1.0 g, 3.6 mmol) and 1-(4-trifluoromethylphenyl)piperazine (1.0 g, 4.4 mmol) following general procedure E afforded **7v** as a pale-yellow semisolid (1.17 g, 66% yield). ¹H NMR (400 MHz, CDCl₃): δ 10.98 (d, *J* = 13.8 Hz, 1H), 8.47 (d, *J* = 13.9 Hz, 1H), 7.37 (d, *J* = 8.6 Hz, 2H), 7.09–7.05 (m, 2H), 6.89 (dd, *J* = 8.2, 2.5 Hz, 1H), 6.80 (d, *J* = 8.6 Hz, 2H), 3.76 (s, 3H), 3.70 (s, 3H), 3.40 (s, 2H), 3.17 (dd, *J* = 6.2, 3.7 Hz, 4H), 2.51 (t, *J* = 5.0 Hz, 4H), 2.26 (s, 3h). ¹³C NMR (101 MHz, CDCl₃): δ 169.0, 165.7, 153.0, 151.9, 137.7, 136.6, 134.0, 131.2, 126.0, 126.0, 125.9, 125.9, 118.3, 115.2, 114.0 (2C), 92.0, 59.9, 52.5 (2C), 51.1, 51.0, 47.6 (2C), 18.3. HRMS (ESI-TOF) calcd for C₂₅H₂₉F₃N₃O₄ [M + H]⁺ 492.2110, found 492.2115.

Dimethyl 2-(((4-Methoxy-3-((4-phenylpiperazin-1-yl)methyl)-phenyl)amino)methylene)malonate **7w.**—A DRA reaction between aldehyde **13c** (300

mg, 1.0 mmol) and 1-phenylpiperazine (200 mg, 1.22 mmol) following general procedure E afforded **7w** as a pale-yellow semisolid (305 mg, 68% yield). ¹H NMR (400 MHz, CDCl₃): δ 11.00 (d, *J* = 13.9 Hz, 1H), 8.46 (d, *J* = 14.0 Hz, 1H), 7.27–7.18 (m, 3H), 7.01 (dd, *J* = 8.7, 2.9 Hz, 1H), 6.94–6.88 (m, 2H), 6.85–6.78 (m, 2H), 3.82 (s, 3H), 3.80 (s, 3H), 3.74 (s, 3H), 3.58 (s, 2H), 3.22–3.19 (m, 4H), 2.66–2.62 (m, 4H). ¹³C NMR (101 MHz, CDCl₃): δ 169.5, 166.1, 155.4, 152.9, 151.3, 132.4, 129.0 (2C), 128.0, 119.8, 119.5, 116.7, 116.0 (2C), 111.4, 91.65, 55.8, 55.6, 53.1 (2C), 51.4, 51.3, 49.1 (2C). HRMS (ESI-TOF) calcd for C₂₄H₃₀N₃O₅ [M + H]⁺ 440.2185, found 440.2199.

Dimethyl 2-(((3-((4-Benzylpiperazin-1-yl)methyl)-4-methoxyphenyl)amino)methylene)malonate **7x.**—A DRA reaction between

aldehyde **13c** (500 mg, 1.7 mmol) and 1-benzylpiperazine (360 mg, 2.0 mmol) following general procedure E afforded **7x** as a pale-yellow semisolid (500 mg, 65% yield). ¹H NMR (400 MHz, CDCl₃): δ 10.97 (d, *J* = 14.0 Hz, 1H), 8.44 (d, *J* = 13.9 Hz, 1H), 7.30–7.26 (m, *J* = 2.6 Hz, 4H), 7.23–7.18 (m, 2H), 6.97 (dd, *J* = 8.7, 2.9 Hz, 1H), 6.80 (d, *J* = 8.7 Hz, 1H), 3.83 (s, 3H), 3.77 (s, 3H), 3.75 (s, 3H), 3.52 (s, 2H), 3.49 (s, 2H), 2.50 (m, 8H). ¹³C NMR (101 MHz, CDCl₃): δ 169.5, 166.1, 155.4, 152.9, 138.0, 132.3, 129.2 (2C), 128.2, 128.1 (2C), 126.9, 119.8, 116.6, 111.3, 91.6, 63.0, 55.7, 55.5, 53.1 (2C), 53.0 (2C), 51.4, 51.3. HRMS (ESI-TOF) calcd for C₂₅H₃₂N₃O₅ [M + H]⁺ 454.2342, found 454.2365.

Dimethyl 2-(((4-Methoxy-3-((4-(4-methoxyphenyl)piperazin-1-yl)methyl)phenyl)amino)methylene)malonate 7y.—A DRA reaction between aldehyde **13c** (350 mg, 1.2 mmol) and 1-(4-methoxybenzyl)-piperazine (295 mg, 1.4 mmol) following general procedure E afforded **7y** as a pale-yellow semisolid (350 mg, 61%). ¹H NMR (400 MHz, CDCl₃) δ 11.02–10.91 (m, 1H), 8.44 (d, *J* = 14.0 Hz, 1H), 7.25–7.17 (m, 3H), 6.98 (dd, *J* = 8.7, 2.9 Hz, 1H), 6.85–6.77 (m, 3H), 3.83 (s, 3H), 3.77 (s, 3H), 3.76 (s, 3H), 3.75 (s, 3H), 3.54 (s, 2H), 3.46 (s, 2H), 2.52 (s, 8H). ¹³C NMR (101 MHz, CDCl₃) δ 169.5, 166.2, 158.8, 155.4, 153.0 (2C), 132.4 (2C), 130.5 (2C), 119.9, 116.8, 113.6 (2C), 111.4, 91.6, 62.3, 55.7, 55.4, 55.2, 52.9, 52.8, 51.5, 51.4, 51.4. HRMS (ESI-TOF) calcd for C₂₆H₃₄N₃O₆ [M + H]⁺ 484.2448, found 484.2357.

Dimethyl 2-(((4-Methoxy-3-((4-(4-methoxyphenyl)piperazin-1-yl)methyl)phenyl)amino)methylene)malonate 7z.—A DRA reaction between aldehyde **13c** (200 mg, 0.7 mmol) and 1-(4-methoxyphenyl)-piperazine hydrochloride (220 mg, 0.82 mmol) following general procedure E afforded **7z** as a pale-yellow semisolid (250 mg, 78%). ¹H NMR (400 MHz, CDCl₃): δ 11.00 (d, *J* = 13.9 Hz, 1H), 8.47 (d, *J* = 13.9 Hz, 1H), 7.28–7.24 (m, 1H), 7.02 (dd, *J* = 8.7, 2.9 Hz, 1H), 6.92–6.77 (m, 5H), 3.83 (s, 4H), 3.82 (s, 3H), 3.75 (s, 3H), 3.74 (s, 3H), 3.61 (s, 2H), 3.14–3.08 (m, 4H), 2.67 (t, *J* = 5.0 Hz, 4H). ¹³C NMR (101 MHz, CDCl₃) δ 169.5, 166.2, 155.5, 153.8, 153.0 (2C), 145.7, 132.4, 119.9, 118.2 (2C), 116.8, 114.4 (2C), 111.5, 91.7, 55.8, 55.6, 55.5, 53.2, 51.5, 51.4, 50.6. HRMS (ESI-TOF) calcd for C₂₅H₃₂N₃O₆ [M + H]⁺ 470.2291, found 470.2309.

Dimethyl 2-(((3-((4-(4-Fluorophenyl)piperazin-1-yl)methyl)-4-methoxyphenyl)amino)methylene)malonate 7aa.—A DRA reaction between aldehyde **13c** (500 mg, 1.7 mmol) and 1-(4-fluorophenyl)-piperazine (220 mg, 2.0 mmol) following general procedure E afforded **7aa** as a pale-yellow semisolid (550 mg, 71%). ¹H NMR (400 MHz, CDCl₃): δ 11.03–10.94 (m, 1H), 8.44 (dd, *J* = 13.9, 12.3 Hz, 1H), 7.25–7.14 (m, 1H), 7.03–6.97 (m, 1H), 6.96–6.89 (m, 2H), 6.87–6.82 (m, 3H), 3.82 (s, 3H), 3.80 (s, 3H), 3.74 (s, 3H), 3.59 (s, 2H), 3.15–3.10 (m, 4H), 2.68–2.61 (m, 4H). ¹³C NMR (101 MHz, CDCl₃) δ 169.5, 166.2, 158.3, 155.9, 155.4, 154.6, 152.9, 152.8, 148.0, 132.5, 132.4, 131.0, 127.8, 119.9, 117.8, 117.7, 117.6, 117.5, 116.8, 115.5, 115.3, 111.5, 111.0, 91.7, 60.9, 55.8, 55.6, 55.5, 53.1, 51.5, 51.4, 51.3, 50.1. HRMS (ESI-TOF) calcd for C₂₄H₂₈FN₃O₅ [M + H]⁺ 458.2091, found 458.2104.

Dimethyl 2-(((4-Methoxy-3-((4-(trifluoromethyl)phenyl)piperazin-1-yl)methyl)phenyl)amino)methylene)malonate 7ab.—A DRA reaction between

aldehyde **13c** (1.0 g, 3.4 mmol) and 1-(4-trifluoromethylphenyl)piperazine (950 mg, 4.1 mmol) following general procedure E afforded **7ab** as a pale-yellow semisolid (1.2 g, 70% yield). ¹H NMR (400 MHz, CDCl₃): δ 11.00 (d, *J* = 13.9 Hz, 1H), 8.48–8.42 (m, 1H), 7.46–7.40 (m, 2H), 7.22 (d, *J* = 2.9 Hz, 1H), 7.00 (dd, *J* = 8.8, 2.9 Hz, 1H), 6.89–6.81 (s, 3H), 3.81 (m, 3h), 3.79 (s, 3H), 3.73 (s, 3H), 3.57 (s, 2H), 3.27 (t, *J* = 5.0 Hz, 4H), 2.61 (t, *J* = 5.0 Hz, 4H). ¹³C NMR (101 MHz, CDCl₃) δ 169.5, 166.2, 155.4, 153.3, 152.9, 132.4, 127.9, 126.3, 126.3, 126.3, 126.2, 119.8, 116.8, 114.4 (2C), 111.5, 91.7, 55.8, 55.6, 52.8 (2C), 51.4, 51.4, 47.9 (2C). HRMS (ESI-TOF) calcd for C₂₅H₂₉F₃N₃O₅ [M + H]⁺ 508.2059, found 508.2065.

Dimethyl 2-(((4-((4-Phenylpiperazin-1-yl)methyl)phenyl)amino)-

methylene)malonate 7af.—A DRA reaction of aldehyde **13d** (500 mg, 1.89 mmol) with 1-phenylpiperazine hydrochloride (370 mg, 2.3 mmol) following general procedure E furnished **7af** as a pale-yellow semisolid (520 mg, 67% yield). ¹H NMR (400 MHz, CDCl₃): δ 11.04 (d, *J* = 13.9 Hz, 1H), 8.52 (d, *J* = 13.7 Hz, 1H), 7.34 (d, *J* = 8.0 Hz, 2H), 7.23 (t, *J* = 7.7 Hz, 2h), 7.09 (d, *J* = 8.0 Hz, 2H), 6.90 (d, *J* = 8.1 Hz, 2H), 6.82 (t, *J* = 7.3 Hz, 1H), 3.84 (s, 3H), 3.76 (s, 3h), 3.52 (s, 2H), 3.17 (t, *J* = 4.8 Hz, 4h), 2.58 (t, *J* = 4.8 Hz, 4H). ¹³C NMR (101 MHz, CDCl₃): δ 169.3, 165.9, 152.2, 151.2, 138.1, 135.1, 130.5 (2C), 129.0 (2C), 119.6, 117.1 (2C), 116.0 (2C), 92.7, 62.2, 53.0 (2C), 51.5, 51.4, 49.1 (2C). HRMS (ESI-TOF) calcd for C₂₄H₃₀N₃O₅ [M + H]⁺ 440.2185, found 440.2173.

Dimethyl 2-(((4-((4-(4-Methoxyphenyl)piperazin-1-yl)methyl)-

phenyl)amino)methylene)malonate 7ag.—A DRA reaction of aldehyde **13d** (850 mg, 3.2 mmol) with 1-(4-methoxyphenyl)-piperazine hydrochloride (1.0 g, 3.86 mmol) following general procedure E furnished **7ag** as a pale-yellow solid (1.0 g, 71% yield). ¹H NMR (400 MHz, CDCl₃): δ 11.01 (d, *J* = 13.8 Hz, 1H), 8.49 (dd, *J* = 13.7, 1.1 Hz, 1H), 7.31 (d, *J* = 8.0 Hz, 2H), 7.07 (d, *J* = 8.1 Hz, 2H), 6.84 (d, *J* = 9.1 Hz, 2H), 6.80–6.76 (m, 2H), 3.81 (s, 3H), 3.73 (s, 3H), 3.70 (s, 3H), 3.49 (s, 2H), 3.04 (t, *J* = 4.8 Hz, 4H), 2.55 (t, *J* = 4.8 Hz, 4H). ¹³C NMR (101 MHz, CDCl₃): δ 169.2, 165.8, 153.6, 152.1, 45.5, 138.0, 135.0, 130.4 (2C), 118.0 (2C), 117.1, 117.0, 114.2 (2C), 92.5, 62.1, 55.3, 53.0 (2C), 51.4, 51.3, 50.4 (2C). HRMS (ESI-TOF) calcd for C₂₄H₃₀N₃O₅ [M + H]⁺ 440.2185, found 440.2173.

Dimethyl 2-(((4-((4-(4-Fluorophenyl)piperazin-1-yl)methyl)-

phenyl)amino)methylene)malonate 7ah.—A DRA reaction of aldehyde **13d** (850 mg, 3.2 mmol) with 1-(4-fluorophenyl)piperazine (695 mg, 3.86 mmol) following general procedure E furnished **7ah** as a pale-white solid (900 mg, 66% yield). ¹H NMR (400 MHz, CDCl₃): δ 11.01 (d, *J* = 13.7 Hz, 1H), 8.49 (d, *J* = 13.8 Hz, 1H), 7.33–7.29 (m, 2H), 7.07 (dd, *J* = 9.0, 2.5 Hz, 2H), 6.92–6.87 (m, 2H), 6.84–6.79 (m, 2H), 3.81 (s, 3H), 3.73 (s, 3H), 3.49 (s, 2H), 3.06 (t, *J* = 5.0 Hz, 4H), 2.54 (dd, *J* = 6.1, 3.9 Hz, 4h). ¹³C NMR (101 MHz, CDCl₃): δ 169.2, 165.8, 158.1, 155.7, 152.1, 147.8, 147.8, 138.0, 135.0, 130.4, 117.6, 117.5, 117.0, 115.4, 115.2, 92.6, 62.1, 52.9 (2C), 51.4, 51.3, 50.0 (2C). HRMS (ESI-TOF) calcd for C₂₃H₂₇FN₃O₄ [M + H]⁺ 428.1986, found 428.1993.

Dimethyl 2-(((4-((4-(4-(Trifluoromethyl)phenyl)piperazin-1-yl)-

methyl)phenyl)amino)methylene)malonate 7ai.—A DRA reaction of aldehyde **13d**

(500 mg, 1.9 mmol) with 1-(4-trifluoromethylphenyl)-piperazine (523 mg, 2.3 mmol) following general procedure E furnished **7ai** as a pale-yellow solid (570 mg, 63% yield). ¹H NMR (400 MHz, CDCl₃): δ 11.03 (d, *J* = 13.7 Hz, 1H), 8.52 (dd, *J* = 13.7, 1.1 Hz, 1H), 7.43 (d, *J* = 1.2 Hz, 2H), 7.34 (d, *J* = 7.4 Hz, 2H), 7.12–7.08 (m, 2H), 6.90–6.86 (m, 2H), 3.83 (s, 3H), 3.76 (s, 3H), 3.51 (s, 2H), 3.27–3.23 (m, 4H), 2.56 (dd, *J* = 6.1, 4.1 Hz, 4H). ¹³C NMR (101 MHz, CDCl₃): δ 169.4, 165.9, 153.3, 152.2, 138.2, 134.9, 130.5 (2C), 126.4, 126.3, 126.3, 126.3, 117.2 (2C), 114.4 (2C), 92.8, 62.2, 52.7 (2C), 51.6, 51.4, 47.9 (2C). HRMS (ESI-TOF) calcd for C₂₄H₂₇F₃N₃O₄ [M + H]⁺ 478.1954, found 478.1966.

Methyl 4-Oxo-7-(4-phenylpiperazin-1-yl)-1,4-dihydroquinoline-3-carboxylate

8a.—**8a** was synthesized from amine **5a** following general procedures C and F in 12% yield over two steps. ¹H NMR (500 MHz, DMSO-*d*₆) δ 11.95 (s, 1H), 8.44 (s, 1H), 7.97 (d, *J* = 9.1 Hz, 1H), 7.25 (t, *J* = 7.8 Hz, 2H), 7.17 (dd, *J* = 9.1, 2.3 Hz, 1H), 7.01 (d, *J* = 8.1 Hz, 2H), 6.88 (d, *J* = 2.4 Hz, 1H), 6.82 (t, *J* = 7.4 Hz, 1H), 3.71 (s, 3H), 3.46 (t, *J* = 5.0 Hz, 4H), 3.30 (d, *J* = 5.2 Hz, 4H). HRMS (ESI-TOF) calcd for C₂₁H₂₂N₃O₃ [M + H]⁺ 364.1661, found 364.1653.

Methyl 7-(4-Benzylpiperazin-1-yl)-4-oxo-1,4-dihydroquinoline-3-carboxylate 8a.

—**8a** was synthesized from amine **5b** following general procedures C and F in 16% yield over two steps. ¹H NMR (500 MHz, DMSO-*d*₆) δ 11.92 (s, 1H), 8.41 (s, 1H), 7.93 (d, *J* = 9.1 Hz, 1H), 7.34 (d, *J* = 4.8 Hz, 4H), 7.30–7.24 (m, 1H), 7.09 (dd, *J* = 9.2, 2.4 Hz, 1H), 6.79 (d, *J* = 2.4 Hz, 1H), 3.70 (s, 3H), 3.53 (s, 2H), 3.30 (t, *J* = 5.1 Hz, 4H), 2.53 (d, *J* = 5.4 Hz, 4H). ¹³C NMR (126 MHz, DMSO-*d*₆) δ 172.8, 165.5, 153.4, 144.7, 140.7, 137.9, 128.9, 128.2, 127.0, 126.7, 119.1, 113.7, 109.0, 100.0, 62.0, 52.2, 51.0, 47.0. HRMS (ESI-TOF) calcd for C₂₂H₂₄N₃O₃ [M + H]⁺ 378.1818, found 378.1816.

Methyl 6-Methyl-4-oxo-7-(4-phenylpiperazin-1-yl)-1,4-dihydroquinoline-3-carboxylate 8c.

—**8c** was synthesized from commercially available **10a** following general procedure H, followed by general procedures B, C, and F in 5% overall yield. ¹H NMR (400 MHz, DMSO-*d*₆) δ 12.12 (s, 1H), 8.46 (d, *J* = 5.9 Hz, 1H), 7.90 (s, 1H), 7.21 (d, *J* = 7.8 Hz, 2H), 7.11 (s, 1H), 6.98 (d, *J* = 8.2 Hz, 2H), 6.79 (t, *J* = 7.2 Hz, 1H), 3.69 (s, 3H), 3.07 (dd, *J* = 6.2, 3.7 Hz, 4H), 2.51 (t, *J* = 5.0 Hz, 4H), 2.35 (s, 3H). HRMS (ESI-TOF) calcd for C₂₂H₂₄N₃O₃ [M + H]⁺ 378.1818, found 378.1827.

Methyl 6-Methoxy-4-oxo-7-(4-phenylpiperazin-1-yl)-1,4-dihydroquinoline-3-carboxylate 8d.

—**8d** was synthesized from commercially available **10a** following general procedure H, followed by general procedures B, C, and F in 4% overall yield. ¹H NMR (400 MHz, DMSO-*d*₆) δ 12.14 (s, 1H), 8.47 (s, 1H), 7.53 (s, 1H), 7.26–7.22 (m, 2H), 7.06 (s, 1H), 7.00 (d, *J* = 8.0 Hz, 2H), 6.81 (t, *J* = 7.2 Hz, 1H), 3.90 (s, 3H), 3.72 (s, 3H), 3.31–3.25 (m, 8H). HRMS (ESI-TOF) calcd for C₂₂H₂₃N₃NaO₃ [M + Na]⁺ 416.1586, found 416.1584.

Methyl 7-(4-(4-Methoxyphenyl)piperazin-1-yl)-4-oxo-1,4-dihydroquinoline-3-carboxylate 8e.

—**8e** was synthesized from **10b** following general procedure H, followed by general procedures B, C, and F in 6% overall yield. ¹H NMR (500 MHz, DMSO-*d*₆) δ 11.93 (s, 1H), 8.43 (d, *J* = 6.0 Hz, 1H), 7.97 (d, *J* = 9.0 Hz, 1H), 7.16 (dd, *J* = 9.1, 2.3 Hz, 1H), 6.96 (d, *J* = 8.8 Hz, 2H), 6.90–6.82 (m, 3H), 3.70 (d, *J* = 9.7 Hz, 6H), 3.44 (t, *J* = 5.1 Hz,

4H), 3.17 (t, $J=5.1$ Hz, 4H). HRMS (ESI-TOF) calcd for $C_{22}H_{24}N_3O_4$ $[M + H]^+$ 394.1767, found 394.1761.

Methyl 6-Methoxy-7-(4-(4-methoxyphenyl)piperazin-1-yl)-4-oxo-1,4-

dihydroquinoline-3-carboxylate 8f.—8f was synthesized from 10b following general procedure H, followed by general procedures B, C, and F in 4% overall yield. 1H NMR (400 MHz, DMSO- d_6) δ 12.41 (s, 1H), 8.65 (s, 1H), 8.01 (s, 1H), 6.96 (d, $J=8.0$ Hz, 2H), 7.11 (s, 1H), 7.08 (d, $J=8.2$ Hz, 2H), 3.84 (s, 3H), 3.78 (s, 3H), 3.61 (s, 3H), 3.48–3.38 (m, 8H). HRMS (ESI-TOF) calcd for $C_{23}H_{26}N_3O_5$ $[M + H]^+$ 424.1872, found 424.1877.

Methyl 7-(4-Benzylpiperazin-1-yl)-6-methyl-4-oxo-1,4-dihydroquinoline-3-

carboxylate 8g.—8g was synthesized from commercially available 10c following general procedure H, followed by general procedures B, C, and F in 6% overall yield. 1H NMR (500 MHz, DMSO- d_6) δ 11.85 (s, 1H), 8.37 (s, 1H), 7.88 (s, 1H), 7.7 (d, $J=4.2$ Hz, 4H), 7.27–7.21 (m, 1H), 6.99 (s, 1H), 3.70 (s, 3H), 3.62 (s, 2H), 3.42 (t, $J=5.1$ Hz, 4H), 3.08 (s, 3H) 2.66 (d, $J=5.4$ Hz, 4H). ^{13}C NMR (126 MHz, DMSO- d_6) δ 172.8, 165.5, 155.3, 144.5, 138.4, 138.0, 129.0, 128.2, 127.5, 127.0, 122.3, 109.1, 106.7, 103.2, 62.1, 52.8, 51.0, 50.9, 18.0. HRMS (ESI-TOF) calcd for $C_{23}H_{26}N_3O_3$ $[M + H]^+$ 392.1974, found 392.1975.

Methyl 7-(4-Benzylpiperazin-1-yl)-6-methoxy-4-oxo-1,4-dihydroquinoline-3-

carboxylate 8h.—8h was synthesized from commercially available 10c following general procedure H, followed by general procedures B, C, and F in 8% overall yield. 1H NMR (500 MHz, DMSO- d_6) δ 12.12 (s, 1H), 8.11 (s, 1H), 7.46 (s, 1H), 7.21 (d, $J=3.9$ Hz, 4H), 7.19–7.11 (m, 1H), 6.89 (s, 1H), 3.58 (s, 3H), 3.51 (s, 2H), 3.37 (t, $J=5.1$ Hz, 4H), 3.01 (s, 3H) 2.64 (d, $J=5.4$ Hz, 4H). HRMS (ESI-TOF) calcd for $C_{23}H_{26}N_3O_4$ $[M + H]^+$ 408.1923, found 408.1918.

Methyl 7-(4-(4-Methoxybenzyl)piperazin-1-yl)-4-oxo-1,4-dihydroquinoline-3-

carboxylate 8i.—8i was synthesized from 10d following general procedure H, followed by general procedures B, C, and F 10% overall yield. 1H NMR (400 MHz, DMSO- d_6) δ 11.90 (s, 1H), 8.41 (s, 1H), 7.93 (d, $J=9.2$ Hz, 1H), 7.26–7.22 (m, 2H), 7.08 (dd, $J=9.2$, 2.3 Hz, 1H), 6.91–6.88 (m, 2H), 6.78 (d, $J=2.4$ Hz, 1H), 3.72 (d, $J=14.9$ Hz, 10H), 3.46 (s, 2H), 3.28 (d, $J=6.8$ Hz, 4H). ^{13}C NMR (126 MHz, DMSO- d_6) δ 172.8, 165.5, 158.4, 153.3, 144.7, 140.7, 130.2, 126.7, 119.1, 113.7, 113.6, 109.0, 99.9, 61.3, 55.0, 52.1, 51.0, 47.0. HRMS (ESI-TOF) calcd for $C_{23}H_{26}N_3O_4$ $[M + H]^+$ 408.1923, found 408.1911.

Methyl 4-Oxo-7-((4-phenylpiperazin-1-yl)methyl)-1,4-dihydroquinoline-3-

carboxylate 8j.—8j was synthesized from 7j following general procedure F as a pale-yellow solid in 32% yield. 1H NMR (400 MHz, DMSO- d_6): δ 12.58 (s, 1H), 8.57 (d, $J=6.4$, 1H), 8.22 (d, $J=7.9$, 1H), 7.69 (s, 1H), 7.51 (d, $J=8.0$, 1H), 7.22 (t, $J=7.9$, 2h), 6.94 (d, $J=8.1$, 2h), 6.82 (t, $J=7.2$, 1H), 3.78 (s, 2h), 3.72 (s, 3h), 3.53 (m, 4H), 3.21 (s, 4H). ^{13}C NMR (101 MHz, DMSO- d_6): 5 173.7, 165.9, 151.4, 145.7, 143.8, 139.8, 129.3 (2C), 126.8, 126.1, 125.8, 119.3, 118.7, 115.8 (2C), 109.8, 61.8, 53.1 (2C), 51.5, 48.7 (2C). HRMS (ESI-TOF) calcd for $C_{22}H_{24}N_3O_3$ $[M + H]^+$ 378.1818, found 378.1815.

Methyl 7-((4-Benzylpiperazin-1-yl)methyl)-4-oxo-1,4-dihydroquinoline-3-carboxylate 8k.—8k was synthesized from 7k following general procedure F as a pale-yellow solid in 26% yield. ¹H NMR (400 MHz, methanol-*d*₄): δ 8.67 (s, 1H), 7.95 (d, *J* = 8.3, 1H), 7.61 (s, 1H), 7.47–7.34 (m, 6H), 4.41 (s, 2H), 4.30 (s, 2H), 3.83 (s, 3H), 3.61 (s, 4H), 3.49 (s, 4H). ¹³C NMR (101 MHz, methanol-*d*₄): δ 175.3, 165.6, 145.8 (2C), 138.8, 137.6, 130.9 (2C), 129.8, 128.8 (2C), 127.1, 126.4, 120.6, 117.7, 108.5, 60.0, 59.7, 50.9, 50.0 (2C), 48.9 (2C). HRMS (ESI-TOF) calcd for C₂₃H₂₆N₃O₃ [M + H]⁺ 392.1974, found 392.1968.

Methyl 7-((4-(4-Methoxybenzyl)piperazin-1-yl)methyl)-4-oxo-1,4-dihydroquinoline-3-carboxylate 8l.—8l was synthesized from 7l following general procedure F as a light-brown solid in 21% yield. ¹H NMR (400 MHz, DMSO-*d*₆): δ 12.27 (s, 1H), 8.52 (s, 1H), 8.08 (d, *J* = 8.0, 1H), 7.52 (s, 1H), 7.32 (d, *J* = 8.1, 1H), 7.17 (d, *J* = 7.0, 2H), 6.85 (d, *J* = 6.8, 2H), 3.74 (s, 2H), 3.57 (s, 3H), 3.36 (m, 4H), 2.38 (m, 4H). ¹³C NMR (126 MHz, DMSO-*d*₆) δ 173.8, 165.6, 159.5, 145.4, 139.4, 132.0, 131.7, 126.8, 126.1, 125.8, 118.7, 114.8, 114.1, 109.8, 79.6, 79.3, 78.9, 61.2, 55.4 (2C), 51.7 (2C), 51.4 (2C). HRMS (ESI-TOF) calcd for C₂₄H₂₈N₃ [M + H]⁺ 422.2080, found 422.2071.

Methyl 7-((4-(Benzo[d][1,3]dioxol-5-ylmethyl)piperazin-1-yl)-methyl)-4-oxo-1,4-dihydroquinoline-3-carboxylate 8m.—8m was synthesized from 7m following general procedure F as a pale-yellow solid in 15% yield. ¹H NMR (400 MHz, DMSO-*d*₆): δ 12.33 (bs, 1H), 8.51 (s, 1H), 8.10 (s, 1H), 7.52 (s, 1H), 7.35 (s, 1H), 6.98–6.89 (m, 3H), 6.00 (s, 2H), 3.92 (m, 4H), 3.70 (s, 3H), 2.82 (m, 8H). ¹³C NMR (126 MHz, DMSO-*d*₆) δ 173.24, 165.39, 147.16, 146.10, 145.01, 143.62, 139.05, 131.94, 126.27, 125.63, 125.27, 121.90, 117.89, 109.45, 109.02, 107.80, 100.74, 61.71, 61.39, 52.72 (2C), 52.42 (2C), 51.09. HRMS (ESI-TOF) calcd for C₂₄H₂₆N₃O₅ [M + H]⁺ 436.1872, found 436.1853.

Methyl 7-((4-(4-Methoxyphenyl)piperazin-1-yl)methyl)-4-oxo-1,4-dihydroquinoline-3-carboxylate 8n.—8n was synthesized from 7n following general procedure F as a pale-yellow solid in 20% yield. ¹H NMR (400 MHz, DMSO-*d*₆): δ 12.31 (s, 1H), 8.55 (s, 1H), 8.12 (d, *J* = 8.2 Hz, 1H), 7.60 (s, 1H), 7.38 (d, *J* = 8.3 Hz, 1H), 6.88 (d, *J* = 8.7 Hz, 2H), 6.81 (d, *J* = 9.1 Hz, 2H), 3.74 (s, 3H), 3.68 (s, 3H), 3.65 (s, 2H), 3.03 (t, *J* = 4.6 Hz, 4H), 2.58–2.53 (m, 4H). ¹³C NMR (101 MHz, DMSO-*d*₆): δ 173.7, 165.9, 153.3, 145.8, 145.5, 143.9, 139.5, 126.8, 126.1, 125.8, 118.5, 117.8 (2C), 114.7 (2C), 109.9, 61.9, 55.6, 53.2 (2C), 51.6, 50.1 (2C). HRMS (ESI-TOF) calcd for C₂₃H₂₆N₃O₄ [M + H]⁺ 408.1923, found 408.1902.

Methyl 7-((4-(4-Fluorophenyl)piperazin-1-yl)methyl)-4-oxo-1,4-dihydroquinoline-3-carboxylate 8o.—8o was synthesized from 7o following general procedure F as a pale-yellow solid in 20% yield. ¹H NMR (400 MHz, DMSO-*d*₆): δ 12.29 (s, 1H), 8.53 (s, 1H), 8.10 (d, *J* = 8.3 Hz, 1H), 7.57 (d, *J* = 1.4 Hz, 1H), 7.35 (dd, *J* = 8.2, 1.5 Hz, 1H), 7.04–6.98 (m, 2H), 6.93–6.89 (m, 2H), 3.72 (s, 3H), 3.63 (s, 2H), 3.07 (t, *J* = 4.9 Hz, 4H), 2.53 (t, *J* = 4.9 Hz, 4H). ¹³C NMR (101 MHz, DMSO-*d*₆): δ 173.7, 165.8, 157.6, 155.3, 148.3, 145.5, 143.8, 139.5, 126.8, 126.1, 125.8, 118.5, 117.6, 117.5, 115.8, 115.6,

109.9, 61.8, 53.1 (2C), 51.5, 49.5 (2C). HRMS (ESI-TOF) calcd for $C_{22}H_{22}FN_3NaO_3$ [M + Na]⁺ 418.1543, found 418.1539.

Methyl 4-Oxo-7-((4-(4-(trifluoromethyl)phenyl)piperazin-1-yl)methyl)-1,4-dihydroquinoline-3-carboxylate 8p.—**8p** was synthesized from **7p** following general procedure F as a pale-yellow solid in 35% yield. ¹H NMR (400 MHz, DMSO-*d*₆): δ 12.30 (s, 1H), 8.54 (s, 1H), 8.12 (d, *J* = 8.2 Hz, 1H), 7.58 (s, 1H), 7.48 (d, *J* = 8.5 Hz, 2H), 7.37 (dd, *J* = 8.2, 1.5 Hz, 1H), 7.04 (d, *J* = 8.6 Hz, 2H), 3.73 (s, 3H), 3.65 (s, 2H), 3.32–3.27 (m, 4H), 2.54 (t, *J* = 5.0 Hz, 4H). HRMS (ESI-TOF) calcd for $C_{23}H_{23}F_3N_3O_3$ [M + H]⁺ 446.1692, found 446.1670.

Methyl 6-Methyl-4-oxo-7-((4-phenylpiperazin-1-yl)methyl)-1,4-dihydroquinoline-3-carboxylate 8q.—**8q** was synthesized from **7q** following general procedure F as a pale-yellow solid in 30% yield. ¹H NMR (400 MHz, DMSO-*d*₆): δ 12.22 (s, 1H), 8.48 (s, 1H), 7.89 (s, 1H), 7.58 (s, 1H), 7.16 (t, *J* = 7.8 Hz, 2H), 6.89 (d, *J* = 8.1 Hz, 2H), 6.73 (t, *J* = 7.3 Hz, 1H), 3.69 (s, 3H), 3.56 (s, 2H), 3.11 (m, 4H), 2.55 (t, *J* = 5.0 Hz, 4H), 2.37 (s, 3H). ¹³C NMR (101 MHz, DMSO-*d*₆): δ 173.6, 165.9, 151.4, 145.0, 137.6, 134.3, 129.4 (2C), 126.5 (2C), 119.3, 118.8 (2C), 115.8 (2C), 109.6, 59.7, 53.3 (2C), 51.5, 48.8 (2C), 19.2. HRMS (ESI-TOF) calcd for $C_{23}H_{26}N_3O_3$ [M + H]⁺ 392.1974, found 392.1981.

Methyl 7-((4-Benzylpiperazin-1-yl)methyl)-6-methyl-4-oxo-1,4-dihydroquinoline-3-carboxylate 8r.—**8r** was synthesized from **7r** following general procedure F as a pale-yellow solid in 23% yield. ¹H NMR (400 MHz, DMSO-*d*₆): δ 12.20 (s, 1H), 8.47 (s, 1H), 7.89 (d, *J* = 1.0 Hz, 1H), 7.52 (s, 1H), 7.33–7.17 (m, 5H), 3.72 (s, 3H), 3.51 (s, 2H), 3.46 (s, 2H), 2.45–2.40 (m, 8H), 2.37 (s, 3H). ¹³C NMR (126 MHz, DMSO-*d*₆): δ 173.07, 165.53, 144.62, 142.18, 138.07, 137.18, 133.88, 128.86 (2C), 128.16 (2C), 126.92, 126.01, 125.94, 118.24, 109.14, 62.07, 59.35, 52.91 (2C), 52.67 (2C), 51.05, 18.68. HRMS (ESI-TOF) calcd for $C_{24}H_{28}N_3O_3$ [M + H]⁺ 406.2131, found 406.2122.

Methyl 7-((4-(4-Methoxybenzyl)piperazin-1-yl)methyl)-6-methyl-4-oxo-1,4-dihydroquinoline-3-carboxylate 8s.—**8s** was synthesized from **7s** following general procedure F as a pale-yellow solid in 20% yield. ¹H NMR (400 MHz, DMSO-*d*₆): δ 12.27 (s, 1H), 8.51 (s, 1H), 7.91 (s, 1H), 7.56 (s, 1H), 7.20 (d, *J* = 7.8 Hz, 2H), 6.88 (d, *J* = 8.0 Hz, 2H), 3.74 (s, 6H), 3.52 (s, 2H), 3.41 (s, 2H), 2.45 (bs, 8H), 2.38 (s, 3H). ¹³C NMR (101 MHz, DMSO-*d*₆): δ 173.6, 165.9, 158.7, 145.0 (2C), 142.6, 137.6, 134.2, 130.6 (2C), 126.5, 126.5, 118.7, 114.0 (2C), 109.6, 61.9, 59.8, 55.4 (2C), 53.3, 53.0 (2C), 51.5, 19.1. HRMS (ESI-TOF) calcd for $C_{25}H_{29}N_3NaO_4$ [M + Na]⁺ 458.2056, found 458.2056.

Methyl 7-((4-(4-Methoxyphenyl)piperazin-1-yl)methyl)-6-methyl-4-oxo-1,4-dihydroquinoline-3-carboxylate 8t.—**8t** was synthesized from **7t** following general procedure F as a pale-yellow solid in 22% yield. ¹H NMR (400 MHz, DMSO-*d*₆): δ 12.26 (s, 1H), 8.55–8.45 (m, 1H), 7.93 (d, *J* = 4.8 Hz, 1H), 7.59 (d, *J* = 4.8 Hz, 1H), 6.87–6.84 (m, 2H), 6.81–6.78 (m, 2H), 3.73 (s, 3H), 3.67 (s, 3H), 3.66 (s, 2H), 3.04 (bs, 4H), 2.66 (bs, 4H), 2.41 (s, 3H). ¹³C NMR (101 MHz, DMSO-*d*₆): δ 173.2, 165.4, 153.0, 144.6 (2C), 137.1

(2C), 133.9, 126.2, 117.4 (2C), 114.2 (2C), 114.2 (2C), 109.1, 79.2, 78.9, 78.5, 55.1, 52.8 (2C), 51.0, 49.6 (2C), 18.8. HRMS (ESI-TOF) calcd for $C_{24}H_{28}N_3O_4$ $[M + H]^+$ 422.2080, found 422.2076.

Methyl 7-((4-(4-Fluorophenyl)piperazin-1-yl)methyl)-6-methyl-4-oxo-1,4-dihydroquinoline-3-carboxylate 8u.—**8u** was synthesized from **7u** following general procedure F as a pale-yellow solid in 30% yield. 1H NMR (400 MHz, DMSO- d_6): δ 12.23 (s, 1H), 8.50 (s, 1H), 7.92 (s, 1H), 7.59 (s, 1H), 7.03 (t, J = 8.7 Hz, 2H), 6.93 (dd, J = 9.2, 4.6 Hz, 2H), 3.72 (s, 3H), 3.59 (s, 2H), 3.10 (t, J = 4.8 Hz, 4H), 2.58 (t, J = 4.7 Hz, 4H), 2.41 (s, 3H). ^{13}C NMR (101 MHz, DMSO- d_6) δ 173.12, 165.48, 157.15, 154.81, 147.91, 144.57, 141.99, 137.19, 133.87, 126.08, 118.38, 117.10, 117.02, 115.36, 115.14, 109.19, 59.30, 52.81 (2C), 51.05, 49.13 (2C), 18.71. HRMS (ESI-TOF) calcd for $C_{23}H_{25}FN_3O_3$ $[M + H]^+$ 410.1880, found 410.1865.

Methyl 6-Methyl-4-oxo-7-((4-(4-(trifluoromethyl)phenyl)-piperazin-1-yl)methyl)-1,4-dihydroquinoline-3-carboxylate 8v.—**8v** was synthesized from **7v** following general procedure F as a pale-yellow solid in 35% yield. 1H NMR (400 MHz, DMSO- d_6): δ 12.25 (s, 1H), 8.51 (s, 1H), 7.92 (s, 1H), 7.60 (s, 1H), 7.49 (d, J = 8.5 Hz, 2H), 7.05 (d, J = 8.6 Hz, 2H), 3.72 (s, 3H), 3.59 (s, 2H), 3.29 (m, 4H), 2.62–2.54 (m, 4H), 2.40 (s, 3H). HRMS (ESI-TOF) calcd for $C_{24}H_{25}F_3N_3O_3$ $[M + H]^+$ 460.1848, found 460.1854.

Methyl 6-Methoxy-4-oxo-7-((4-phenylpiperazin-1-yl)methyl)-1,4-dihydroquinoline-3-carboxylate 8w.—**8w** was synthesized from **7w** following general procedure F as a pale-yellow solid in 16% yield. 1H NMR (400 MHz, DMSO- d_6): δ 12.29 (s, 1H), 8.52–8.42 (m, 1H), 7.72 (d, J = 14.8 Hz, 1H), 7.59–7.51 (m, 1H), 7.25–7.12 (m, 2H), 6.93 (d, J = 8.3 Hz, 2H), 6.76 (t, J = 7.2 Hz, 1H), 3.87 (s, 3H), 3.70 (m, 3H), 3.61 (d, J = 13.9 Hz, 2H), 3.21–3.12 (m, 4H), 2.61 (t, J = 5.0 Hz, 4H). ^{13}C NMR (126 MHz, DMSO- d_6) δ 172.79, 165.56, 154.83, 151.04, 143.70, 133.30, 133.24, 128.95 (2C), 127.12, 119.10, 118.85, 115.34 (2C), 108.33, 104.08, 55.65, 55.22, 52.93 (2C), 51.06, 48.36 (2C). HRMS (ESI-TOF) calcd for $C_{23}H_{26}N_3O_4$ $[M + H]^+$ 408.1923, found 408.1903.

Methyl 7-((4-Benzylpiperazin-1-yl)methyl)-6-methoxy-4-oxo-1,4-dihydroquinoline-3-carboxylate 8x.—**8x** was synthesized from **7x** following general procedure F as a pale-yellow solid in 15% yield. 1H NMR (500 MHz, DMSO- d_6): 12.30 (bs, 1H), δ 8.48 (s, 1H), 7.67 (s, 1H), 7.53 (s, 1H), 7.33–7.23 (m, 5H), 3.85 (s, 3H), 3.72 (s, 3H), 3.55 (s, 2H), 3.47 (s, 2H), 2.44 (m, 8H). HRMS (ESI-TOF) calcd for $C_{24}H_{28}N_3O_4$ $[M + H]^+$ 422.2080, found 422.2093.

Methyl 6-Methoxy-7-((4-(4-methoxybenzyl)piperazin-1-yl)-methyl)-4-oxo-1,4-dihydroquinoline-3-carboxylate 8y.—**8y** was synthesized from **7y** following general procedure F as a pale-yellow solid in 15% yield. 1H NMR (500 MHz, DMSO- d_6) δ 12.30 (s, 1H), 8.49 (s, 1H), 7.68 (s, 1H), 7.54 (s, 1H), 7.20 (d, J = 8.1 Hz, 2H), 6.88 (d, J = 8.1 Hz, 2H), 3.87 (s, 3H), 3.74 (s, 3H), 3.72 (s, 3H), 3.56 (s, 2H), 3.42 (s, 2H), 2.44 (bs, 8H). ^{13}C NMR (126 MHz, DMSO- d_6) δ 172.6, 165.5, 158.3, 154.6, 143.5, 133.3, 133.2, 130.1 (2C), 129.9, 126.9, 118.7, 113.5 (2C), 108.3, 104.0, 61.5, 55.6, 55.2, 55.0, 53.0 (2C), 52.5 (2C), 51.0. HRMS (ESI-TOF) calcd for $C_{25}H_{30}N_3O_5$ $[M + H]^+$ 452.2185, found 452.2175.

Methyl 6-Methoxy-7-((4-(4-methoxyphenyl)piperazin-1-yl)methyl)-4-oxo-1,4-dihydroquinoline-3-carboxylate 8z.—8z was synthesized from 7z following general procedure F as a pale-yellow solid in 20% yield. ¹H NMR (400 MHz, DMSO-*d*₆): δ 12.29 (s, 1H), 8.48 (s, 1H), 7.72 (s, 1H), 7.55 (s, 1H), 6.91–6.85 (m, 2H), 6.80 (d, *J* = 9.0 Hz, 2H), 3.87 (s, 3H), 3.71 (s, 3H), 3.66 (s, 3H), 3.62 (s, 2H), 3.05 (t, *J* = 4.7 Hz, 4H), 2.60 (t, *J* = 4.8 Hz, 4H). ¹³C NMR (101 MHz, DMSO-*d*₆): δ 173.2, 165.9, 155.2, 153.3, 145.8, 144.1, 133.7 (2C), 127.5, 119.5, 117.7 (2C), 114.7 (2C), 108.8, 104.5, 56.1, 55.6, 53.4 (2C), 51.5, 50.2 (2C). HRMS (ESI-TOF) calcd for C₂₄H₂₈N₃O₅ [M + H]⁺ 438.2029, found 438.2009.

Methyl 7-((4-(4-Fluorophenyl)piperazin-1-yl)methyl)-6-methoxy-4-oxo-1,4-dihydroquinoline-3-carboxylate 8aa.—8aa was synthesized from 7aa following general procedure F as a pale-yellow solid in 28% yield. ¹H NMR (400 MHz, DMSO-*d*₆): δ 12.29 (s, 1H), 8.49 (s, 1H), 7.73 (s, 1H), 7.56 (s, 1H), 7.03 (t, *J* = 8.7 Hz, 2H), 6.94 (dd, *J* = 9.2, 4.7 Hz, 2h), 3.88 (s, 3h), 3.72 (s, 3H), 3.63 (s, 2H), 3.12 (t, *J* = 4.6 Hz, 4H), 2.61 (t, *J* = 4.8 Hz, 4H). ¹³C NMR (101 MHz, DMSO-*d*₆): δ 173.2, 166.0, 157.6, 155.2, 148.4, 144.1, 133.7, 133.6, 127.6, 119.5, 1117.5, 115.8, 115.6, 108.8, 104.5, 56.1, 55.6, 53.3 (2C), 51.5, 49.6 (2C). HRMS (ESI-TOF) calcd for C₂₃H₂₅FN₃O₄ [M + H]⁺ 426.1829; found 426.1817.

Methyl 6-Methoxy-4-oxo-7-((4-(4-(trifluoromethyl)phenyl)piperazin-1-yl)methyl)-1,4-dihydroquinoline-3-carboxylate 8ab.—8ab was synthesized from 7ab following general procedure F as a pale-yellow solid in 30% yield. ¹H NMR (400 MHz, DMSO-*d*₆): δ 12.29 (s, 1H), 8.49 (s, 1H), 7.73 (s, 1H), 7.56 (s, 1H), 7.49 (d, *J* = 8.5 Hz, 2H), 7.06 (d, *J* = 8.6 Hz, 2H), 3.88 (s, 3h), 3.72 (s, 3H), 3.63 (s, 2H), 3.32 (m, 4H), 2.61 (t, *J* = 4.8 Hz, 4H). ¹³C NMR (101 MHz, DMSO-*d*₆) δ 172.78, 165.40, 154.77 (2C), 153.10, 143.78, 143.61, 133.17 (2C), 126.08 (2C), 126.03 (2C), 114.07 (2C), 108.26, 104.07, 55.56, 55.02, 52.45 (2C), 50.92, 46.98 (2C). HRMS (ESI-TOF) calcd for C₂₄H₂₅F₃N₃O₄ [M + H]⁺ 476.1797, found 476.1796.

Methyl 4-Oxo-7-(2-(4-phenylpiperazin-1-yl)ethyl)-1,4-dihydroquinoline-3-carboxylate 8ac.—8ac was synthesized from 5ac following general procedures C and F as a pale-brown solid in 23% yield over two steps. ¹H NMR (400 MHz, DMSO-*d*₆): δ 12.59 (bs, 1H), 8.55 (s, 1H), 8.25 (m, 1H), 7.49 (s, 1h), 7.35 (d, *J* = 10.5, 1H), 7.26 (t, *J* = 7.9, 2h), 7.01 (d, *J* = 8.1, 2h), 6.86 (t, *J* = 7.3, 1H), 3.85 (m, 2h), 3.73 (s, 3h), 3.51–3.43 (m, 4H), 3.24–3.16 (m, 4H), 3.02 (m, 2H). HRMS (ESI-TOF) calcd for C₂₃H₂₆N₃O₃ [M + H]⁺ 392.1974, found 392.1955

Methyl 7-(2-(4-Benzylpiperazin-1-yl)ethyl)-4-oxo-1,4-dihydroquinoline-3-carboxylate 8ad.—8ad was synthesized from 5ad following general procedures C and F as a brown solid in 15% yield over two steps. ¹H NMR (400 MHz, DMSO-*d*₆): δ 12.22 (s, 1H), 8.50 (s, 1H), 8.04 (s, 1H), 7.41 (s, 1H), 7.28 (m, 6H), 3.72 (s, 3H), 3.44 (s, 2h), 3.31 (s, 2H), 2.84 (m, 2H), 2.48–2.37 (m, 8H). HRMS (ESI-TOF) calcd for C₂₄H₂₈N₃O₃ [M + H]⁺ 406.2131, found 406.2123.

Methyl 7-(2-(4-(4-Methoxybenzyl)piperazin-1-yl)ethyl)-4-oxo-1,4-dihydroquinoline-3-carboxylate 8ae.—8ae was synthesized from 5ae following general procedures C and F as a brown solid in 11% yield over two steps. ¹H NMR (400

MHz, DMSO- d_6) δ 12.24 (bs, 1H), 8.52 (s, 1H), 8.05 (d, J = 7.9 Hz, 1H), 7.42 (s, 1H), 7.29 (s, 1H), 7.19 (d, J = 7.9 Hz, 2H), 6.87 (d, J = 8.1 Hz, 2H), 3.77 (m, 6H), 3.46–3.36 (m, 4H), 2.85 (t, J = 7.4 Hz, 2H), 2.60–2.37 (m, 8H). HRMS (ESI-TOF) calcd for $C_{25}H_{30}N_3O_4$ [M + H]⁺ 436.2236, found 436.2235.

Methyl 4-Oxo-6-((4-phenylpiperazin-1-yl)methyl)-1,4-dihydroquinoline-3-carboxylate 8af.—8af was synthesized following general procedure F as a pale-yellow solid in 42% yield. ¹H NMR (400 MHz, DMSO- d_6): δ 12.36 (s, 1H), 8.55 (s, 1H), 8.09 (s, 1H), 7.67 (s, 1H), 7.61 (s, 1H), 7.19 (s, 2H), 6.91 (d, J = 7.2 Hz, 2H), 6.76 (s, 1H), 3.74 (s, 3H), 3.64 (s, 2H), 3.13 (m, 4H), 2.50 (m, 4H). HRMS (ESI-TOF) calcd for $C_{22}H_{24}N_3O_3$ [M + H]⁺ 378.1818, found 378.1803.

Methyl 6-((4-(4-Methoxyphenyl)piperazin-1-yl)methyl)-4-oxo-1,4-dihydroquinoline-3-carboxylate 8ag.—8ag was synthesized following general procedure F as a pale-yellow solid in 36% yield. ¹H NMR (400 MHz, DMSO- d_6): δ 12.34 (s, 1H), 8.53 (s, 1H), 8.07 (s, 1H), 7.68–7.63 (m, 1H), 7.57 (d, J = 8.4 Hz, 1H), 6.85 (d, J = 9.1 Hz, 2H), 6.78 (d, J = 9.1 Hz, 2H), 3.72 (s, 3H), 3.65 (s, 3H), 3.61 (s, 2H), 2.99 (m, 4H), 2.49 (m, 4H). HRMS (ESI-TOF) calcd for $C_{23}H_{26}N_3O_4$ [M + H]⁺ 408.1923, found 408.1935.

Methyl 6-((4-(4-Fluorophenyl)piperazin-1-yl)methyl)-4-oxo-1,4-dihydroquinoline-3-carboxylate 8ah.—8ah was synthesized following general procedure F as a pale-yellow solid in 45% yield. ¹H NMR (400 MHz, DMSO- d_6): δ 12.36 (s, 1H), 8.54 (s, 1H), 8.08 (s, 1H), 7.67 (d, J = 7.7 Hz, 1H), 7.58 (d, J = 8.4 Hz, 1H), 7.01 (t, J = 8.3 Hz, 2H), 6.92 (d, J = 4.1 Hz, 2H), 3.73 (s, 3H), 3.62 (s, 2H), 3.06 (s, 4H), 2.50 (s, 4H). HRMS (ESI-TOF) calcd for $C_{22}H_{23}FN_3O_3$ [M + H]⁺ 396.1723, found 396.1714.

Methyl 4-Oxo-6-((4-(4-(trifluoromethyl)phenyl)piperazin-1-yl)-methyl)-1,4-dihydroquinoline-3-carboxylate 8ai.—8ai was synthesized following general procedure F as a pale-yellow solid in 45% yield. ¹H NMR (400 MHz, DMSO- d_6): δ 12.29 (s, 1H), 8.50 (s, 1H), 8.06 (s, 1H), 7.63 (d, J = 8.5 Hz, 1H), 7.54 (d, J = 8.5 Hz, 1H), 7.42 (d, J = 8.6 Hz, 2H), 6.97 (d, J = 8.7 Hz, 2H), 3.69 (d, J = 10.0 Hz, 3H), 3.60 (s, 2H), 3.23 (m, 4H), 2.49 (m, 4H). HRMS (ESI-TOF) calcd for $C_{23}H_{23}F_3N_3O_3$ [M + H]⁺ 446.1692, found 446.1685.

3-Bromo-7-((4-(4-fluorophenyl)piperazin-1-yl)methyl)quinolin-4(1H)-one 8ak.—The enamine intermediate **15aj** (270 mg, 0.61 mmol) in toluene was subjected to microwave heating at 260 °C for 5 min. The reaction was allowed to cool to RT and concentrated under reduced pressure. The resultant crude was an inseparable mixture of quinolone regioisomers. To a stirred solution of quinolone isomers in anhydrous CH_2Cl_2 was added freshly recrystallized NBS (127.0 mg, 0.71 mmol) at RT, and the resulting mixture was stirred overnight. The reaction mixture was concentrated under reduced pressure and the residue was purified by preparative HPLC to give the desired **8ak** as a pale-yellow solid (40 mg, 16% over two steps). ¹H NMR (400 MHz, DMSO- d_6): δ 12.50 (d, J = 6.4 Hz, 1H), 8.53 (d, J = 6.3 Hz, 1H), 8.24 (d, J = 8.3 Hz, 1H), 7.73 (s, 1H), 7.54 (d, J = 8.4 Hz, 1H), 7.13–7.06 (m, 2H), 7.02–6.97 (m, 2H), 3.74 (d, J = 13.3 Hz, 2H), 3.44 (d, J = 12.2 Hz, 3H), 3.25 (d, J = 11.1

Hz, 3h), 2.97 (d, J = 12.6 Hz, 2H). ^{13}C NMR (126 MHz, DMSO- d_6) δ 171.16, 155.72, 146.31, 140.70, 139.13, 133.29, 126.48, 126.21, 12–4.56, 121.79, 117.98, 117.92, 115.65, 115.48, 104.77, 58.11, 50.69 (2C), 46.23 (2C). HRMS (ESI-TOF) calcd for $\text{C}_{20}\text{H}_{20}\text{BrFN}_3\text{O}$ $[\text{M} + \text{H}]^+$ 416.0774, found 416.0778.

3-Chloro-7-((4-(4-fluorophenyl)piperazin-1-yl)methyl)quinolin-4(1H)-one 8al.—

The enamine intermediate **15aj** (270 mg, 0.61 mmol) in toluene was subjected to microwave heating at 260 °C for 5 min. The reaction was allowed to cool to RT and concentrated under reduced pressure. The resultant crude was an inseparable mixture of quinolone regio-isomers. To a stirred solution of quinolone isomers in anhydrous CH_2Cl_2 was added freshly recrystallized NCS (94.0 mg, 0.71 mmol) at RT, and the resulting mixture was stirred overnight. The reaction mixture was concentrated under reduced pressure, and the residue was purified by preparative HPLC to give the desired **8al** as a pale-yellow solid (34 mg, 15% over two steps). ^1H NMR (400 MHz, DMSO- d_6): δ 12.71 (s, 1H), 8.39 (d, J = 4.8 Hz, 1H), 8.20 (d, J = 8.3 Hz, 1H), 7.86 (d, J = 1.5 Hz, 1H), 7.65 (dd, J = 8.4, 1.5 Hz, 1H), 7.08 (dd, J = 9.9, 7.8 Hz, 2H), 7.01–6.94 (m, 2H), 3.70 (d, J = 12.5 Hz, 2h), 3.37 (d, J = 11.5 Hz, 2H), 3.26–3.03 (m, 6H). ^{13}C NMR (101 MHz, methanol- d_6 and 3 drops of CDO_3) δ 173.02, 160.83, 158.42, 145.88, 140.41, 139.95, 133.89, 128.07, 127.54, 125.78, 123.04, 120.55, 120.47, 116.84, 116.61, 110.91, 60.34, 52.47 (2C), 48.94 (2C). HRMS (ESI-TOF) calcd for $\text{C}_{20}\text{H}_{20}\text{ClFN}_3\text{O}$ $[\text{M} + \text{H}]^+$ 372.1279, found 372.1279.

7-((4-(4-Fluorophenyl)piperazin-1-yl)methyl)-2-methylquinolin-4(1H)-one 8am.

—A mixture of aniline **5aj** (2.0 g, 7.01 mmol) and ethyl acetoacetate (1.34 mL, 10.5 mmol) in benzene (20 mL) and AcOH (cat.) was heated to reflux in an oven-dried round-bottom flask equipped with Dean—Stark trap and a reflux condenser until no water separates out (usually overnight). The solvents were removed under reduced pressure, and the resulting crude intermediate after thorough drying under vacuo was used in next step without further purification. The enamine intermediate in toluene was subjected to microwave heating at 260 °C for 5 min. The reaction mixture was allowed to cool to RT. The crude mixture containing quinolone regio-isomers was then refluxed in methanol for 1 h and filtered to give the unwanted isomer as a white solid. The methanolic solution (filtrate) after evaporation gave 950 mg (39% yield) of light-brown amorphous **8am** in pure form. ^1H NMR (400 MHz, methanol- d_6): δ 8.14 (t, J = 5.5 Hz, 1H), 7.54 (s, 1H), 7.38 (dd, J = 8.4, 1.4 Hz, 1H), 6.94 (d, J = 2.2 Hz, 2H), 6.93 (d, J = 2.4 Hz, 2H), 6.17 (s, 1h), 3.69 (s, 2h), 3.13–3.09 (m, 4H), 2.67–2.62 (m, 4H), 2.44 (s, 3H). HRMS (ESI-TOF) calcd for $\text{C}_{21}\text{H}_{23}\text{FN}_3\text{O}$ $[\text{M} + \text{H}]^+$ 352.1825, found 352.1829.

3-Bromo-7-((4-(4-Fluorophenyl)piperazin-1-yl)methyl)-2-methylquinolin-4(1H)-one 8an.—

To a stirred solution of quinolone **8am** (50.0 mg, 0.14 mmol) in anhydrous CH_2Cl_2 was added freshly recrystallized NBS (30.0 mg, 0.17 mmol) at RT, and the resulting mixture was stirred overnight. The reaction mixture was filtered, and the solid was washed with EtOAc followed by MeOH to give the purest **8an** as an off-white solid (25 mg, 42% yield). ^1H NMR (400 MHz, DMSO- d_6): δ 12.07 (s, 1H), 8.04 (d, J = 8.3 Hz, 1H), 7.54 (s, 1H), 7.31 (d, J = 8.3 Hz, 1H), 7.03 (t, J = 8.7 Hz, 2H), 6.93 (dd, J = 9.3, 4.6 Hz, 2H), 3.65 (s, 2H), 3.10–3.08 (m, 4H), 2.58–2.55 (m, 4H), 2.54 (s, 3H). ^{13}C NMR (126 MHz, DMSO- d_6)

δ 171.20, 158.04, 156.16, 149.85, 146.83, 138.97, 126.62, 126.46, 123.53, 118.42, 118.36, 116.09, 115.92, 109.99, 106.97, 58.70, 51.19 (2C), 46.83 (2C), 21.86. HRMS (ESI-TOF) calcd for C₂₁H₂₂BrFN₃O [M + H]⁺ 430.0930, found 430.0938.

3-Chloro-7-((4-(4-fluorophenyl)piperazin-1-yl)methyl)-2-methylquinolin-4(1H)-one 8ao.—To a stirred solution of quinolone **8am** (50.0 mg, 0.14 mmol) in anhydrous CH₂Cl₂ was added freshly recrystallized NCS (23.0 mg, 0.17 mmol) at RT, and the resulting mixture was stirred overnight. The reaction mixture was concentrated under reduced pressure, and the residue was purified by preparative HPLC to give the purest **8ao** as a white solid (30 mg, 55% yield). ¹H NMR (400 MHz, DMSO-*d*₆): δ 12.03 (s, 1H), 8.05 (d, *J* = 8.2 Hz, 1H), 7.54 (s, 1H), 7.30 (d, *J* = 8.3 Hz, 1H), 7.03 (t, *J* = 8.9 Hz, 2H), 6.97–6.85 (m, 2H), 3.65 (s, 2H), 3.09 (t, *J* = 4.7 Hz, 4H), 2.55 (t, *J* = 4.6 Hz, 4H), 2.50 (s, 3h). HRMS (ESI-TOF) calcd for C₂₁H₂₂OFN₃O [M + h]⁺ 386.1435, found 386.1434.

3-Bromo-2-methyl-7-((4-(4-(trifluoromethyl)phenyl)piperazin-1-yl)methyl)quinolin-4(1H)-one 8aq.—A mixture of aniline **5ap** (380 mg, 1.12 mmol), ethyl acetoacetate (280 μ L, 2.98 mmol), and acetic acid (cat.) were stirred overnight in benzene (2 mL) at 100 °C in an oven-dried round-bottom equipped with a Dean–Stark trap and reflux condenser. Solvents were removed under reduced pressure, and the resulting crude intermediate was transferred with toluene (2 mL) into a microwave vessel and subjected to 260 °C in the microwave for 5 min. The resulting crude was a mixture of two quinolone isomers. The quinolone mixture (100 mg, 0.249 mmol) was brominated using NBS (53 mg, 0.299 mmol) according to the general method G. The reaction mixture was filtered, and the solid was recrystallized in methanol to give **8aq** as a pale-brown solid (6 mg, 5% yield). ¹H NMR (399 MHz, DMSO) δ 12.10 (s, 1H), 8.05 (d, *J* = 8.2 Hz, 1H), 7.54 (s, 1H), 7.49 (d, *J* = 8.6 Hz, 2H), 7.32 (d, *J* = 8.4 Hz, 1H), 7.05 (d, *J* = 8.7 Hz, 2H), 3.66 (s, 2H), 3.30 (s, 4H), 2.55 (s, 7H).

3-Chloro-2-methyl-7-((4-(4-(trifluoromethyl)phenyl)piperazin-1-yl)methyl)quinolin-4(1H)-one 8ar.—A mixture of aniline **5ap** (380 mg, 1.12 mmol), ethyl acetoacetate (280 μ L, 2.98 mmol), and acetic acid (cat.) were stirred overnight in benzene (2 mL) at 100 °C in an oven-dried round-bottom equipped with a Dean–Stark trap and reflux condenser. Solvents were removed under reduced pressure, and the resulting crude intermediate was transferred with toluene (2 mL) into a microwave vessel and subjected to 260 °C in the microwave for 5 min. The resulting crude was a mixture of two quinolone isomers. The quinolone mixture (100 mg, 0.249 mmol) was chlorinated using NCS (40 mg, 0.299 mmol) according to the general method G. The reaction mixture was filtered, and the solid was recrystallized in methanol to give **8ar** as a pale-brown solid (19 mg, 18% yield). ¹H NMR (399 MHz, DMSO) δ 12.06 (s, 1H), 8.06 (d, *J* = 8.1 Hz, 1H), 7.54 (s, 1H), 7.49 (d, *J* = 8.6 Hz, 2h), 7.31 (d, *J* = 8.4 Hz, 1h), 7.05 (d, *J* = 8.6 Hz, 2H), 3.66 (s, 2h), 3.30 (s, 4H), 2.55 (s, 4H), 2.51 (s, 3H). ¹³C NMR (100 MHz, DMSO) δ 170.5, 153.2, 142.6, 138.6, 126.2, 125.2, 122.6, 119.1, 117.1, 115.5, 114.2, 113.7, 61.4, 52.4, 47.1, 18.7.

3-Bromo-6-methoxy-2-methyl-7-((4-(4-(trifluoromethyl)phenyl)-piperazin-1-yl)methyl)quinolin-4(1H)-one 8at.—A mixture of aniline **5as** (760 mg, 1.37 mmol),

ethyl acetoacetate (520 μL , 2.74 mmol), and acetic acid (cat.) were stirred overnight in benzene (3.5 mL) at 100 °C in an oven-dried round-bottom equipped with a Dean–Stark trap and reflux condenser. Solvents were removed under reduced pressure, and the resulting crude intermediate was transferred with toluene (3.5 mL) into a microwave vessel and subjected to 260 °C in the microwave for 5 min. The resulting crude was a mixture of two quinolone isomers. The quinolone mixture (500 mg, 1.16 mmol) was brominated using NBS (250 mg, 1.39 mmol) according to the general method G. The reaction mixture was filtered, and the solid was recrystallized in methanol to give **8at** as a yellow solid (74 mg, 12% yield). ^1H NMR (399 MHz, CDCl_3 and 3 drops of TFA-*d*) δ 11.12 (s, 1H), 8.60 (s, 1h), 7.76 (d, J = 8.6 Hz, 2H), 7.73 (s, 1H), 7.59 (d, J = 8.7 Hz, 2H), 4.80 (s, 2h), 4.10 (s, 3h), 4.01 (s, 8H), 3.03 (s, 3H). ^{13}C NMR (100 MHz, CDCl_3 and 3 drops TFA-*d*) δ 162.71, 157.95, 155.49, 132.61, 132.35, 128.12 (d, J = 2.9 Hz), 126.5, 121.0, 120.1, 118.8, 116.0, 113.1, 110.3, 105.1, 102.5, 57.2, 55.2, 50.7, 50.1, 22.2.

2,2'-((4-Methoxyphenyl)azanediyl)bis(ethan-1-ol) 10b.—A mixture of *p*-anisole (36 mmol) and 2-chloroethan-1-ol (90 mmol) were added to a round-bottom flask along with DMF (72 mL) and K_2CO_3 (72 mmol) and refluxed overnight. The reaction was then concentrated and purified using flash chromatography (hexanes/ethyl acetate) to give the title compound in 85% yield as an off-white solid. ^1H NMR (500 MHz, CDCl_3) δ 7.31 (d, J = 8.3 Hz, 2H), 6.82–6.77 (m, 2H), 3.62 (dd, J = 9.4, 7.9 Hz, 4H), 3.89 (s, 3H), 2.64–2.58 (m, 4H). ^{13}C NMR (126 MHz, CDCl_3) δ 260.63, 232.07, 215.63, 210.11, 164.62, 161.32, 157.38, 157.08, 249.2, 239.6, 218.4, 214.9, 178.3, 151.8, 149.6.

2,2'-((4-Methoxybenzyl)azanediyl)bis(ethan-1-ol) 10d.—A mixture of (4-methoxyphenyl)methanamine (36 mmol) and 2-chloroethan-1-ol (90 mmol) were added to a round-bottom flask along with DMF (70 mL) and K_2CO_3 (72 mmol) and refluxed overnight. The reaction was then concentrated and purified using flash chromatography (hexanes/ethyl acetate) to give the title compound in 91% yield as an off-white solid. ^1H NMR (500 MHz, CDCl_3) δ 7.20 (d, J = 8.7 Hz, 2H), 6.86–6.81 (m, 2H), 3.76 (s, 2h), 3.62 (dd, J = 10.3, 8.6 Hz, 4H), 3.47 (s, 3H), 2.70–2.60 (m, 4H). ^{13}C NMR (126 MHz, CDCl_3) δ 260.6, 232.1, 215.6, 210.1, 164.6, 161.3, 157.4, 157.1.

Dimethyl 2-(((3-(Hydroxymethyl)phenyl)amino)methylene)-malonate 12a.—**12a** was prepared from 3-aminobenzyl alcohol (3 g, 24.4 mmol) according to general procedure C (pale-yellow solid, 6.4 g, quantitative yield). ^1H NMR (400 MHz, CDCl_3): δ 10.93 (d, J = 13.8 Hz, 1H), 8.44 (d, J = 13.8 Hz, 1H), 7.26 (t, J = 7.8 Hz, 1H), 7.11–7.04 (m, 2H), 6.97–6.93 (m, 1H), 4.63 (s, 2H), 3.77 (s, 3H), 3.70 (s, 3H), 2.83 (bs, 1H). ^{13}C NMR (101 MHz, CDCl_3): δ 169.1, 166.0, 151.9, 143.2, 139.1, 129.7, 123.2, 116.0, 115.2, 92.6, 64.3, 51.5, 51.4. HRMS (ESI-TOF) calcd for $\text{C}_{13}\text{H}_{16}\text{NO}_5$ [$\text{M} + \text{H}$] $^+$ 266.1028, found 266.1021.

Dimethyl 2-(((3-(Hydroxymethyl)-4-methylphenyl)amino)-methylene)malonate 12b.—**12b** was prepared from 5-amino-2-methoxybenzyl alcohol (3.0 g, 21.9 mmol) according to general procedure C (pale-white solid, 5.5 g, 95% yield). ^1H NMR (400 MHz, CDCl_3): δ 10.94 (d, J = 13.9 Hz, 1H), 8.44 (dd, J = 13.9, 0.7 Hz, 1H), 7.15 (d, J = 2.5 Hz, 1H), 7.07 (d, J = 8.1 Hz, 1H), 6.88 (dd, J = 8.0, 2.6 Hz, 1H), 4.62 (s, 2H), 3.76 (s, 3H), 3.71

(s, 3H), 2.21 (s, 3H). ^{13}C NMR (101 MHz, CDCl_3): δ 169.2, 166.1, 152.1, 140.8, 137.0, 132.2, 131.2, 115.7, 115.6, 92.0, 62.4, 51.4, 51.3, 17.9. HRMS (ESI-TOF) calcd for $\text{C}_{14}\text{H}_{18}\text{NO}_5$ $[\text{M} + \text{H}]^+$ 280.1185, found 280.1182.

Dimethyl 2-(((3-(Hydroxymethyl)-4-methoxyphenyl)amino)-methylene)malonate

12c.—**12c** was prepared from 5-amino-2-methoxybenzyl alcohol (3.0 g, 19.6 mmol) according to general procedure C (violet-red semisolid, 5.3 g, 92% yield). ^1H NMR (400 MHz, CDCl_3) δ 10.96 (d, J = 13.8 Hz, 1H), 8.40 (d, J = 13.9 Hz, 1H), 7.13 (d, J = 2.9 Hz, 1H), 7.01–6.95 (m, 1H), 6.83–6.78 (m, 1H), 4.65 (s, 2H), 3.81 (s, 3H), 3.80 (s, 3H), 3.73 (s, 3H). ^{13}C NMR (101 MHz, CDCl_3): δ 169.4, 166.1, 154.6, 152.8, 132.4, 130.9, 117.6, 117.5, 111.0, 91.8, 61.0, 55.6, 51.4, 51.3. HRMS (ESI-TOF) calcd for $\text{C}_{14}\text{H}_{18}\text{NO}_6$ $[\text{M} + \text{H}]^+$ 296.1134, found 296.1128.

Dimethyl 2-(((4-(Hydroxymethyl)phenyl)amino)methylene)-malonate 12d.—**12d**

was prepared from 4-aminobenzyl alcohol (3 g, 24.4 mmol) according to general procedure C (pale-yellow solid, 6.4 g, quantitative yield). ^1H NMR (400 MHz, CDCl_3): δ 10.94 (d, J = 13.8 Hz, 1H), 8.43 (ddd, J = 13.8, 8.2, 5.5 Hz, 1H), 7.38–7.28 (m, 2H), 7.06–7.02 (m, 2H), 4.60 (s, 2H), 3.79 (s, 3H), 3.71 (m, 3H). ^{13}C NMR (101 MHz, CDCl_3): δ 169.2, 166.0, 152.0, 138.1, 138.1, 128.3 (2C), 117.1 (2C), 92.6, 64.2, 51.5, 51.4. HRMS (ESI-TOF) calcd for $\text{C}_{13}\text{H}_{16}\text{NO}_5$ $[\text{M} + \text{H}]^+$ 266.1028, found 266.1032.

5-(((3-((4-(4-Fluorophenyl)piperazin-1-yl)methyl)phenyl)amino)-methylene)-2,2-dimethyl-1,3-dioxane-4,6-dione 15aj.—Trimethyl orthoformate (3.7 g, 35.0 mmol) and Meldrum's acid (0.3 g, 2.10 mmol) were refluxed for 3 h under N_2 and then cooled to RT.

The aniline **5aj** (0.5 g, 1.75 mmol) was then added to the reaction, and the resulting mixture was refluxed for another 1 h. The reaction mixture was cooled to RT, ether was added to allow precipitation, and the excess solvents were decanted (the addition of ether and decanting can be repeated couple of times to get rid of excess $\text{CH}(\text{OCH}_3)_3$ and Meldrum's acid). The resulting orange yellow solid was dried under vacuum to give an NMR-pure enamine **15aj** in 84% yield (650 mg) that was used directly in next cyclization step without further purification. ^1H NMR (400 MHz, CDCl_3): δ 11.19 (m, 1H), 8.64 (d, J = 14.4 Hz, 1H), 7.35 (t, J = 7.8 Hz, 1H), 7.28 (s, 1H), 7.21 (d, J = 7.6 Hz, 1H), 7.12 (dd, J = 7.9, 1.8 Hz, 1H), 6.95–6.87 (m, 2H), 6.86–6.80 (m, 2H), 3.56 (d, J = 12.8 Hz, 2H), 3.14–3.04 (m, 4H), 2.63–2.55 (m, 4H), 1.72 (s, 6H). ^{13}C NMR (101 MHz, CDCl_3) δ 165.38, 163.43, 152.43 (2C), 147.81, 140.78, 137.83, 129.83, 127.34, 118.23, 117.76, 117.69, 116.72 (2C), 115.45, 115.23, 105.02, 62.32, 53.04 (2C), 49.97 (2C), 26.90 (2C). HRMS (ESI-TOF) calcd for $\text{C}_{24}\text{H}_{27}\text{FN}_3\text{O}_4$ $[\text{M} + \text{H}]^+$ 440.1986, found 440.1996.

Supplementary Material

Refer to Web version on PubMed Central for supplementary material.

ACKNOWLEDGMENTS

We thank Susan A. Charman and Karen L. White (Monash Institute of Pharmaceutical Sciences, Parkville, Australia) for valuable discussions and for proof reading the manuscript. We also thank the Genshaft Family Doctoral Fellowship from the University of South Florida for financial support of J.R.M. and C.L.L. We thank the

Medicines for Malaria Venture (MMV 11/ 0022) and the National Institutes of Health (R01 GM097118) for financial support.

ABBREVIATIONS USED

Ac	acetyl
ACT	artemisinin combination therapy
DMF	<i>N,N</i> -dimethylformamide
EC₅₀	half-maximal effective concentration
ED₅₀	half-maximal effective dose
HPLC	high performance liquid chromatography
LBI	liver blood index
NBS	<i>N</i> -bromosuccinimide
NCS	<i>N</i> -chlorosuccinimide
ND	not determined
Pb	<i>Plasmodium berghei</i>
PI	post infection
RI	resistance index
RT	room temperature
SAR	structure—activity relationship
SPR	structure—property relationship
WHO	World Health Organization

REFERENCES

- (1). World Malaria Report 2016; World Health Organization: Geneva, 2016.
- (2). Lacrue AN; Saenz FE; Cross RM; Udenze KO; Monastyrskiy A; Stein S; Mutka TS; Manetsch R; Kyle DE 4(1H)-Quinolones with liver stage activity against *Plasmodium berghei*. *Antimicrob. Agents Chemother.* 2013, 57, 417–24. [PubMed: 23129047]
- (3). Teixeira C; Vale N; Perez B; Gomes A; Gomes JR; Gomes P “Recycling” classical drugs for malaria. *Chem. Rev.* 2014, 114, 11164–220. [PubMed: 25329927]
- (4). Zhang Y; Guiguemde WA; Sigal M; Zhu F; Connelly MC; Nwaka S; Guy RK Synthesis and structure-activity relationships of antimalarial 4-oxo-3-carboxyl quinolones. *Bioorg. Med. Chem.* 2010, 18, 2756–66. [PubMed: 20206533]
- (5). Zhang Y; Clark JA; Connelly MC; Zhu F; Min J; Guiguemde WA; Pradhan A; Iyer L; Furimsky A; Gow J; Parman T; El Mazouni F; Phillips MA; Kyle DE; Mirsalis J; Guy RK Lead optimization of 3-carboxyl-4(1H)-quinolones to deliver orally bioavailable antimalarials. *J. Med. Chem.* 2012, 55, 4205–19. [PubMed: 22435599]

- (6). Cross RM; Monastyrskiy A; Mutka TS; Burrows JN; Kyle DE; Manetsch R Endochin optimization: structure-activity and structure-property relationship studies of 3-substituted 2-methyl-4(1H)-quinolones with antimalarial activity. *J. Med. Chem.* 2010, 53, 7076–94. [PubMed: 20828199]
- (7). Cross RM; Namelikonda NK; Mutka TS; Luong L; Kyle DE; Manetsch R Synthesis, antimalarial activity, and structure-activity relationship of 7-(2-phenoxyethoxy)-4(1H)-quinolones. *J. Med. Chem.* 2011, 54, 8321–7. [PubMed: 22111907]
- (8). Cross RM; Maignan JR; Mutka TS; Luong L; Sargent J; Kyle DE; Manetsch R Optimization of 1,2,3,4-tetrahydroacridin-9(10H)-ones as antimalarials utilizing structure-activity and structure-property relationships. *J. Med. Chem.* 2011, 54, 4399–426. [PubMed: 21630666]
- (9). Cross RM; Flanigan DL; Monastyrskiy A; LaCrue AN; Saenz FE; Maignan JR; Mutka TS; White KL; Shackelford DM; Bathurst I; Fronczek FR; Wojtas L; Guida WC; Charman SA; Burrows JN; Kyle DE; Manetsch R Orally Bioavailable 6-Chloro-7-methoxy-4(1H)-quinolones Efficacious against Multiple Stages of Plasmodium. *J. Med. Chem.* 2014, 57, 8860–8879. [PubMed: 25148516]
- (10). Saenz FE; LaCrue AN; Cross RM; Maignan JR; Udenze K; Manetsch R; Kyle DE 4-(1H)-Quinolones and 1,2,3,4-tetrahydroacridin-9(10H)-ones prevent the transmission of Plasmodium falciparum to Anopheles freeborni. *Antimicrob. Agents Chemother.* 2013, 57, 6187–6195. [PubMed: 24080648]
- (11). Bueno JM; Manzano P; Garcia MC; Chicharro J; Puente M; Lorenzo M; Garcia A; Ferrer S; Gomez RM; Fraile MT; Lavandera JL; Fiandor JM; Vidal J; Herreros E; Gargallo-Viola D Potent antimalarial 4-pyridones with improved physico-chemical properties. *Bioorg. Med. Chem. Lett.* 2011, 21, 5214–5218. [PubMed: 21824778]
- (12). Winter RW; Kelly JX; Smilkstein MJ; Dodean R; Hinrichs D; Riscoe MK Antimalarial quinolones: synthesis, potency, and mechanistic studies. *Exp. Parasitol.* 2008, 118, 487–97. [PubMed: 18082162]
- (13). Winter R; Kelly JX; Smilkstein MJ; Hinrichs D; Koop DR; Riscoe MK Optimization of endochin-like quinolones for antimalarial activity. *Exp. Parasitol.* 2011, 127, 545–51. [PubMed: 21040724]
- (14). Monastyrskiy A; Kyle DE; Manetsch R 4(1H)-Pyridone and 4(1H)-Quinolone Derivatives as Antimalarials with Erythrocytic, Exoerythrocytic, and Transmission Blocking Activities. *Curr. Top. Med. Chem.* 2014, 14, 1693–1705. [PubMed: 25116582]
- (15). Puri SK; Dutta GP Quinoline esters as potential antimalarial drugs: effect on relapses of Plasmodium cynomolgi infections in monkeys. *Trans. R. Soc. Trop. Med. Hyg.* 1990, 84, 759–60. [PubMed: 2096498]
- (16). Ryley JF; Peters W The antimalarial activity of some quinolone esters. *Ann. Trop. Med. Parasitol.* 1970, 64, 209–22. [PubMed: 4992592]
- (17). Maignan JR; Lichorowic CL; Giarrusso J; Blake LD; Casandra D; Mutka TS; LaCrue AN; Burrows JN; Willis PA; Kyle DE; Manetsch R ICI 56,780 Optimization: Structure-Activity Relationship Studies of 7-(2-Phenoxyethoxy)-4(1H)-quinolones with Antimalarial Activity. *J. Med. Chem.* 2016, 59, 6943–60. [PubMed: 27291102]
- (18). Cowley R; Leung S; Fisher N; Al-Helal M; Berry NG; Lawrenson AS; Sharma R; Shone AE; Ward SA; Biagini GA; O'Neill PM The development of quinolone esters as novel antimalarial agents targeting the Plasmodium falciparum bc(1) protein complex. *MedChemComm* 2012, 3, 39–44.
- (19). Reddy MV; Akula B; Cosenza SC; Athuluridivakar S; Mallireddigari MR; Pallela VR; Billa VK; Subbaiah DR; Bharathi EV; Vasquez-Del Carpio R.; Padgaonkar A; Baker SJ; Reddy EP Discovery of 8-cyclopentyl-2-[4-(4-methyl-piperazin-1-yl)-phenylamino]-7-oxo-7,8-dihydro-pyrid o[2,3-d]pyrimidine-6-carbonitrile (7x) as a potent inhibitor of cyclin-dependent kinase 4 (CDK4) and AMPK-related kinase 5 (ARK5). *J. Med. Chem.* 2014, 57, 578–99. [PubMed: 24417566]
- (20). Liu KG; Robichaud AJ A general and convenient synthesis of N-aryl piperazines. *Tetrahedron Lett.* 2005, 46, 7921–7922.
- (21). Gould RG; Jacobs WA The Synthesis of Certain Substituted Quinolines and 5,6-Benzoquinolines. *J. Am. Chem. Soc.* 1939, 61, 2890–2895.

- (22). Dess DB; Martin JC Readily Accessible 12-I-5 Oxidant for the Conversion of Primary and Secondary Alcohols to Aldehydes and Ketones. *J. Org. Chem.* 1983, 48, 4155–4156.
- (23). Kuhhorn J; Hubner H; Gmeiner P Bivalent dopamine D2 receptor ligands: synthesis and binding properties. *J. Med. Chem.* 2011, 54, 4896–903. [PubMed: 21599022]
- (24). Rossi C; Porcelloni M; D'Andrea P; Fincham CI; Ettore A; Mauro S; Squarcia A; Bigioni M; Parlani M; Nardelli F; Binaschi M; Maggi CA; Fattori D Alkyl piperidine and piperazine hydroxamic acids as HDAC inhibitors. *Bioorg. Med. Chem. Lett.* 2011, 21, 2305–8. [PubMed: 21420859]
- (25). Ghosh B; Antonio T; Reith ME; Dutta AK Discovery of 4-(4-(2-((5-Hydroxy-1,2,3,4-tetrahydronaphthalen-2-yl)(propyl)-amino)ethyl)piperazin-1-yl)quinolin-8-ol and its analogues as highly potent dopamine D2/D3 agonists and as iron chelator: in vivo activity indicates potential application in symptomatic and neuroprotective therapy for Parkinson's disease. *J. Med. Chem.* 2010, 53, 2114–25. [PubMed: 20146482]
- (26). Nilsen A; LaCrue AN; White KL; Forquer IP; Cross RM; Marfurt J; Mather MW; Delves MJ; Shackelford DM; Saenz FE; Morrisey JM; Steuten J; Mutka T; Li Y; Wirjanata G; Ryan E; Duffy S; Kelly JX; Sebayang BF; Zeeman AM; Noviyanti R; Sinden RE; Kocken CH; Price RN; Avery VM; Angulo-Barturen I; Jimenez-Diaz MB; Ferrer S; Herreros E; Sanz LM; Gamo FJ; Bathurst I; Burrows JN; Siegl P; Guy RK; Winter RW; Vaidya AB; Charman SA; Kyle DE; Manetsch R; Riscoe MK Quinolone-3-diarylethers: a new class of antimalarial drug. *Sci. Transl. Med.* 2013, 5, 177rara37.
- (27). Plowe CV Malaria: Resistance nailed. *Nature* 2014, 505, 30–31. [PubMed: 24352240]
- (28). Looareesuwan S; Viravan C; Webster HK; Kyle DE; Hutchinson DB; Canfield CJ Clinical studies of atovaquone, alone or in combination with other antimalarial drugs, for treatment of acute uncomplicated malaria in Thailand. *Am. J. Trop. Med. Hyg.* 1996, 54, 62–66. [PubMed: 8651372]
- (29). Milhous WK; Gerena L; Kyle DE; Oduola AM In vitro strategies for circumventing antimalarial drug resistance. *Prog. Clin. Biol. Res.* 1989, 313, 61–72. [PubMed: 2675118]
- (30). Yeates CL; Batchelor JF; Capon EC; Cheesman NJ; Fry M; Hudson AT; Pudney M; Trimming H; Woolven J; Bueno JM; Chicharro J; Fernandez E; Fiandor JM; Gargallo-Viola D; Gomez de las Heras F; Herreros E; Leon ML Synthesis and structure-activity relationships of 4-pyridones as potential antimalarials. *J. Med. Chem.* 2008, 51, 2845–52. [PubMed: 18396855]
- (31). Bueno JM; Herreros E; Angulo-Barturen I; Ferrer S; Fiandor JM; Gamo FJ; Gargallo-Viola D; Derimanov G Exploration of 4(IH)-pyridones as a novel family of potent antimalarial inhibitors of the plasmodial cytochrome bcl. *Future Med. Chem.* 2012, 4, 2311–2323. [PubMed: 23234553]
- (32). Biagini GA; Fisher N; Shone AE; Mubarak MA; Srivastava A; Hill A; Antoine T; Warman AJ; Davies J; Pidathala C; Amewu RK; Leung SC; Sharma R; Gibbons P; Hong DW; Pacorel B; Lawrenson AS; Charoensutthivarakul S; Taylor L; Berger O; Mbekeani A; Stocks PA; Nixon GL; Chadwick J; Hemingway J; Delves MJ; Sinden RE; Zeeman AM; Kocken CH; Berry NG; O'Neill PM; Ward SA Generation of quinolone antimalarials targeting the Plasmodium falciparum mitochondrial respiratory chain for the treatment and prophylaxis of malaria. *Proc. Natl. Acad. Sci. U. S. A.* 2012, 109, 8298–303. [PubMed: 22566611]
- (33). Capper MJ; O'Neill PM; Fisher N; Strange RW; Moss D; Ward SA; Berry NG; Lawrenson AS; Hasnain SS; Biagini GA; Antonyuk SV Antimalarial 4(IH)-pyridones bind to the Qi site of cytochrome bcl. *Proc. Natl. Acad. Sci. U. S. A.* 2015, 112, 755–60. [PubMed: 25564664]
- (34). Birth D; Kao WC; Hunte C Structural analysis of atovaquone-inhibited cytochrome bcl complex reveals the molecular basis of antimalarial drug action. *Nat. Commun.* 2014, 5, 4029. [PubMed: 24893593]
- (35). Van Horn KS; Burda WN; Fleeman R; Shaw LN; Manetsch R Antibacterial activity of a series of N2,N4-disubstituted quinazoline-2,4-diamines. *J. Med. Chem.* 2014, 57, 3075–93. [PubMed: 24625106]
- (36). Van Horn KS; Zhu X; Pandharkar T; Yang S; Vesely B; Vanaerschot M; Dujardin JC; Rijal S; Kyle DE; Wang MZ; Werbovetz KA; Manetsch R Antileishmanial activity of a series of N(2),N(4)-disubstituted quinazoline-2,4-diamines. *J. Med. Chem.* 2014, 57, 5141–56. [PubMed: 24874647]

- (37). Nilsen A; LaCrue AN; White KL; Forquer IP; Cross RM; Marfurt J; Mather MW; Delves MJ; Shackelford DM; Saenz FE; Morrisey JM; Steuten J; Mutka T; Li Y; Wirjanata G; Ryan E; Duffy S; Kelly JX; Sebayang BF; Zeeman AM; Noviyanti R; Sinden RE; Kocken CHM; Price RN; Avery VM; Angulo-Barturen I; Jimenez-Diaz MB; Ferrer S; Herreros E; Sanz LM; Gamo FJ; Bathurst I; Burrows JN; Siegl P; Guy RK; Winter RW; Vaidya AB; Charman SA; Kyle DE; Manetsch R; Riscoe MK Quinolone-3-diarylethers: a new class of antimalarial drug. *Sci. Transl. Med.* 2013, 5, 177ra37.
- (38). Mwakingwe A; Ting LM; Hochman S; Chen J; Sinnis P; Kim K Noninvasive real-time monitoring of liver-stage development of bioluminescent Plasmodium parasites. *J. Infect. Dis.* 2009, 200, 1470–8. [PubMed: 19811100]
- (39). Madhavi Sastry G.; Adzhigirey M; Day T; Annabhimoju R; Sherman W Protein and ligand preparation: parameters, protocols, and influence on virtual screening enrichments. *J. Comput.-Aided Mol. Des.* 2013, 27, 221–234. [PubMed: 23579614]
- (40). Friesner RA; Banks JL; Murphy RB; Halgren TA; Klicic JJ; Mainz DT; Repasky MP; Knoll EH; Shelley M; Perry JK; Shaw DE; Francis P; Shenkin PS Glide: a new approach for rapid, accurate docking and scoring. 1. Method and assessment of docking accuracy. *J. Med. Chem.* 2004, 47, 1739–49. [PubMed: 15027865]
- (41). Friesner RA; Murphy RB; Repasky MP; Frye LL; Greenwood JR; Halgren TA; Sanschagrin PC; Mainz DT Extra precision glide: docking and scoring incorporating a model of hydrophobic enclosure for protein-ligand complexes. *J. Med. Chem.* 2006, 49, 6177–96. [PubMed: 17034125]
- (42). Halgren TA; Murphy RB; Friesner RA; Beard HS; Frye LL; Pollard WT; Banks JL Glide: a new approach for rapid, accurate docking and scoring. 2. Enrichment factors in database screening. *J. Med. Chem.* 2004, 47, 1750–9. [PubMed: 15027866]

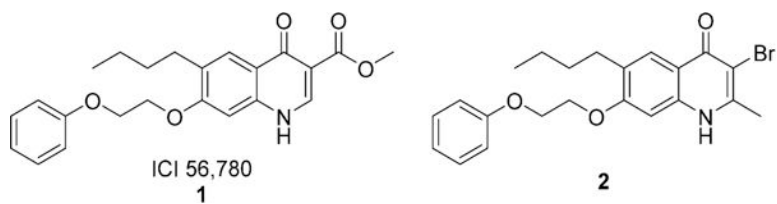


Figure 1.
Antimalarial 4(1*H*)-quinolones.

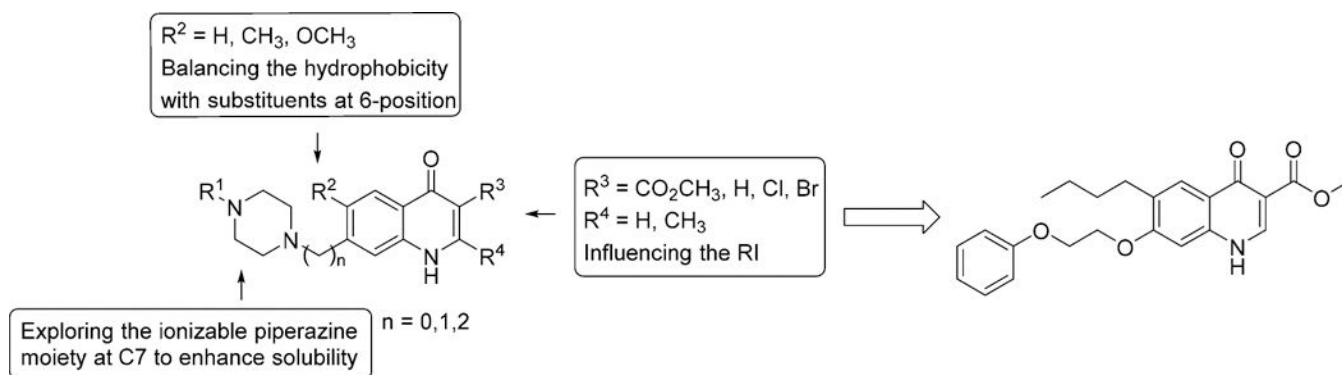


Figure 2.
Design of piperazinyl-substituted scaffolds based on **1**.

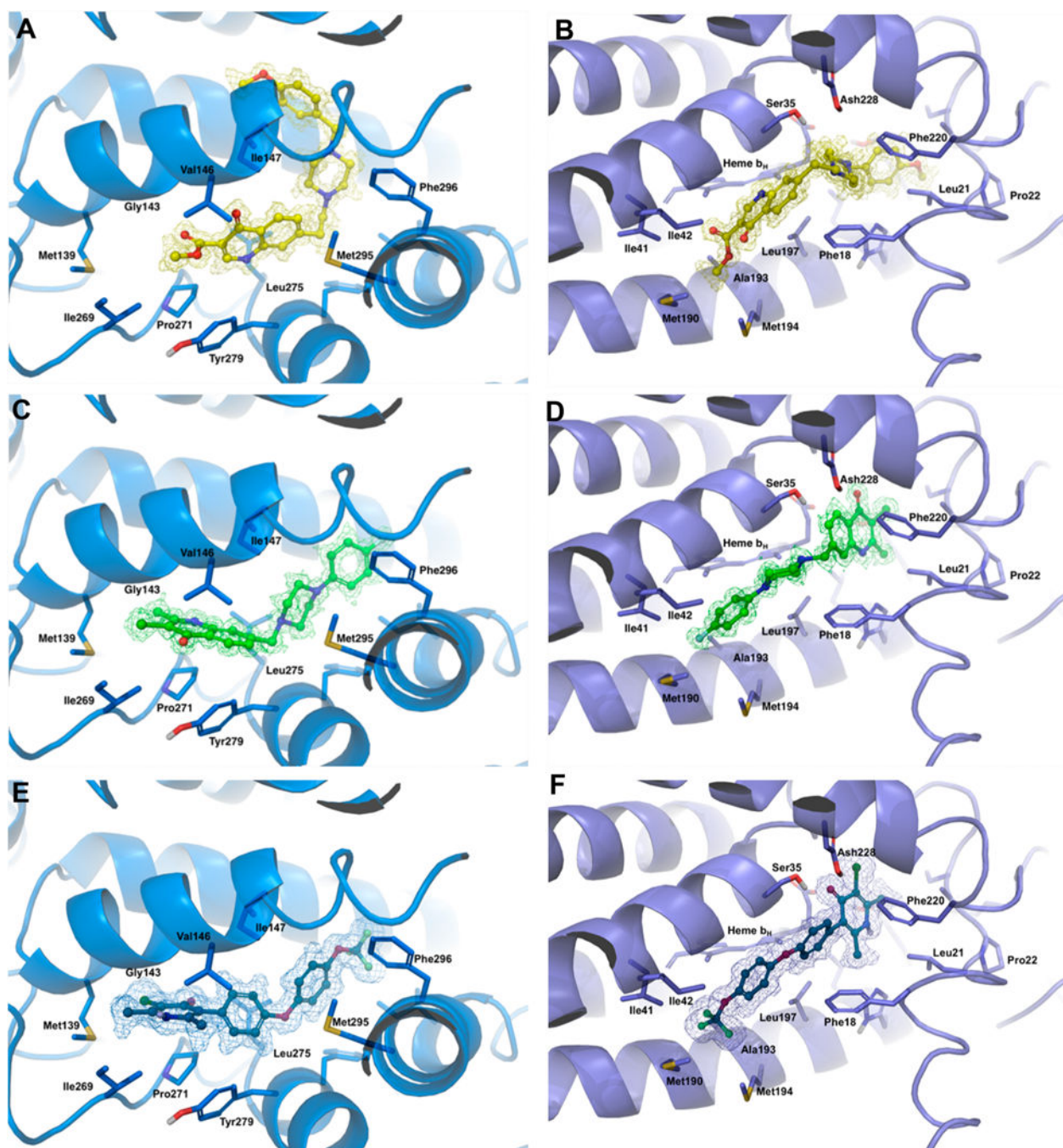


Figure 3.

Binding of **8ae** (yellow), **8ao** (green) and GW844520 (blue) within the hydrophobic Q₀ and Q₁ cavities as predicted by Glide docking. The electron density map (Gaussian type, yellow or green, contoured at level 1.0 in Pymol) was calculated after docking of the ligands to the model. Protein residues within 5 Å to Q₀ site (marine blue) or Q₁ site (deep blue) are shown in stick representation. (A) Docking pose of **8ae** (yellow sticks) within Q₀ binding site (marine blue). (B) Docking pose of **8ae** (yellow sticks) within Q₁ binding site (deep blue). (C) Docking pose of **8ao** (green sticks) within Q₀ binding site (marine blue). (D) Docking

pose of **8ao** (green sticks) within Q_i binding site (deep blue). (E) Docking pose of GW844520 (blue sticks) within Q_o binding site (marine blue). (F) Docking pose of GW844520 (blue sticks) within Q_i binding site (deep blue).

Author Manuscript

Author Manuscript

Author Manuscript

Author Manuscript

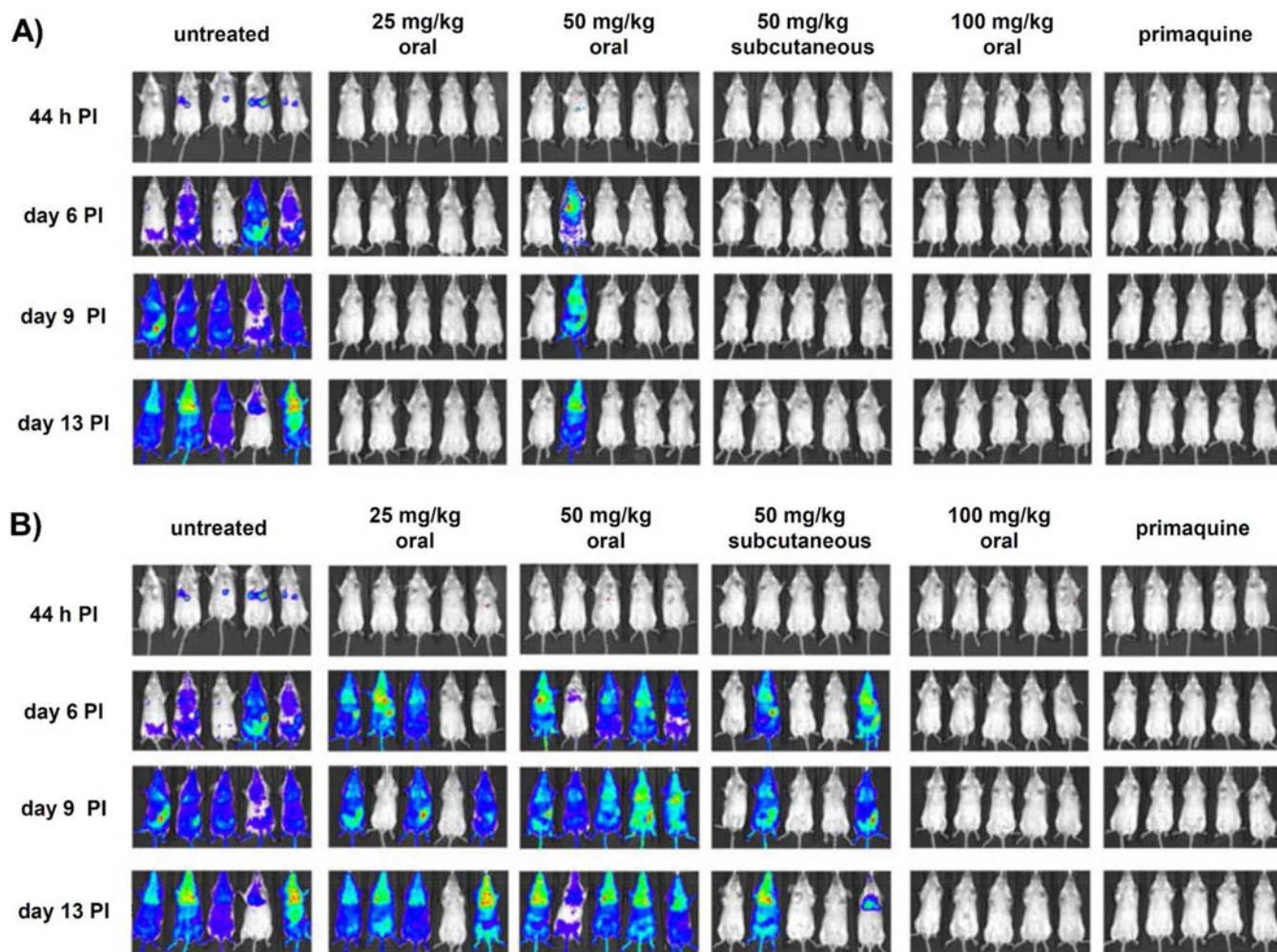


Figure 4. Whole-animal bioluminescence imaging of mice infected with luciferase-transfected *P. berghei* sporozoites. Mice were treated with different doses of **8j** (A), **81** (B), and primaquine (50 mg/kg, oral). Animals ($n = 5$ per group) received a single dose by gavage 1 h after inoculation with sporozoites. Representative images taken at 44 h, day 6, day 9, and day 13 after infection are shown. At 44 h, bioluminescent signal was detected in control untreated animals, with the highest intensity noted in the area overlaying the liver, consistent with the presence of liver-stage parasites.

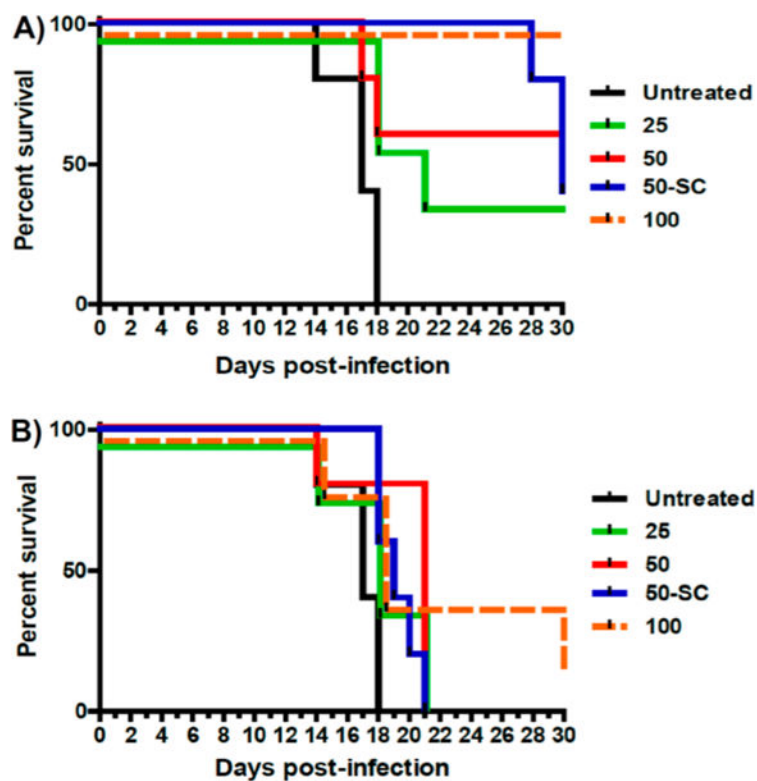
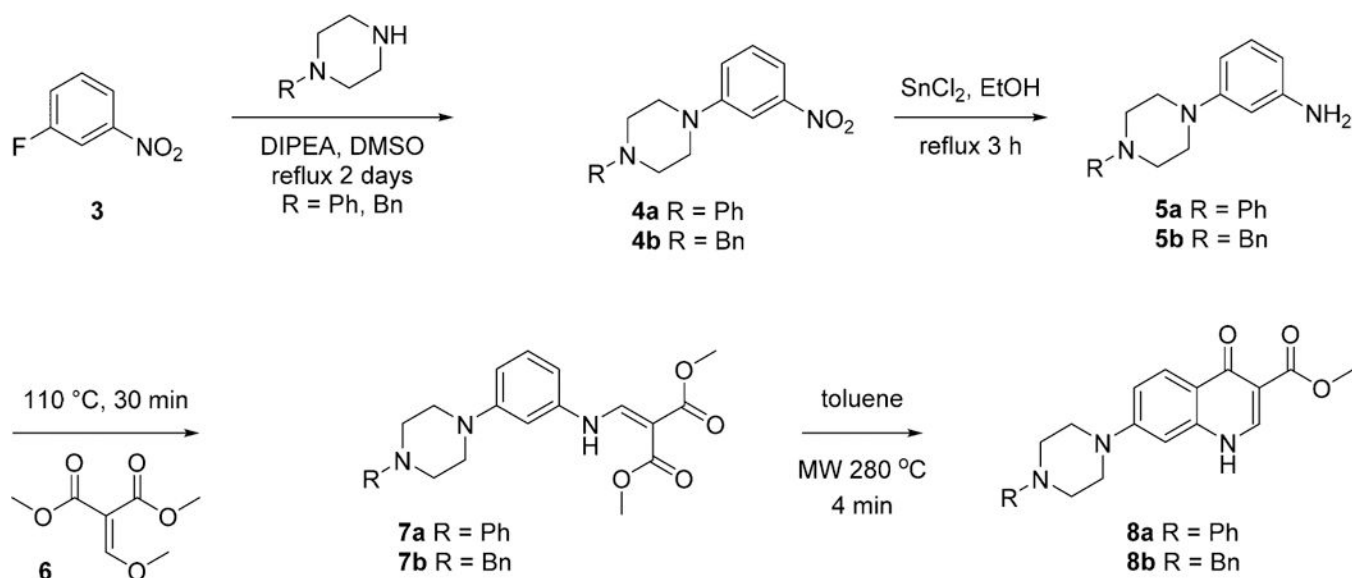
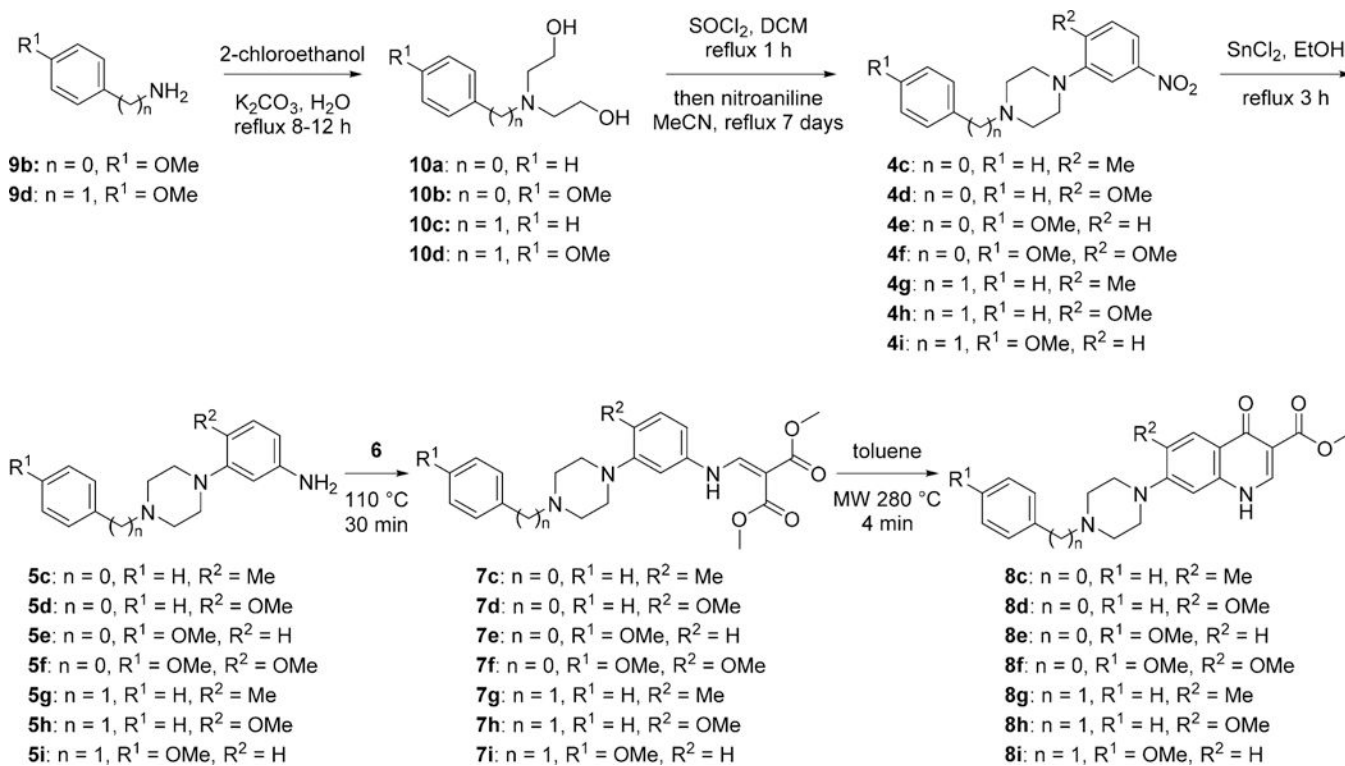


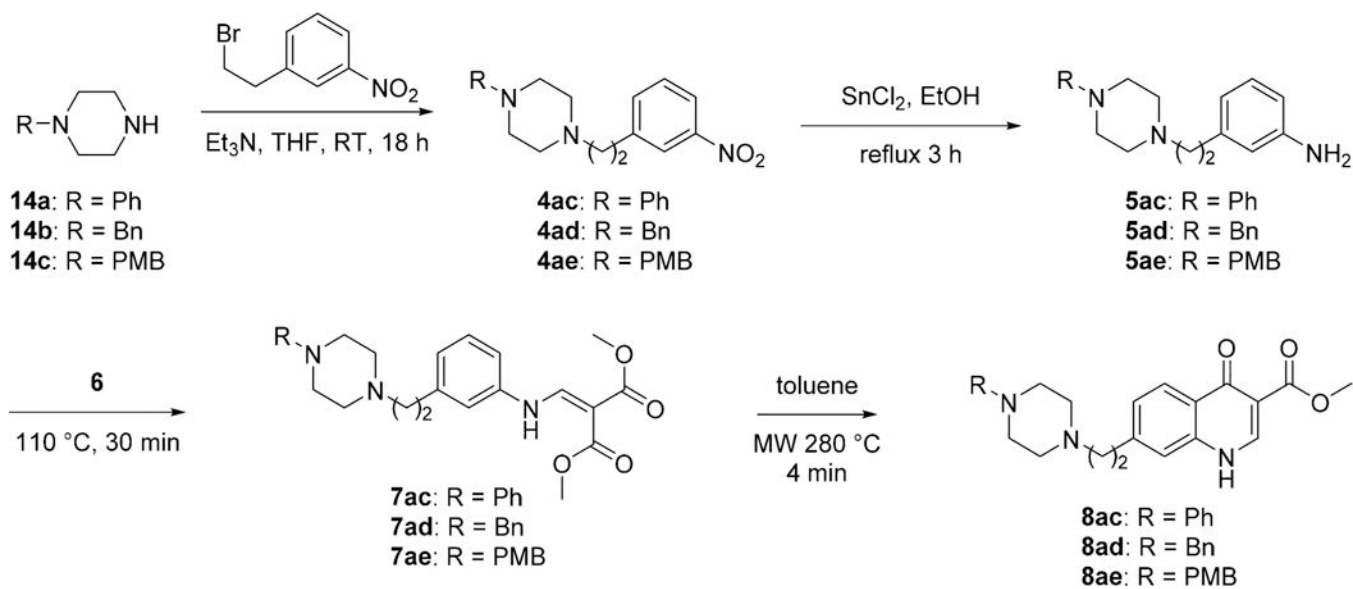
Figure 5. Survival curves for 4(1*H*)-quinolones **8j** (A) and **8l** (B) that demonstrate antimalarial activity against liver stages of the parasite. Compounds have been tested oral at 25 mg/kg (25), 50 mg/kg (50), and 100 mg/kg (100) and subcutaneous at 50 mg/kg (50-SC) doses.



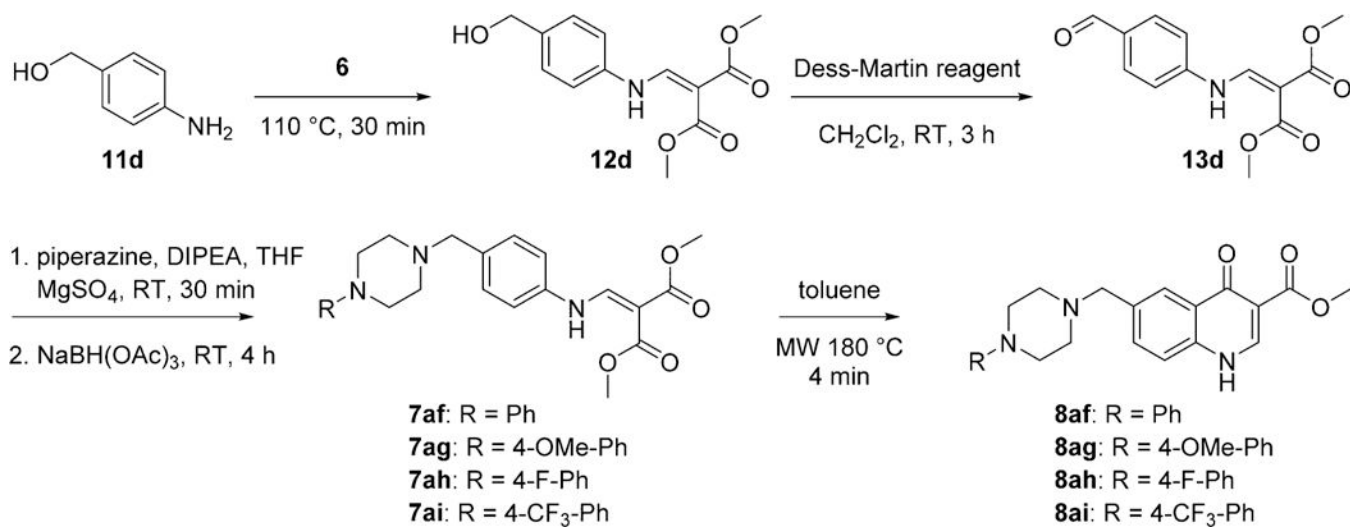
Scheme 1.
Synthesis of 4(1*H*)-Quinolones with Direct Attachment of Piperazinyl Moiety

**Scheme 2.**

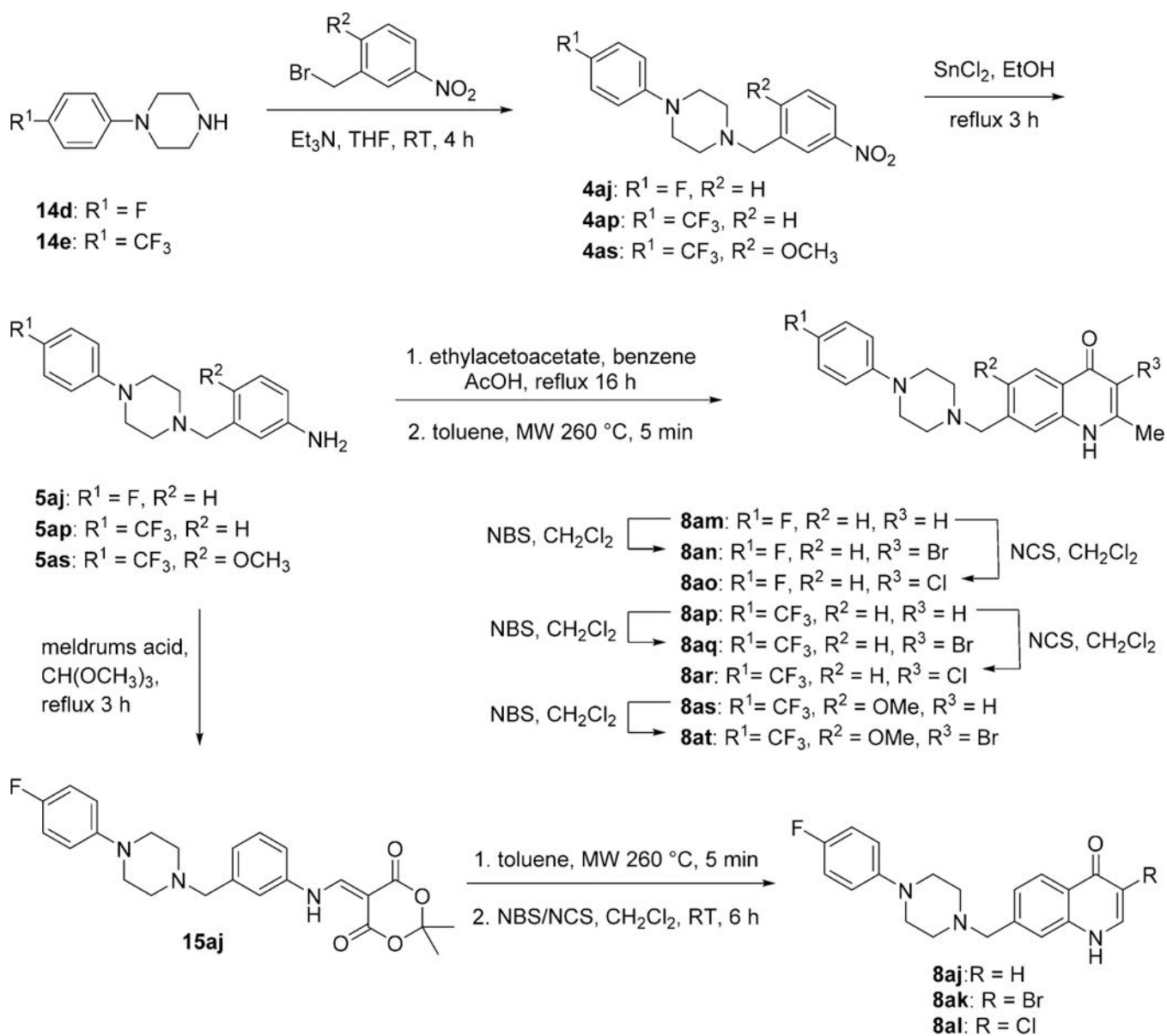
Alternate Synthesis of 4(1*H*)-Quinolones with Direct Attachment of the Piperazinyl Moiety to the 4(1*H*)-Quinolone Core

**Scheme 4.**

Synthesis of 4(1*H*)-Quinolones with an Ethylene between the Piperazinyl Moiety to the 4(1*H*)-Quinolone Core



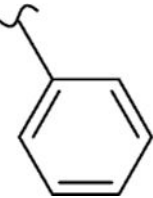

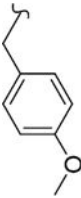
Scheme 5.
Synthesis of 6-Piperazinyl-4(1*H*)-Quinolones



Scheme 6.
Synthesis of 3-Halo Substituted 4(1*H*)-Quinolones

Table 1.

Exploration of Various *N*-Substituted Piperazinyl Moieties on 7-Position of 4(1*H*)-Quinolone Benzenoid Ring to Enhance the Solubility and Antimalarial Activity

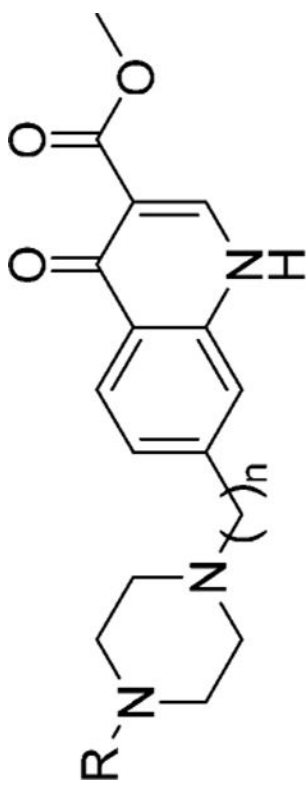
compd	R	n	EC ₅₀ W2 (nM) ^a	EC ₅₀ TM90-C2B (nM)	RI ^b	EC ₅₀ Pb (nM)	EC ₅₀ J774 (μM)
8ac		2	25	1500	60	^c	>20
8ad		2	120	>2000	>17	160	>20
8ae		2	12	>2000	>167	^c	>20

Author Manuscript

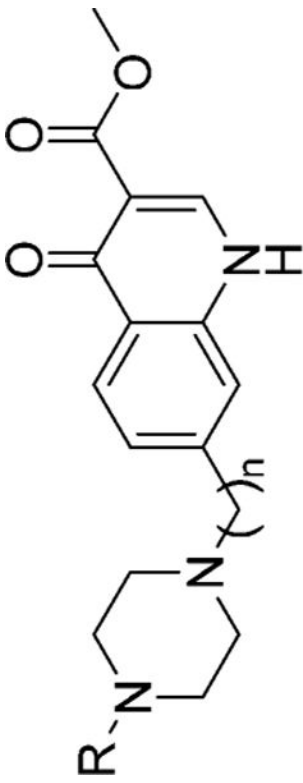
Author Manuscript


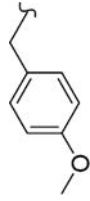
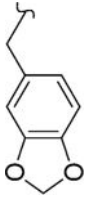
Author Manuscript

Author Manuscript



compd	R	n	EC ₅₀ W2 (nM) ^a	EC ₅₀ TM90-C2B (nM)	RI ^b	EC ₅₀ Pb (nM)	EC ₅₀ J774 (μM)
8a		0	4.5	250	56	74	>20
8b		0	16	860	53	85	>20
8i		0	20	1300	65	c	c
8j		1	1.3	480	369	4.7	3.9



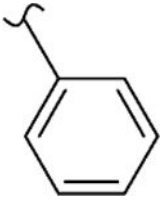

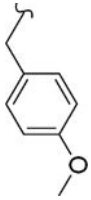
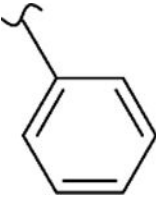
compd	R	n	EC ₅₀ W2 (nM) ^a	EC ₅₀ TM90-C2B (nM)	RI ^b	EC ₅₀ Pb (nM)	EC ₅₀ J774 (μM)
8k		1	1.4	150	106	44	10
8l		1	2.5	800	320	83	5.1
8m		1	160	>2000	>12	^c	>20

^aChloroquine (CQ), atovaquone (ATO), and dihydroartemisinin (DHA) are internal controls for each in vitro assay: CQ, 0.42 μM W2, 0.23 μM TM90-C2B, and 47.2 μM J774; ATO, 1.4 nM W2, 18 μM TM90-C2B, and 28 μM J774; DHA, 5.5 nM W2, 5.9 nM TM90-C2B and 1.5 μM J774.

^bRI = TM90-C2B/W2.

^cNot determined.

Table 2. Effect of Various Substitutions in 6-Position of the 4(1*H*)-Quinolone's Benzenoid Ring on Antimalarial Activity

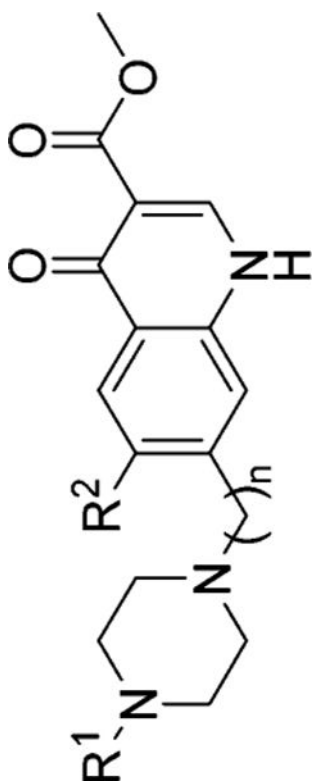
compd	R ¹	R ²	n	EC ₅₀ W2 (nM) ^a	EC ₅₀ TM90-C2B (nM)	RI ^b	EC ₅₀ Pb (nM)	EC ₅₀ J774 (μM)
8q		-CH ₃	1	0.44	150	345	6.9	12
8r		-CH ₃	1	1.5	890	614	9.5	>20
8s		-CH ₃	1	2.4	1000	417	c	>20
8w		-OCH ₃	1	1.6	490	306	110	>20

Author Manuscript

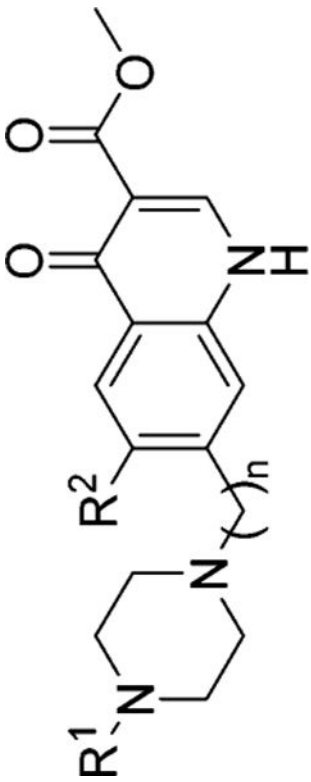
Author Manuscript

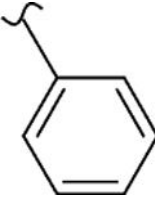

Author Manuscript

Author Manuscript



compd	R ¹	R ²	n	EC ₅₀ W2 (nM) ^a	EC ₅₀ TNM90-C2B (nM)	RI ^b	EC ₅₀ P ₆ (nM)	EC ₅₀ J774 (μM)
8x		-OCH ₃	1	5.5	>2000	>364	9.3	>20
8y		-OCH ₃	1	10	>2000	>200	52	>20
8c		-CH ₃	0	46	1100	24	c	17
8g		-CH ₃	0	13	980	75	>100	>20



compd	R ¹	R ²	n	EC ₅₀ W2 (nM) ^a	EC ₅₀ TM90-C2B (nM)	RI ^b	EC ₅₀ Pb (nM)	EC ₅₀ J774 (μM)
8d		-OCH ₃	0	37	800	22	- ^c	17
8h		-OCH ₃	0	64	200	3	- ^c	12

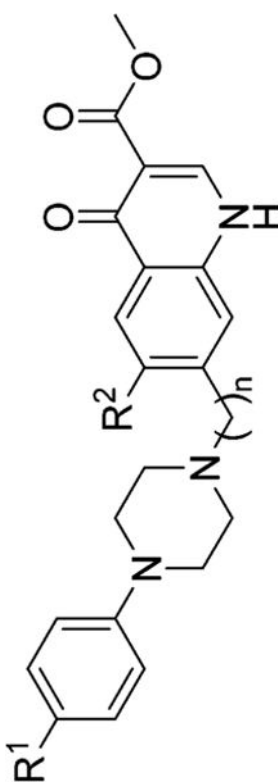
^aChloroquine (CQ), atovaquone (ATO), and dihydroartemisinin (DHA) are internal controls for each in vitro assay: CQ, 0.42 μM W2, 0.23 μM TM90-C2B, and 47.2 μM J774; ATO, 1.4 nM W2, 18 μM TM90-C2B, and 28 μM J774; DHA, 5.5 nM W2, 5.9 nM TM90-C2B, and 1.5 μM J774.

^bRI = TM90-C2B/W2.

^cNot determined.

Steric and Electronic Effects of the Phenyloiperazine Moiety and the 4(1*H*)-Quinolone 6-Position on Antimalarial Activity

Table 3.



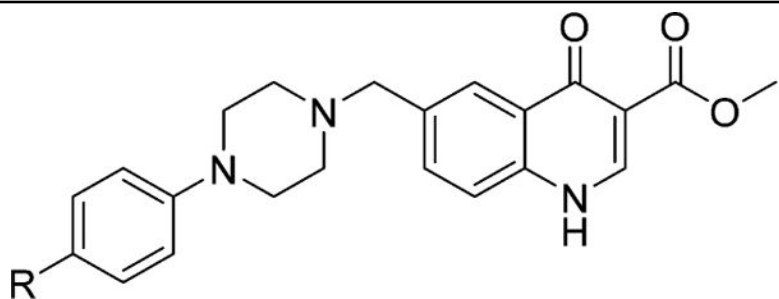
compd	R ¹	R ²	n	EC ₅₀ W2 (nM) ^d	EC ₅₀ TM90-C2B (nM)	RT ^b	EC ₅₀ P _b (nM)	EC ₅₀ J774 (μM)
8o	-F	-H	1	1.8	130	74	1.1	2.0
8u	-F	-CH ₃	1	0.84	350	417	2.6	16
8aa	-F	-OCH ₃	1	1.8	220	122	32	>20
8e	-OCH ₃	-H	0	7.8	150	20	c	>20
8f	-OCH ₃	-OCH ₃	0	43	2000	47	>100	>20
8n	-OCH ₃	-H	1	3.6	220	61	0.12	4.7
8t	-OCH ₃	-CH ₃	1	0.57	180	316	4.1	>20
8z	-OCH ₃	-OCH ₃	1	3.4	860	253	10	16
8p	-CF ₃	-H	1	0.32	120	375	16	11
8v	-CF ₃	-CH ₃	1	0.066	100	1515	c	>20
8ab	-CF ₃	-OCH ₃	1	6.4	210	33	9.6	>20

^dChloroquine (CQ), atovaquone (ATO), and dihydroartemisinin (DHA) are internal controls for each in vitro assay: CQ, 0.42 μM W2, 0.23 μM TM90-C2B, and 47.2 μM J774; ATO, 1.4 nM W2, 18 μM TM90-C2B, and 28 μM J774; DHA, 5.5 nM W2, 5.9 nM TM90-C2B, and 1.5 μM J774.

^bR¹ = TM90-C2B/W2.

^cNot determined.

Table 4.

4(1*H*)-Quinolones Substituted in 6-Position with the Piperazine Moiety

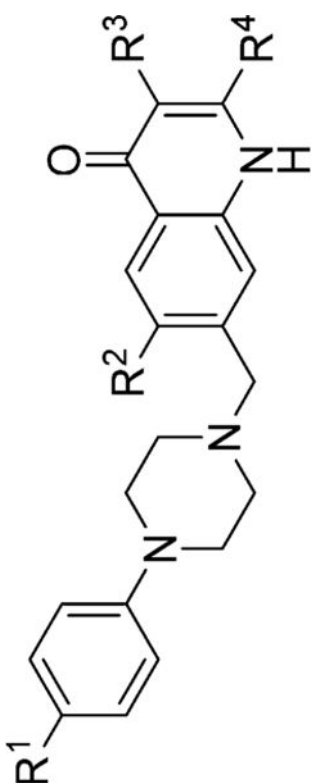
compd	R	EC ₅₀ W2 (nM) ^a	EC ₅₀ TM90-C2B (nM)	^b RI	EC ₅₀ Pb (nM)	EC ₅₀ J774 (μM)
8af	-H	150	>2000	>13	91	>20
8ag	-OCH ₃	160	>2000	>12	>100	>20
8ah	-F	110	>2000	>18	^c	>20
8ai	-CF ₃	45	>2000	>44	85	>20

^aChloroquine (CQ), atovaquone (ATO), and dihydroartemisinin (DHA) are internal controls for each in vitro assay: CQ, 0.42 μM W2, 0.23 μM TM90-C2B, and 47.2 μM J774; ATO, 1.4 nM W2, 18 μM TM90-C2B, and 28 μM J774; DHA, 5.5 nM W2, 5.9 nM TM90-C2B, and 1.5 μM J774.

^bRI = TM90-C2B/W2.

^cNot determined.

Table 5.

3-Halo-Substituted 4(1*H*)-Quinolones


compd	R ¹	R ²	R ³	R ⁴	EC ₅₀ W2 (nM) ^a	EC ₅₀ TM90-C2B (nM)	RI ^b	EC ₅₀ P <i>b</i> (nM)	EC ₅₀ J774 (μM)
8ak	-F	-H	-Br	-H	810	>2000	>2.5	0.86	>20
8al	-F	-H	-Cl	-H	1100	>2000	>1.8	<i>c</i>	>20
8am	-F	-H	-H	-CH ₃	1200	1500	1.2	<i>c</i>	>20
8an	-F	-H	-Br	-CH ₃	25	26	1.0	26	>20
8ao	-F	-H	-Cl	-CH ₃	39	52	1.3	<i>c</i>	>20
8aq	-CF ₃	-H	-Br	-CH ₃	120	95	0.8	<i>c</i>	>20
8ar	-CF ₃	-H	-Cl	-CH ₃	140	1500	11	<i>c</i>	>20
8at	-CF ₃	-OCH ₃	-Br	-CH ₃	130	>2000	>15	<i>c</i>	>20

^a Chloroquine (CQ), atovaquone (ATO), and dihydroartemisinin (DHA) are internal controls for each in vitro assay: CQ, 0.42 μM W2, 0.23 μM TM90-C2B and 47.2 μM J774; ATO, 1.4 nM W2, 18 μM TM90-C2B and 28 μM J774; DHA, 5.5 nM W2, 5.9 nM TM90-C2B and 1.5 μM J774.

^b RI = TM90-C2B/W2.

^c Not determined

Table 6.

In Vivo Efficacy Scout Screening

compd	% inhibition day 3 PI ^d	% inhibition day 6 PI ^d	compd	% inhibition day 3 PI ^d	% inhibition day 6 PI ^d
8a	38.5	27.5	8u	100	98.3
8b	46.2	43.1	8v	100	100
8c	80.0	31.6	8w	100	82.4
8d	70.0	33.0	8x	80.0	19.3
8h	100	<1	8y	100	24.6
8k	100	12.3	8z	100	70.6
8l	69.2	41.2	8aa	100	56.9
8m	40.0	<1	8ab	100	100
8n	100	39.2	8ad	46.2	<1
8o	100	98.0	8ag	84.6	31.4
8p	100	100	8ak	100	94.2
8q	46.2	15.7	8al	100	71.9
8r	100	24.6	8an	100	100
8s	80.0	14.0	8ao	100	86.4
8t	100	<1	atovaquone	96.3	99.8
amodiaquine	95.5	99.9			

^dPercent inhibition compared to untreated animals.

Table 7.

In Vivo Efficacy Thompson Test

compd	dose (mg/kg)	% inhibition day 6 PI ^a	av day of death	no. of cures
8o	10	100	21	0/5
8p	10	100	21	0/5
8u	10	100	21	0/5
8v	10	100	N/A	3/5
8ab	10	100	N/A	3/5
8ak	10	33.0	13	0/5
8an	10	90.9	13	0/5
8ao	10	11.0	13	0/5
atovaquone	10	100	N/A	5/5

^aPercent inhibition as compared to untreated control animals.

Table 8.

In Vivo Efficacy of Compounds 8j and 8l Against Liver Stages of the Parasite

compd	dose (mg/kg)	route	% inhibition day 9	
			PI ^a	no. of cures
8j	25	oral	65.3	2/5
8j	50	oral	85.1	2/5
8j	50	subcutaneous	>99.0	3/5
8j	100	oral	>99.0	5/5
8l	25	oral	49.1	0/5
8l	50	oral	38.8	0/5
8l	50	subcutaneous	20.1	0/5
8l	100	oral	43.9	1/5
primaquine	50	oral	>99.0	2/5

^aPercent inhibition as compared to untreated control animals.